MASARYKOVA UNIVERZITA
PŘÍRODOVĚDECKÁ FAKULTA
ÚSTAV TEORETICKÉ FYZIKY A ASTROFYZIKY

Diplomová práce

BRNO 2019 **JAKUB FAKTOR**

MASARYKOVA UNIVERZITA
PŘÍRODOVĚDECKÁ FAKULTA
ÚSTAV TEORETICKÉ FYZIKY A ASTROFYZIKY

Vývoj moderního nástroje pro spektrální klasifikaci

Diplomová práce

Jakub Faktor

Vedoucí práce: doc. Mgr. Ernst Paunzen, Dr. **Brno 2019**

Bibliografický záznam

Autor:	Bc. Jakub Faktor Přírodovědecká fakulta, Masarykova univerzita Ústav teoretické fyziky a astrofyziky
Název práce:	Vývoj moderního nástroje pro spektrální klasifikaci
Studijní program:	Fyzika
Studijní obor:	Teoretická fyzika a astrofyzika
Vedoucí práce:	doc. Mgr. Ernst Paunzen, Dr.
Akademický rok:	2018/2019
Počet stran:	xiii + 80
Klíčová slova:	klasifikace hvězd; spektrální čáry; ekvivalentní šířky; Pickles MK standardy; horké hvězdy; chladné hvězdy; software

Bibliographic Entry

Author:	Bc. Jakub Faktor Faculty of Science, Masaryk University Department of Theoretical Physics and Astrophysics
Title of Thesis:	Development of a modern tool for spectral classification
Degree Programme:	Physics
Field of Study:	Theoretical Physics and Astrophysics
Supervisor:	doc. Mgr. Ernst Paunzen, Dr.
Academic Year:	2018/2019
Number of Pages:	xiii + 80
Keywords:	stellar classification; spectral lines; equivalent widths; Pickles MK standards; hot stars; cool stars; software

Abstrakt

Software umožňující klasifikaci hvězd je již mnoho let jedním z diskutovaných témat hvězdné spektroskopie. Klasifikace hvězd je v současnosti jednou z nejvíce prominentních disciplín moderní astrofyziky, jež se rapidně vyvíjí již od publikace Yerkes klasifikačního systému v roce 1943. Kritéria klasifikace byla za uplynulé roky prodiskutována, některá byla zanechána, jiná zůstávají až dodnes. Tato práce se mimo vývoje softwarového nástroje pro spektrální klasifikaci rovněž zabývá systémem kritérií aplikovatelných při klasifikaci spekter hvězd luminositních tříd I-V spektrálních typů O-M viditelné až blízké infračervené části spektra v rozsahu vlnový délek 3 800 – 8 400 Å, zejména pak dle flexibilních MK standardů Pickles rozlišení 5 Å. Za tím účelem byl v programovacím jazyku C# vyvinut software SpecOp 2. SpecOp 2 je softwarové rozhraní pro uživatele-experty, poskytující vizuální kontrolu při manipulaci se spektrálními daty, zahrnující širokou škálu nástrojů a obsahující několik knihoven hvězdných spekter, která je schopná vykreslit a zpracovat hvězdné spektrum a určit ekvivalentní šířky důležitých spektrálních čar a rovněž vynést tyto eqvivalentní šířky na HR diagram. Navíc přímá podpora softwaru MKClass vytvořeného skupinou R. O. Gray *et al.* poskytuje možnost vysoce kvalitní automatické klasifikace, k níž by jinak uživatelé systémů Win NT měli obtížný přístup.

Abstract

Software capable of stellar classification has been for years a topic of discussion on the field of stellar spectroscopy. Stellar classification is presently one of the most prominent disciplines of modern astrophysics, that has been developing rapidly, ever since the publishing of Yerkes classification system in 1943. The criteria of the classification were broadly debated over the years, some were left behind and some remain to this day. Apart from the development of a modern tool for spectral classification, this thesis ponders on the various criteria applicable in the classification of spectra of stars of luminosity classes I-V of spectral types O-M in the visible to near infrared region, ranging the wavelength interval of 3 800 – 8 400 Å, particularly according to the flexible Pickles MK standards of resolution 5 Å. For this purpose, the software SpecOp 2 was developed in the C# programming language. The SpecOp 2 is a spectroscopy suite software for expert users, granting enhanced visual control when manipulating with spectral data, containing a number of toolsets and multiple stellar spectra libraries, that is capable of plotting and processing stellar spectra and determining equivalent widths of important spectral lines and also plot these equivalent on the HR diagram. Additionally, direct support of the MKClass software created by R. O. Gray *et al.* provides an option of high quality automatic classification, access to which would otherwise be difficult for users of Win NT systems.

MASARYKOVA UNIVERZITA
Přírodovědecká fakulta

ZADÁNÍ DIPLOMOVÉ PRÁCE

Akademický rok: 2018/2019

Ústav: Ústav teoretické fyziky a astrofyziky

Student: Bc. Jakub Faktor

Program: Fyzika

Obor: Teoretická fyzika a astrofyzika

Směr: Astrofyzika

Ředitel *Ústavu teoretické fyziky a astrofyziky* PřF MU Vám ve smyslu Studijního a zkušebního řádu MU určuje diplomovou práci s názvem:

Název práce: Vývoj moderního nástroje pro spektrální klasifikaci

Název práce anglicky: Development of a modern tool for spectral classification

Oficiální zadání:
With the availability of spectrosopic all-sky surveys (e.g. LAMOST), the need for a modern tool to perform spectral classification within a GUI is very much needed. The classification process is mainly based on line ratios of different species. Important points when classifying stars is the rotational line broadening, the normalization, resolution and the radial velocity shift of the spectra. These items can be efficiently treated in a GUI based tool. Within this thesis, such a tool should be developed, tested and make public available for the community. The tool will be applied to a list of new observations of bona-fide chemically peculiar star candidates to determine their true nature.

Literatura:
GRAY, R. O., C. J. CORBALLY a Adam J. BURGASSER. *Stellar spectral classification*. Princeton, N.J.: Princeton University Press, 2009. xvi, 592. ISBN 9780691125114.

GALITZ, Wilbert O. *The Essential Guide to User Interface Design: An Introduction to GUI Design Principles and Tech-niques*. 2007. ISBN 978-0-470-05342-3.

Jazyk závěrečné práce: angličtina

Vedoucí práce: doc. Ernst Paunzen, Dr.

Datum zadání práce: 22. 11. 2016

V Brně dne: 30. 11. 2018

Souhlasím se zadáním (podpis, datum):

Bc. Jakub Faktor
student

doc. Ernst Paunzen, Dr.
vedoucí práce

prof. Rikard von Unge, Ph.D.
ředitel Ústavu teoretické fyziky a astrofyziky

Poděkování

Poděkování patří především vedoucímu práce, doc. Mgr. Ernstu Paunzenovi, Dr., za odborné vedení, ochotu a čas, který mi po dobu zpracování práce věnoval.

Prohlášení

Prohlašuji, že jsem svoji diplomovou práci vypracoval samostatně s využitím informačních zdrojů, které jsou v práci citovány.

Brno 2. ledna 2019 .....

Jakub Faktor

Table of Contents

List of Figures

List of Tables

Introduction

Modern spectroscopy is a highly developed method of studying electromagnetic radiation and retains its position as the method making possible a significant portion of scientific discoveries worldwide. Spectra, products of our spectroscopic measurements, are essentially distribution functions of radiation intensity respective to wavelength of the objects we observe. Analysis of measured spectra is one of the main tasks of astrophysics. No matter what object we are currently observing, be it stars, nebulae or galaxies, spectroscopy always brings us some extra useful information, gaining which would possibly be very difficult in other ways. Spectroscopic methods are of great importance especially when it comes to classifying stars according to their spectra. Stellar spectra can tell us much not only about the physical nature of observed stars, like temperature, surface gravity and chemical composition, but also give us a crucial piece of information needed to identify larger celestial systems and structures, for instance determining the radial velocity or the rate of rotation. Some stellar parameters can be obtained quite simply, however when attempting to gain knowledge of the very important parameters of mass, temperature, luminous power, radius, element abundances or distance we often lack a critical piece of information, that is, any combination of said physical properties of the star. A very solid estimate of the star's characteristics can be achieved through the use of stellar classification, which is mostly based on classifying stars according to ratios of relative strengths of specific spectral lines. In the present, the majority of stars are classified according to the Yerkes system. The classification is done by determining both the spectral and luminosity class, effectively describing the star's position in the Hertzsprung-Russell diagram. Observed spectra are different for each spectral type and so the ratios of intensities of lines used for classification are type-specific. Correct choice of criteria spectral lines is critical: the number of spectral lines usable for classification is somewhat reduced by the possibility of varying degrees of metallicity and chemical peculiarity that may affect the certain spectral lines greatly.

The software SpecOp 2 was developed for the Win NT operation systems, in the C# programming language from a reworked code of the original SpecOp software and was designed as greatly expanded, advanced and more lightweight version of its predecessor.

It is a comfortably controllable application capable of semi-automatic to automatic MK system stellar classification.

Development of forementioned software is not the sole goal of this thesis, as I also attempt to compile a set of stellar classification criteria used for classification according to the MK system, using a refined set of spectral lines, amounting to nearly hundred spectral lines collected from literature. This thesis is considering criteria applicable to classification of stars of types O-M, of the luminosity classes I-V. Collection of criteria included in this thesis spans the wavelength region of 3 800 – 8 400 Å. As this is direct continuation of my previous work, several sections of the text not needing revisions are directly cited from [1].

Chapter 1

Spectroscopy

1.1 Historical introduction

In the historical introduction to spectroscopy of my bachelor thesis, I pondered whether Isaac Newton could have foreseen the importance of his discovery, upon first splitting the beam of light with a prism in the 17th century, possibly indirectly recognizing his forefather-like role in the field of spectroscopy, not because of his brilliant works in other fields of physics, but because this moment represents the "Eureka", a crucial scientific breakthrough for the subtle and delicate science of analyzing spectra, stellar or otherwise. In similar spirit, I'd like to address two other milestones of spectroscopy. The first one is the moment Victor Schumann used fluorite lens and discovered vacuum ultraviolet radiation in 1893, leading to discovery of Lyman series by Theodore Lyman in 1914. The second major event are the flights of V-2 rockets in 1946 and 1947, carrying not an explosive payload, but a scientific one, pioneering spectroscopy out of the bounds of our atmospheric prison. Perhaps this one also serves as a testament to the fact that science has no agenda: as the theory of nuclear fission was misused for war in atomic bombs, so can instruments, made originally for war, be used for the greater good of science and humanity in turn. V-2 rockets were designed by the pioneer of rocketry, Wernher von Braun, and modified and flown by a team of scientists of the Naval Research Laboratory (Baum, Johnson, Oberly, Rockwood, Strain). The measurements brought another breakthrough for spectroscopy and not only shifted our interest from ground based spectroscopy to a space-craft based one but also to different regions of spectrum.

As already mentioned, Isaac Newton was the first to use a prism to disperse a beam of light and document it. He began studying the found spectrum, as he called it, and spectroscopy was born. Many great minds of physics studied the phenomenon throughout the history in attempt to explain its physical nature and improve the methods used

in spectroscopic measurements. Josef von Fraunhofer increased the precision of spectroscopic measurements by replacing the dispersing prism by a diffraction grating, using concepts of Thomas Young's theory of interference. Later on, he made systematic observations of the Sun, where he, in the year 1814, detected dark lines that bear his name to this day. However, what he was unaware of, was the origin of these lines. The fact that there is some relation between the measured spectrum and the chemical composition of the observed object was discovered independently by Léon Foucault and Anders Angström. This dependency was first quantitatively explained in 1859 by Gustav Kirchoff and Robert Bunsen. These gentlemen have shown that every element and compound has its own characteristic spectrum and also provided experimental evidence, as they observed flames produced by many elements, including Lithium, Potassium, Strontium, Calcium and Barium. [2] In the 19th century studies of black body radiation by Gustav Kirchhoff and Ludwig Boltzmann advanced our understanding of spectra. Max Planck explained that the energy transmission is not continuous, but travels in the form of energy quanta and in the year 1900 he achieved a breakthrough by developing the equation that we know today as Planck's Law. The path to modern spectroscopy has been paved by the works of Niels Bohr, mainly by his 1913 Theory of atomic hydrogen, which revolutionized not only spectroscopy, but all of physics. [1, 3]

1.2 Electromagnetic radiation

Spectroscopy, at its core, is a discipline studying various regions of electromagnetic radiation, so before advancing to the problematics of spectra and their origin, some description of characteristics of electromagnetic radiation is in order. According to Maxwell theory of electromagnetic fields, electromagnetic radiation is a transverse wave propagating through the vacuum at the speed of light. The frequency ν [Hz] and the wavelength λ [nm] of electromagnetic radiation are governed by the dependency (1.1):

$$c = \nu\lambda, \tag{1.1}$$

where c is the speed of light. Electromagnetic radiation is formed by photons, elementary boson particles (thus possessing an integer spin, 0 specifically for photons) that have a rest mass equal to zero. Max Planck explained that the energy E [J] of an energy quantum, a photon, is given by the equation (1.2):

$$E = h\nu = \frac{hc}{\lambda}, \tag{1.2}$$

where h is Planck's constant, ν [Hz] is frequency and λ [nm] is wavelength of the radiation. In the various disciplines of astrophysics that study stars, electromagnetic radiation has the major role of one of the means transporting energy, maintaining the so called radiative transfer, carrying the energy from the inner regions to the outer regions and even to the star's surroundings. Furthermore, it is the source of radiation pressure, which in turn has a major role in the physics of hot stars. [1, 4, 5]

1.3 Radiation of an Absolutely Black body

All objects that are made of matter emit light and the hotter they are, the more luminous energy they radiate. To quantitatively describe radiation that is being emitted by an ideal black body, a physical model of the absolutely black body, described by the Planck function, is used. The model consists of several constraints: it is defined as a non-reflective body that's surface is uniformly held at constant temperature. Absolutely black body is a physical approximation applicable in many scientific fields. In this model, the scientific fields of thermodynamics and atomic physics seem to have meeting point. For astrophysics it holds major importance, as absolutely black body is a good approximation for stars and other astrophysical objects of interest, even though stars are not completely non-reflective, nor are they in thermal equilibrium with their surroundings and the spectral distribution of an ABB is different from that of a star, especially in the blue and ultraviolet region. It was Kirchhoff's 1859 work that showed that the black body radiation only depends on the temperature of the absolutely black body's surface and not on the properties of the surface itself. [4] The black body radiation spectrum is in the form of continuum, consisted in a continuous interval of wavelengths, with spectral distribution changing according to temperature. Generally, with increasing temperature, the radiation of an absolutely black body is more intensive and in higher frequencies (thus in shorter wavelengths). Quantitatively, this is described by Planck's Law (1.3):

$$B_\nu(\nu,T) = 2\pi\frac{\nu^2}{c^2}\frac{h\nu}{exp(h\nu/kT)-1}, \tag{1.3}$$

where B_ν is monochromatic intensity in specific radiation frequency and temperature, ν is frequency, T is temperature of the black body, h is Planck's constant and k is Boltzmann's constant. [4] The characteristically shaped spectral distribution to which this equation leads is shown below in the figure 1.1:

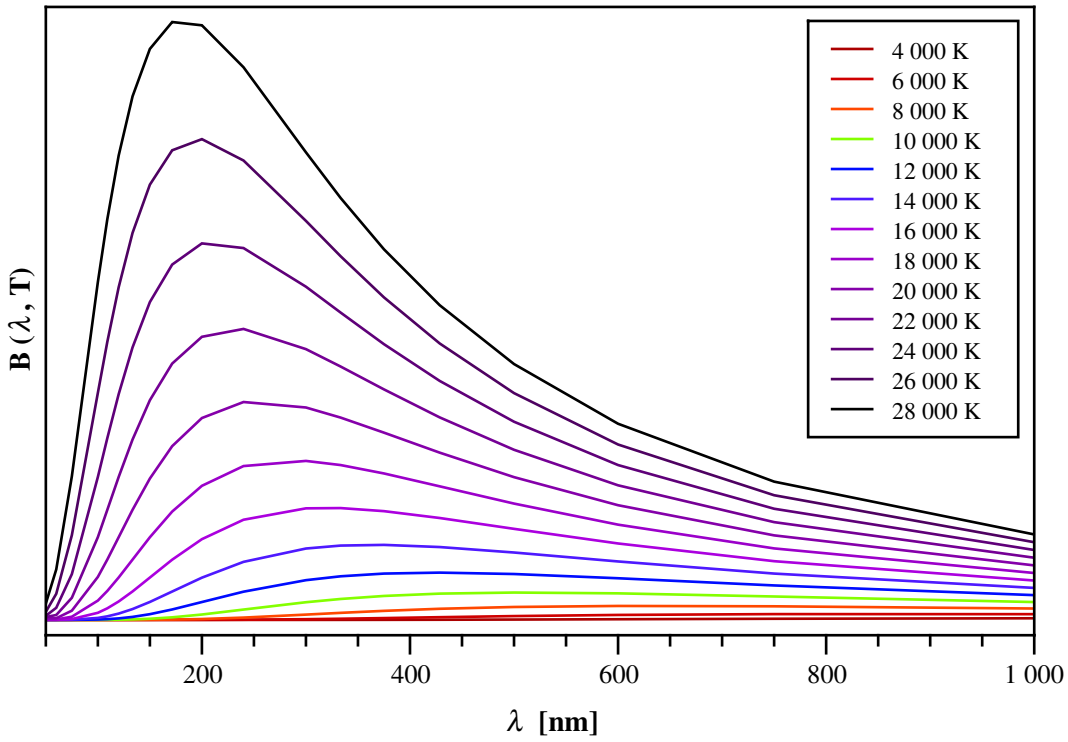

Figure 1.1: Spectral distribution of a black body at several values of temperature T [K].

As it can be noticed in this graphical representation, the wavelength of the maximum of the spectral distribution is decreasing with increasing temperature, as higher energy radiation is being radiated. Wien's displacement law is an example of an approximation that makes use of this fact. [6] Luminous energy that is radiated by the black body is tied to the black body's effective temperature T_{eff} [K] by the Stefan- Boltzmann's Law (1.4): [1, 4]

$$\Theta_e = \sigma S T_{eff}^4, \tag{1.4}$$

where σ is Stefan-Boltzmann constant and S is the radiating surface area of the black body. If we consider that we intend to approximate stars as spherical black bodies we arrive at the equation (1.5), that describes luminosity L [Js^{-1}] of a star with radius R [m] and effective temperature T_{eff} [K]:

$$L = \sigma T_{eff}^4 4\pi R^2. \tag{1.5}$$

1.4 Photon absorption and emission

Absorption and emission of a photon are processes resulting from the change of momentum state of a charged particle. The lighter the charged particle is, the easier it is to change its momentum and the easier a photon is emitted. In practical astrophysics, radiation that is product of changes in the momentum state of electrons is studied nearly exclusively. [4] In the case of electrons bound in atoms, the electron's movement state is represented by its quantized energy levels. Fundamental characteristic of photons is the fact that their energy is always exactly equal to the energy difference of the emitting electron's initial and final energy states. In the case of absorption of photon by electron bound in an atom, the final state of the atom is the more energetic of the two energy levels and the term excitation is used. In the majority of cases the atom only remains in an excited state for a relatively short amount of time, before an opposite effect of de-excitation takes place. As stated, only a photon with energy equal to the energy difference between initial and final energy states of the electron can be emitted. This, of course, holds true for the inverse scenario, where a photon can only be absorbed by an electron, if the electron's energy levels allow it. This leads to the distinctive shape of atomic spectra, that is formed by a collection of spectral emission and absorption lines. If, on the other hand, the energy of interacting charged particle is not limited to discreet distribution, for instance a situation in which a free electron is changing its momentum after entering an electrostatic field, energy of the photon that is emitted will depend on the initial energy of the charged particle. Thus, if the studied matter allows its charged particles' energy continuous intervals of possible energy values, for example in the state of plasma, the spectrum is in the form of continuum. [1, 4, 7]

1.4.1 Spectral lines

Both absorption and emission spectral lines are product of bound-bound transitions between two states of an atom – electronic spectral lines, or a molecule – rotational and vibrational spectral lines and bands of lines. The nomenclature is apparent, if an atom absorbs a photon, the spectra contain absorption lines, while if the atom emits a photon, we observe emission lines. Sets of hydrogen and helium emission lines, which are product of de-excitation of an atom to a specific energy level, are ordered in series named after their discoverers. Hydrogen spectral series are, in the order of ascending principal quantum number, Lyman series (n = 1) in the ultraviolet region of the spectra, very important Balmer series (n = 2) in the visible region, and Paschen series (n = 3), Brackett (n = 4), Pfund series (n = 5) and Humphreys series (n = 6) in the infrared region. Further series are not named. As goes for helium line series, which are not quite as famous as hydrogen line series, the named series are Fowler series (n = 3) and Pickering series (n = 4), which,

originally Edward Pickering wrongly attributed to some unknown state of hydrogen. Lines belonging to the series are then labeled with Greek characters, for instance the first Lyman line, which is product of n = 2 to n = 1 transition of hydrogen atom, is named Lα, the first Balmer line (n = 3 to n = 2) is Hα and so on. Knowledge of specific energy levels of studied spectral line enables us to calculate its wavelength. For single electron atoms, including hydrogen and singly ionized helium atoms, we can use equation (1.6):

$$h\nu = \Delta E = Z^2 E_1 \left(\frac{1}{n_i^2} - \frac{1}{n_j^2} \right) \rightarrow \frac{1}{\lambda} = -\frac{E_1}{hc} Z^2 \left(\frac{1}{n_i^2} - \frac{1}{n_j^2} \right) = Z^2 R \left(\frac{1}{n_i^2} - \frac{1}{n_j^2} \right), \quad (1.6)$$

where h is Planck's constant, ν is frequency of the photon, E_1 is the energy of the ground state, c is the speed of light, n_i and n_j are the principal quantum numbers of the transitioning states and R is the Rydberg's constant. The wavelength difference for the neighbouring lines in a series is decreasing with the higher principal quantum number n_i, until they are zero in the case $n_i \rightarrow$ infinity. Here the spectral line series turn into a continuum and the wavelength at which this continuum begins is defined as the series limit. [4, 5]

The fact that spectral lines form due to precisely defined transitions would seem to suggest that the energy and thus the wavelength of spectral line photons is a specific value, however, due to quantum mechanical principles, both the energy and the wavelength of these photons are an interval of values, we can say that the lines are not perfectly sharp and that they posses certain profiles. In order to evaluate individual line profiles, usually equivalent widths of the spectral lines are used. [4] Equivalent width W_λ [Å] at wavelength λ [Å] is a measure of a photometric strength of the studied line and is formally defined with the equation (1.7):

$$W_\lambda \equiv \int_0^\infty (1 - r_\lambda) d\lambda, \quad (1.7)$$

where r_λ is residual flux, which we gain after normalizing the flux values of the spectrogram. The equivalent width can be interpreted as the length of a rectangle possessing height equal to one, that spans the same area as the profile of the spectral line as shown in the illustration 1.2. [1, 8]

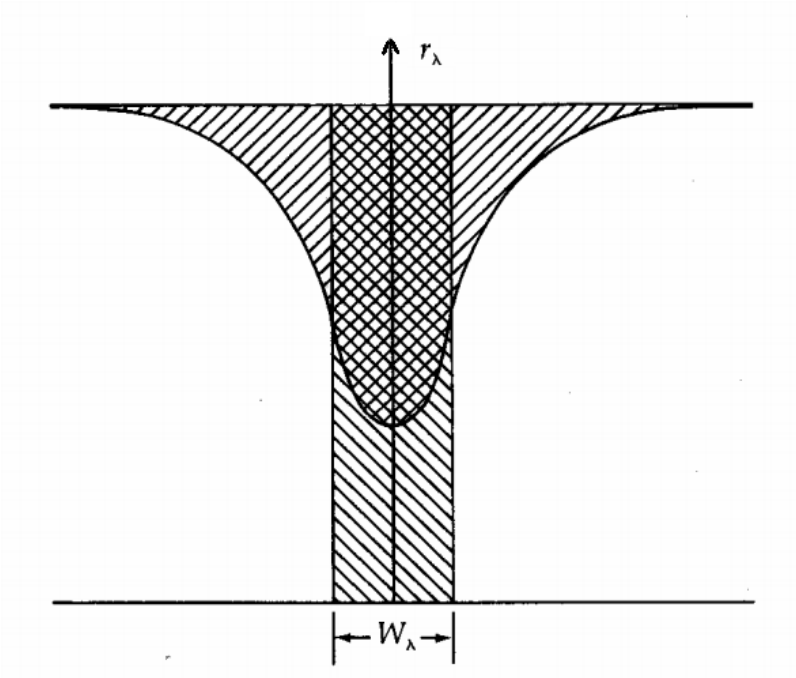

Figure 1.2: Equivalent width W_λ of an absorption spectral line. [8]

1.4.2 Continuum

Both the series limit and following continuum are labeled according to the related series, hence Lyman limit, Lyman continuum, Balmer limit, Balmer continuum etc. Apart from the continua related to the series, continua that are product of multitude of other phenomena can be observed as well. These phenomena include bound-free transitions and free-free transitions. In bound-free transitions the electron that was being held by the nucleus is emitted with some kinetic energy, while also emitting a photon accordingly. This is what we call ionization and the reverse, where an ion catches an electron, is called recombination. In free-free transitions, an electron moving through space near an ion emits a photon, yet still has high enough kinetic energy to escape. [4]

1.4.3 Balmer, Lyman and other jumps

Another spectral feature connected to the generation of series of spectral lines are the spectroscopic jumps. Leaving spectral lines aside, the continua of stellar spectra themselves differ from spectra of absolutely black bodies of the same effective temperature, firstly because of nuclear reactions in their cores, implying greater spectral flux in the extreme UV region than that of an ABB and secondly because of various spectral effects in the stellar atmosphere, of which perhaps the most dominant are Balmer

and Lyman jumps. We can observe these as sharp drops in spectral flux for wavelengths shorter than certain threshold – Balmer Jump at 3647 Å and Lyman Jump at 912 Å – and also as physical region in the stars atmosphere, where opacity for said wavelengths rises significantly. This is due to the values of ionization energy of the element dominant in the stellar spectrum. If for instance the spectrum continuum is mainly formed by hydrogen bound-free quantum transitions, ionization of an electron with the main quantum number n = 2 will take at least a photon with 3.4 keV, which means the area has high opacity for any photon with greater energy and thus it will also have a Balmer Jump. [9] Radiation of shorter wavelengths than the jump is in this way greatly reduced and partly redistributed to the wavelengths of longer wavelengths, which is also quite noticeable in the vicinity of the jump. Going further into the longer wavelengths, their look starts somewhat appear like that of the Planck function distribution.

1.4.4 Transitions in stars

The stellar spectra are not as dependent on chemical composition of the observed star, as the chemical compositions of most stars are mostly not very different, but rather are determined by the possible state transitions of particles enabled by the star's effective temperature. Transitions that happen in stars are usually of cyclic character, progressing in a rapid succession of events of opposite character, creating a statistical equilibrium. Neutral atoms get ionized, ionized atoms recombine, atoms get excited / de-excited, molecules vibrate and rotate. However, if the temperature does not change, the ratios of atoms in specific states remain statistically unchanged, they are in the state called detailed equilibrium. For N_m and N_n particles in the states m and n in statistical equilibrium, the ratios of N_m to N_n can be calculated using Boltzmann's equation (1.8):

$$\frac{N_m}{N_n} = \frac{g_m}{g_n} exp\left(-\frac{E_m - E_n}{kT}\right), \tag{1.8}$$

where g_m and g_n are the state statistical weights, given by the level of degeneracy of the given level, E_m and E_n are energies at said states, k is Boltzmann's constant and T is what we call excitation temperature. The ratio between number of atoms that are $i+1$ times ionized and number of atoms i times ionized, again in the state of statistical equilibrium, can be expressed using Saha's equation (1.9):

$$\frac{N_{i+1}}{N_i} = \frac{2}{N_e}\frac{Z_{i+1}}{Z_i}\left(\frac{2\pi m_e kT}{h^2}\right)^{3/2} exp\left(\frac{E_i}{kT}\right), \tag{1.9}$$

where Z_i is partition function of given level of ionization, N_e is the concentration of free electrons, E_i is the energy of the specific ionization, h is Planck's constant and T in this equation is called ionization temperature. The ratios of number of atoms in specific states is important for stellar classification due to the fact, that the spectral distribution, or more precisely, the ratios of relative intensities, that are being studied, is depending on the number of atoms of each present element in each state. [4]

1.4.5 Other spectral features

Apart from the continuum and atomic spectral absorption and emission lines, sometimes spectra may contain also various other features, including molecular bands, tightly packed series of spectral lines originating from bound-bound transitions of molecular rotational and vibrational states, also blends of spectral lines that happen to coincide on a given wavelength interval, and other spectral features. The profile of the spectral lines may be a spectral feature itself as well, for instance in the spectra of the very hot stars we can observe the so called P Cygni profile, characteristic by absorption in the blue wings and emission in the red wings, creating a very steep rise of intensity at the position of the line's central core, indicating an existence of expanding envelope surrounding the star, as well as powerful stellar winds.

1.5 Spectrograph

Spectrographs, the scientific instruments used to measure observed light's spectral distribution, the spectra, exist in many different designs, providing measurements of varying qualities. Apart from the major dividing characteristic of type of dispersing element used, spectrographic systems possess further properties, most importantly dispersion D and resolving power R resulting in spectral resolution $\Delta\lambda$.

1.5.1 Dispersion

The purpose of a spectrographic instrument is to isolate and measure monochromatic components of the studied radiation, in other words, its spectra, described by the dependency of intensity related quantity, most often spectral flux of the radiation on wavelength. The physical effect of splitting a light beam into a multitude of monochromatic beams of different angles relative to the original beam's direction is called dispersion, or sometimes chromatic dispersion. The greater these angles are, the more spread the measured

spectral lines are, and the greater is the dispersion D [$^{\circ}m^{-1}$] of the measuring system. It is defined (1.10) in the following way:

$$D = \frac{\Delta\theta}{\Delta\lambda}, \tag{1.10}$$

where $\Delta\theta$ [$^{\circ}$] is the angular spread of the neighbouring spectral lines and $\Delta\lambda$ [nm] is the difference of the wavelengths of said lines. [5] In astrophysics, different values of dispersion are used when observing spectral lines of different strengths. If the measured spectra were obtained in low dispersion, only the strong spectral lines will be present in the spectrogram. Higher values of dispersion will yield results with weaker lines observable alongside the strong ones.

1.5.2 Dispersing element

A crucial part of any of any spectrograph is its dispersing element, which enables us to separate the component wavelengths of the studied radiation. Generally, spectrographs can be divided into two groups: instruments using either a prism or a diffraction grating as a dispersing element. In modern times, the former has been largely superseded by the latter, mainly due to the higher possible resolving power of the diffraction grating. The two types of dispersers physically work in different ways. While prisms work based on refraction of light, diffraction gratings make use of interference of light. This fundamental difference gives the two dispersing counterparts several important traits. [7]

1.5.3 Spectral resolution

Quality of a spectrogram is given by the measure of possibility of resolving detailed spectral features in the measured spectra, hence the name of this property – spectral resolution $\Delta\lambda$. This characteristic is strongly tied to the resolving power R of the used instrument. The relation of spectral resolution and resolving power of a spectrograph can be described by the equation (1.11):

$$R = \frac{\lambda}{\Delta\lambda}, \tag{1.11}$$

where spectral lines of wavelengths λ and $(\lambda + \Delta\lambda)$ are the closest possibly resolved lines of the spectrogram. [5] It was earlier stated that Josef von Fraunhofer increased the precision of spectroscopic measurements, when he replaced the dispersing prism by a diffraction grate. To articulate this in less vague terms, this substitution allowed designing

of spectrographs with greater resolving power, resulting in spectrograms of higher spectral resolution. [7]

1.5.4 Prism

Prisms as dispersing elements are based on refraction of light and the main characteristic of a dispersing prism is its refractive index $n(\lambda)$, which is related to the speed of light c inside the prismatic medium and dependent on the incoming wavelength (λ). Snell's law, derived from Fermat's principle, describes the angle of refraction of light (and in turn dispersion) on the refracting interface between two media (1.12):

$$n_1(\lambda)\sin\alpha = n_2(\lambda)\sin\beta, \tag{1.12}$$

where $n_1(\lambda)$ and $n_2(\lambda)$ are the refractive indices of the two media, α is the angle between the direction of incoming light and the direction of a normal vector of the surface of the interface and β is the angle between the direction of the beam of the refracted radiation and the direction of the normal vector of the interface surface. As for spectral resolution, the equation (1.13) [7] applicable in this case is:

$$R = b\frac{dn}{d\lambda}, \tag{1.13}$$

where R is the resolving power, b is a constant and $dn/d\lambda$ is the rate of change of refractive index with respect to wavelength. It is apparent that the component $dn/d\lambda$ is directly proportional to the resolving power, but it should also be noted that this factor depends on the material of the disperser. This fact is fundamental to the limit of resolving power of any spectrograph that makes use of a dispersing prism, as we lack materials that would accommodate our spectrographic needs. [7]

1.5.5 Diffraction grating

Another approach in submitting radiation to chromatic dispersion is the use of the forementioned diffraction grating. It consists of a series of either closely spaced parallel slits or grooves ruled on a hard glassy or metallic material. As the term suggests, diffraction gratings make use of diffraction of light. Diffraction is the phenomena, that occurs when radiation passes through a slit of a size similar to the radiation's wavelength, as a consequence of the wavelike character of radiation and the principles of interference. General equation (1.14) of diffraction on a grating states:

$$m\lambda = d(\sin i + \sin\theta), \tag{1.14}$$

where i [°] and θ [°] are the angles of incidence and reflection, d [mm^{-1}] is the groove spacing that represents the proximity of individual grooves, λ [nm] is the wavelength of radiation and m is an integer quantity, that is called the order of diffraction. Diffraction gratings as dispersing elements do not disperse the incident light into merely one spectral projection as do prisms. Instead, multitude of spectral projections, hence orders of diffraction, is created by the interaction of the radiation after passing through the grating. [7] The equation of dispersion then becomes (1.15):

$$D = \frac{m}{d\cos\theta}, \tag{1.15}$$

which shows the inverse dependence of dispersion D on groove's spacing θ. [5] Instead of dispersion D, the inverse measure called plate factor P [Åmm^{-1}] is more often used. [10] It is therefore described by the equation (1.16):

$$P = \frac{dcos\theta}{m}. \tag{1.16}$$

The equation of spectral resolution can be similarily rewritten as (1.17):

$$R = Nm, \tag{1.17}$$

where N is the number of diffraction grating's grooves. [5] It is apparent, that for a set order of diffraction m, the spectral resolution R increases with the number of grooves N of a spectrograph linearly.

Chapter 2

Stellar Classification

2.1 History of stellar classification

The first attempt at creating a system of stellar classification was made by Angelo Secchi in 1868. He published a catalogue consisting of 4 000 stellar spectra at low dispersion and proposed a system of four classes denoted by Roman numerals: I – white stars with hydrogen lines, II – yellow stars with metallic lines, III – orange stars with absorption lines and IV – red stars with absorption lines sharp at their high wavelength side and blurred at their short wavelength side. In 1890 Secchi's classification was superseded by the Harvard classification scheme, that was created by Edward Pickering and Williamina Fleming and later refined by Antonia Maury. The refined class system became O-B-A-F-G-K-M, which we today know to be the progression order of descending temperature, the original alphabetical progression was based on the strength of hydrogen lines. In the years 1890 to 1924, the Harvard classification underwent further development and had a major role in the creation of the Henry Draper catalogue – the famous HD catalogue, consisting of about half a million stars with identified spectral types in even a more refined system where each class was divided into ten subclasses temperature-wise, for instance F0 being the hottest spectral class F star and F9 being the coolest spectral class F star. [4]

The problem of the Harvard classification lies in its single parameter criterion – temperature. The Hertzsprung-Russell diagram is a perfect display of the reason why this is a problem. It is apparent, that the distribution of stars in the HR diagram as a whole cannot be viewed upon as a function of only temperature, because the mapping of temperature to luminosity would violate the definition of function, where every element of the function's codomain is the image of at most one element of its domain. In the year 1943 a new system, named the Yerkes spectral classification, but also called MKK, bearing the names of its creators William Wilson Morgan, Philip C. Keenan, and Edith Kellman,

was introduced as the first two-parametric model. The new system used both temperature (spectral classification) and luminosity (luminosity classification) in order to classify the star and quickly started gaining popularity. In 1953 Morgan and Keenan published a revised version of MKK, now named MK system, which is still used to this day. [1]

2.2 Morgan-Keenan system

The Morgan-Keenan system is a phenomenology of spectral lines, blends, and bands, based on general progression of colour index and luminosity. It is defined by an array of standard stars, located on the two-dimensional spectral type vs luminosity-class diagram. These standard reference points are not depending on values of any specific line intensities or ratios of intensities; they have come to be defined by the appearance of the totality of lines, blends and bands in the ordinary photographic region. [11]

In this way, the authors themselves retrospectively defined their creation in their 1973 MK system edition. One of the most crucial thoughts of the original introduction of the MK system is consisted in the definition, that is, the emphasis on study of stars and their spectra in the relation to the many different groups of stars, separated by differently looking spectra, while using as little theoretical assumptions as possible. It is obvious, that as there are very many stars, the best course of action is to attempt to find these characteristic stellar specimen, that can be used as a solid general representation of the group and in turn use them to classify the less typical ones. [12] Hence, in the MK system, standard stars are used to classify the stars of unknown type. MK's precursor, the MKK system, published by William W. Morgan, Philip C. Keenan and Edith Kellman in the year 1943, was a vast improvement of the Harvard classification system used at the time, as it brought the second parameter of luminosity classification. After being published, the two-dimensional classification system underwent more improvements and ten years later, re-named as Morgan-Keenan system, gained worldwide acceptance. It did not mean that the MK system has reached its final form, on the contrary the system thrived, as many upstanding individuals of the scientific community sought to refine it even further.

As it was mentioned earlier, MK system is defined at specific value of dispersion 125 Åmm^{-1}. This value was originally discussed in the publication of MKK – An Atlas of Stellar Spectra, 1943.

The dispersion used (125 Åmm^{-1} at Hγ) is near the lower limit for the determination of spectral types and luminosities of high accuracy. The stars of types F5-M can be classified with fair accuracy on slit spectra of lower dispersion, but there is probably a definite decrease in precision if the dispersion is reduced much below 150 Åmm^{-1}. The lowest dispersion capable of giving high accuracy for objective-prism spectra is

higher; the limit is probably near 100 Åmm^{-1}. The minimum dispersion with which an entirely successful two-dimensional classification on objective-prism plates can be made is probably near 140 Åmm^{-1}. This value was arrived at from a study of several plates of exquisite quality taken by Dr. J. Gallo, director of the Astronomical Observatory at Tacubaya, Mexico. [1, 13]

2.3 Spectral classification

The first dimension of classification according to the MK system is essentially a present day, refined, form of the Harvard classification, defining a set of spectral classes with effective temperature decreasing in the order of progression: O-B-A-F-G-K-M, or more precisely with the supplementary classes added throughout the modern era of astrophysics (fig. 2.1):

R N
W O B A F G K M L T
S

Figure 2.1: Hardvard classification with supplementary classes.

As for the early types, O and B type stars have strong helium lines and A type stellar spectra have the strongest hydrogen spectral lines. W type stars are the hot, massive and very luminuous Wolf-Rayet stars, originally massive O type stars that lost a portion of their mass through strong stellar winds and their spectra exhibit similar lines to O type spectra, but some lines of strongly ionized carbon, oxygen and nitrogen are also observable. Spectral lines of metals gain in strength towards the late types, as do spectral lines of molecules. R and N type stars are sometimes called C type or carbon stars, cool stars with strong carbon lines in their spectra, S type stars are similar to the giant M type stars, except for the fact that their spectra contain strong zirconium oxide instead of titanium oxide lines, T type stars are brown dwarfs with strong methane spectral lines. The overview of spectral types, their intervals of temperatures and observable spectral lines is listed in the table 2.1 below [4, 14]:

Table 2.1: Table listing spectral types, their effective temperatures and associated strong lines.

Spectral type	Temperature [K]	Spectral lines
W	$>$ 25 000	He II, He I, H I, O III-VI, N III-V, C III, C IV, Si IV
O	28 000 - 50 000	He II, He I, H I, O III, N III, C III, Si IV
B	10 000 - 28 000	He I, H I, C II, N II, Fe III, Mg III
A	7 300 - 10 000	H I, ionized metals
F	6 000 - 7 300	H I, C II , Ti II, Fe II
G	5 300 - 6 000	Ca II, neutral metals, simple molecules
K	3 800 - 5 300	Ca I, neutral metals, molecules
M	2 500 - 3 800	Ca I, molecular bands of TiO
L	1 300 - 2 100	TiO, VO, FeH, CrH, H_2O
T	600 - 1 300	CH_4, Na I
R	3 655 - 5 350	CH, CN, C_2
N	2 940 - 5 030	CH, CN, C_2, SiC_2, C_3
S	2 400 - 3 500	Ca I, ZrO

An even better overview of the dependency of strength of spectral lines of specific elements on spectral type can be gained from the graphical interpretation (fig. 2.2) of some of the strong lines [14]:

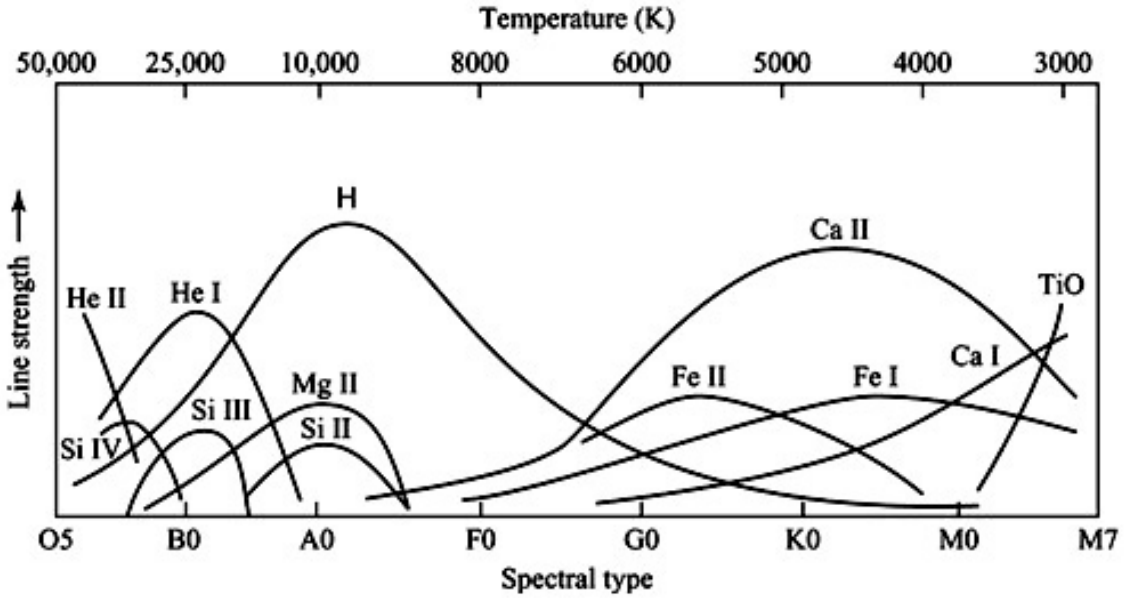

Figure 2.2: Illustration of the presence of strong spectral lines in the temperature progression. Figure taken from: `https://cmswork.nau.edu/CEFNS/Labs/Meteorite/About/Glossary-Ss/`.

As it can be seen, stars with higher effective temperature radiate at spectral lines of higher ionization order and elements with higher ionization energies. The major thought behind the general approach of using ratios of intensities of specific spectral lines can be seen in this illustration. Combinations of ratios of spectral lines are virtually always unique to their temperatures, even if the ratios themselves are not unique or if they reach similar values. Some of the general characteristics of the stellar spectra are contained here as well, for instance strong helium lines of class O and B stars, strong Hydrogen lines of the A type stellar spectra, strong ionized Iron and Calcium lines of type F and G stars and so on. A more detailed description of the characteristic spectra of the different stellar types is given in the chapter 4.

While ratios of intensities at the wavelengths of selected spectral lines should be in principle usable for the classification, or its estimate, at the very least, the most common, scientific way of evaluating the differences between the tested spectra and the standard spectra is using the ratios *W'* of equivalent widths *W* of selected lines instead. Such ratio is traditionally formally described, in the likeness of the following ratio (2.1), proposed by Conti and Alschuler, [15] with the spectral line identifiers included [1, 15, 16]:

$$W' = \frac{W(4471\ \ He\ \ I)}{W(4541\ \ He\ \ II)}. \tag{2.1}$$

2.4 Luminosity classification

The luminosity classification, describing the total radiation output of a star, brings the second parameter of luminosity into stellar classification. The method is based on the fact that the measured stellar spectra not only give us information about the effective temperature, but also information about the surface gravitational acceleration. Spectra of stars with lower surface gravitational acceleration possess sharp and thin spectral lines, while spectra of those with larger surface gravitational acceleration have broad spectral lines, caused by frequent particle collisions. [4] This is due to the the gas pressure of the photosphere – that is a function of surface gravitational acceleration – and we call this effect pressure broadening.

The star's surface gravitational acceleration is tied to the mass of the star M and radius R by the equation (2.2): [17]

$$g = \kappa \frac{M}{R^2}, \tag{2.2}$$

where constant κ is the gravitational constant ($\kappa = 6.6742 \cdot 10^{-11}$ $m^3kg^{-1}s^{-2}$). In practice, however, the surface gravitational acceleration is more typically used in its logarithmic form (2.3): [18]

$$\log g = \log M - 2\log R + 4.437. \tag{2.3}$$

The MK system classes use eight luminosity classes in total: Ia – Luminous supergiants, Ib – Supergiants, II – Bright giants, III – Giants, IV – Subgiants, V – Main sequence stars, also called dwarfs, VI – Subdwarfs and VII – White dwarfs. Often, only classes I-V are used for practical reasons. The stars of each luminosity class typically have similar values of the logarithm of surface gravitational acceleration $\log g$: for the class I stars the $\log g \approx -0.5$, for the class II stars $\log g \approx 0.5$, for the class III stars $\log g \approx 1.5$, for the class IV stars $\log g \approx 3$ and finally, for class V stars, the point of the interest of this thesis, the $\log g \approx 4.5$. [19]

In the subchapter 1.3, it was shown how we can approximate a star as a black body using Stefan-Boltzmann's law. However, according to the equation, the star's luminosity is depending on the fourth power of its effective temperature and the radiating surface area S, which only contains the second power of its radius R. What this implies is that the luminosity is less influenced by the radius in hot stars and more influenced in cool stars. This fact also means that luminosities of stars of particular luminosity classes of hot stars differ less than those of cool stars. [1, 6]

Chapter 3

General Characteristics of main sequence stars

3.1 Hot and cool star distinction

Earlier theories of stellar evolution supposed that stars evolutionarily are born as hot stars and progress by gradual cooling to cool stars. We know today that this is not correct, but the evolutionary series retained the labels that were used. And so, hot stars are sometimes called early, while cool stars are called late. The two groups were separated at the temperature of the Sun (5 780 K). Today we prefer to divide the stars into groups according to their physical characteristics, that we can observe (thus mostly at the outer layers) or quantify. These include the mass, luminosity, radius of the layer, from which the observed radiation is originating, the surface gravity and most importantly the effective temperature of the area of origin of observed radiation. With our current knowledge of stellar physics, it can be stated that the effective temperature is the factor that has the major role in both state of stellar atmospheres and inner regions of the star, that can not be observed directly. The fact that hotter stars also differ from the cool ones in the existence of local magnetic fields and active regions on the surface enables us to find a separation point between hot stars with calm atmospheres and cool atmospheres that possess these features. The role of effective temperature is even more determining in stars, where the energy flux rising from the inner regions is carried prevalently either by radiation or by convection. The former is true for the hot stars, whereas the latter is true for the cool stars. It turns out that the separation point fitting this criterion lies at the effective temperature of spectral type F2, which is approximately 7 000 K. Most often the group of hot stars is considered to consist of spectral types O, B and A, while F, G, K and M are considered cool stars. [1, 17]

3.2 Hot main sequence stars

Hot stars are a diverse group of stars, that are typically very large and bright. Hot stars are rare due to their relatively short times spent on the main sequence. Even so, they form a significant portion of all of the observed stars, since their greater luminosity enables us to detect them from greater distances. The largest subgroup of hot stars is made up of hot main sequence stars. To attain a better perception of what these are, let us observe the famous Hertzprung-Russell (fig. 3.1):

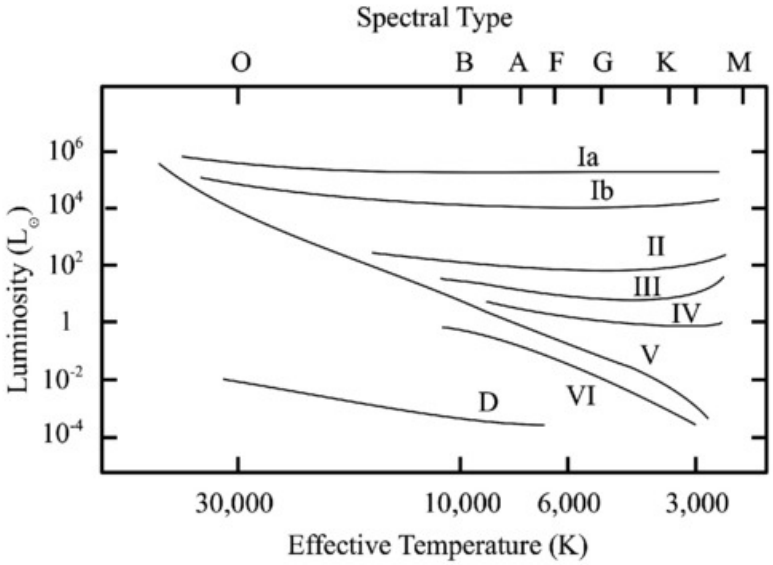

Figure 3.1: HR diagram showing the eight luminosity classes. Figure taken from: `https://ase.tufts.edu/cosmos/print_images.asp?id=49`.

If considering positions of spectral types O, B and A in the HR diagram, they are mostly situated in the area of stars of the main sequence population I on the upper left side of the diagram. Most stars of the spectral types F, G, K and M on the other hand are situated on the lower right side, although their luminosities may vary significantly more.

Main sequence stars are defined as stars that radiate exclusively at the expense of energy produced in the thermonuclear fusion. Among the fusion reactions in the hot main sequence stars dominates the CNO cycle, where carbon, nitrogen and oxygen act as catalyzers in the reaction of fusion of hydrogen into helium. The dominant type of thermonuclear reaction ongoing in the stellar core is dependent on the chemical composition of the core, but mainly on the core temperature. In cool stars, the low temperature does not allow CNO cycle reactions to occur, instead, energy is produced by other fusion reactions, mainly the proton-proton chain, which is another distinction between the two groups. Characteristics of the main sequence stars are primarily given by their

mass, which is nearly invariant in time for most stars, their rotation and chemical composition are secondary factors. [17]

One of the things main sequence stars have in common, is that they follow the mass-luminosity relation (3.1) between the star's luminosity L and the star's mass M:

$$L \propto M^{\eta}, \tag{3.1}$$

where the slope η is only changing slightly with time. Why such aproximation is possible is shown in the illustration 3.2 below, that is depicting the dependency between the star's mass and luminosity of a collection of main sequence stars.

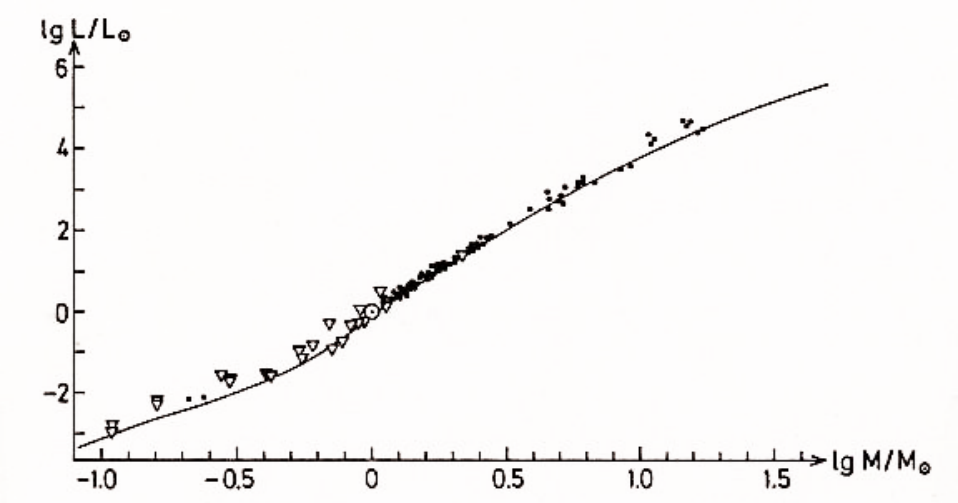

Figure 3.2: The mass-luminosity relation for main sequence stars. Figure taken from: `http://www2.astro.psu.edu/users/rbc/a534/lec18.pdf` [20].

For stars with masses between one and ten solar masses a solid general approximation lies at the value of $\eta \approx 3.88$ [20], for more precise approximation, the equations (3.2, 3.3) are sometimes used [21].

$$\frac{L}{L_{\odot}} = \left(\frac{M}{M_{\odot}}\right)^{4.0} (M > 0.43M_{\odot}), \tag{3.2}$$

$$\frac{L}{L_{\odot}} = 0.23\left(\frac{M}{M_{\odot}}\right)^{2.3} (M < 0.43M_{\odot}). \tag{3.3}$$

In a similar way to the previous rule, the main sequence star's mass M and radius R are tied by the relation (3.4)

$$R \propto M^{\xi}, \tag{3.4}$$

however, the dependency in reality contains a significant change in slope around $M \approx M_{\odot}$, as can be seen in the illustration 3.3.

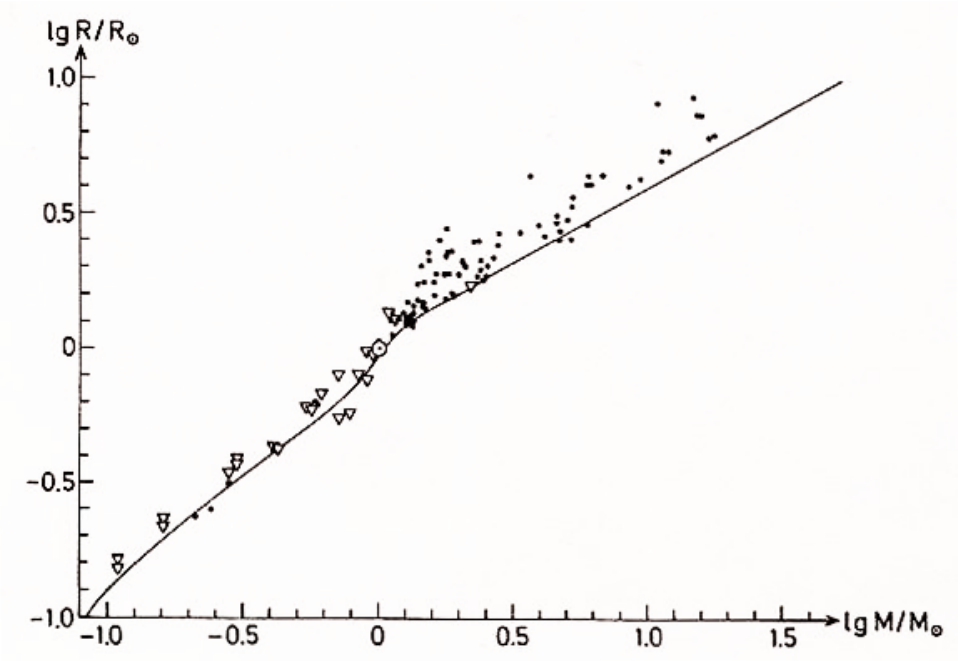

Figure 3.3: The mass-radius relation for main sequence stars. Figure taken from: `http://www2.astro.psu.edu/users/rbc/a534/lec18.pdf` [20].

Because of that, two different values of the slope ξ are usually used in practice: $\xi \approx 0.57$ for stars with $M < M_{\odot}$ and $\xi \approx 0.80$ for stars with $M > M_{\odot}$. This change of slope is caused by the fact, that the convective envelope, that is present below the star's photosphere, extends much deeper in the atmospheres of hot stars and the star's radius is then smaller, as the radiation pressure is lower due to radiation easier leaving the inner regions of the star. [1, 20]

3.3 Cool main sequence stars

Cool main sequence stars on the other hand are quite different from their hot counterparts. Among the group we call cool stars are included the stars of types F (often only the later F-type stars are called cool stars), G, K, and M of the original progression. Compared to O,

B and A main sequence stars, cool main sequence stars are generally of lesser masses and have denser atmospheres. These stars often have complex chromospheres, that transform the spectrum of the radiation coming from the stellar depths. Another major difference in the spectra is the presence of many molecular bands, a manifestation of the fact that their atmospheres are cool enough to allow formation of diatomic, triatomic, but sometimes even very complex molecules. Different is also the dominant part of transfer of energy, as in cool stars, that are generally of lower masses, radiation is the dominant part of energy transfer in their cores, while their envelopes are more convective while hot stars have it the other way around. A somewhat special case are the M type dwarfs of masses lower than 0,25 M_S, that are fully convective during much of their stay on the main sequence, which enables them to use much greater percentage of their hydrogen than other stars and leads to their grand lifetimes. Lifetimes in general are also a point of difference in these two groups – usually, the cooler a main sequence star is, the longer it will exist on main sequence, going hand in hand with their lower masses, lesser luminosities and greater rates of convective mixing. [14]

Chapter 4

O-M type stars and their spectral characteristics

The following chapter more deeply describes the characteristics of the stars of the original Harvard classification and their spectra and ponders on the applicable classification criteria. All of the shown spectrograms were obtained on the Gray / Miller spectrograph on the 0.8m telescope of the Dark Sky Observatory, using the 1 200 gmm^{-1} grating which gives a resolution of 1.8 Å. [22]

4.1 O type stars

O type stars with temperatures ranging from 28 000 K to 50 000 K [23] are massive (18 – 150 M_S), blue and hot. In fact, with the exception of Wolf-Rayet stars, O type stars are the hottest stars in the existence, which, of course, implies immense luminosities, especially if we consider their typically large radii (> 6.6 R_S). Such losses of energy through radiation, of course, shorten the time the star exists as main sequence star, making O type stars very rare, as this time only amounts to millions of years. The wavelength at which O type stars radiate the most lies in the ultra-violet part of the spectrum. O type stars are often observed in OB associations, cosmologically compact areas in the giant molecular clouds, containing a large number of O type and B type stars, that share a common origin, but have gradually become gravitationally unbound, although they are still moving through space together. Stellar evolution of O type is happening at cosmologically rapid scales of millions of years.

Spectra of O type stars are defined as spectra simultaneously exhibiting helium lines in both neutral and ionized states. The intensity of the singly ionized helium line is maximal in the spectra of early O type stars, while the intensity of the neutral helium

line grows towards its maximum in spectra of later O type stars [23]. This antagonistic behaviour is caused by the fact that the ratio of atoms in two said states is only a function of temperature as says the Saha's equation, while the total amount of helium atoms remains constant. This enables us to classify the star in terms of temperature and the MK system uses this principle for classification of O3-O9 stars [24]. Apart from helium, the spectra also contain weak lines of hydrogen. It can be noted that at the temperatures of O type stars, the majority of hydrogen in the photosphere is ionized and as such does not emit radiation. Furthermore, lines of ionized metals including Si IV, C III and O II. N III emission line can be present and if that is the case, while the spectrum also includes a He II emission line, the star is classified as Of. On the other hand, if the spectrum exhibits emission in Balmer and He lines, the star is classified as Oe. For the classification of later O type stars, namely O6-O9, ratio of C III 4649 / He II 4648 can be used for main sequence stars, if the ratio is less than one. Another possible criterion of classifying the O6-O9 stars is the ratio of Si IV 4089 / He I 4143 in high dispersion used by Conti and Alschuler, 1971. [15, 24]

As it was already stated, O type stars are characterized by weak hydrogen lines, lines of neutral helium He I and by lines of singly ionized helium He II, that can be observed in the figure 4.1.

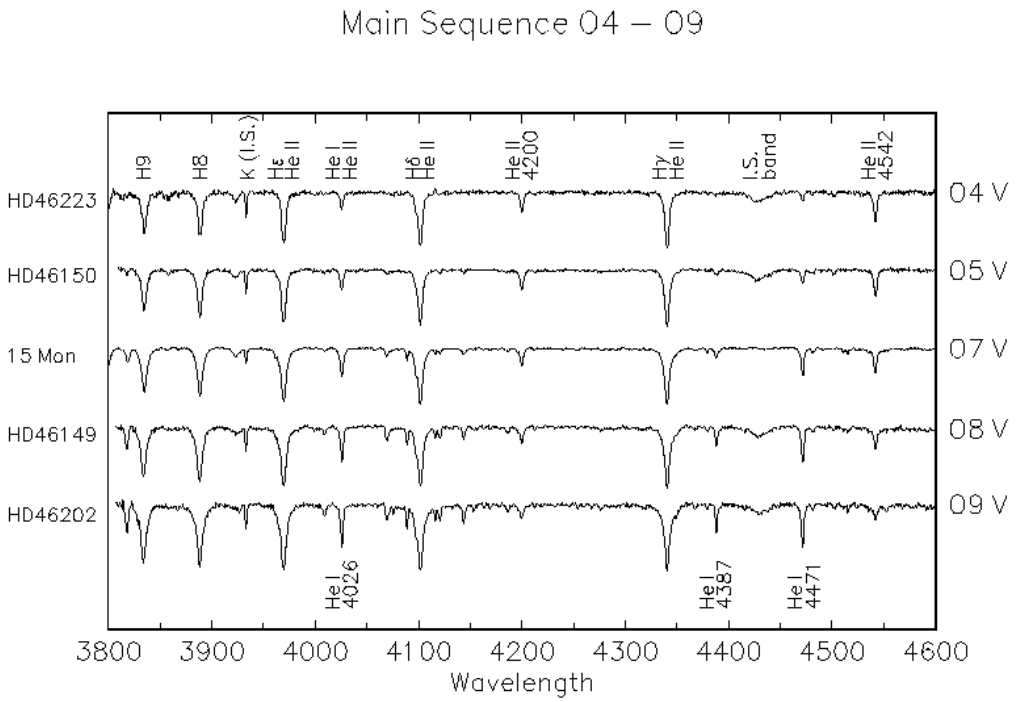

Figure 4.1: The O type main sequence stars. Figure taken from: `http://ned.ipac.caltech.edu/level5/Gray/frames.html`. [22]

The ratio He I 4471 to He II 4542 shows the antagonistic trend of neutral / singly ionized helium spectral line strengths. In several of the shown spectra two interstellar features can be observed. The Ca II K-line, labeled "K (I.S.)", as well as the diffuse interstellar band, labeled "I.S. band" at a wavelength of about 4430 Å are both interstellar features attributed to interstellar gas. [22, 25, 26]

Considering criteria applicable to luminosity classification, O type star spectra show a number of their spectral features to be luminosity sensitive. In the spectra of O type supergiants, the hydrogen spectral lines are slightly weaker, while the He I spectral lines show little to none sensitivity to differences in luminosity class. Their spectra also contain the N III 4634-42 spectral emission blend, that is present in absorption in dwarf stars. Furthermore, the neighboring He II 4686 absorption line decreases in strength with luminosity to the extent, that in spectra of O6 supergiant stars it flips to be an emission spectral line. Another He II spectral line already mentioned, the He II 4542, on the other hand slightly increases with luminosity instead. [22, 25, 26] All these effects are shown in the figure 4.2.

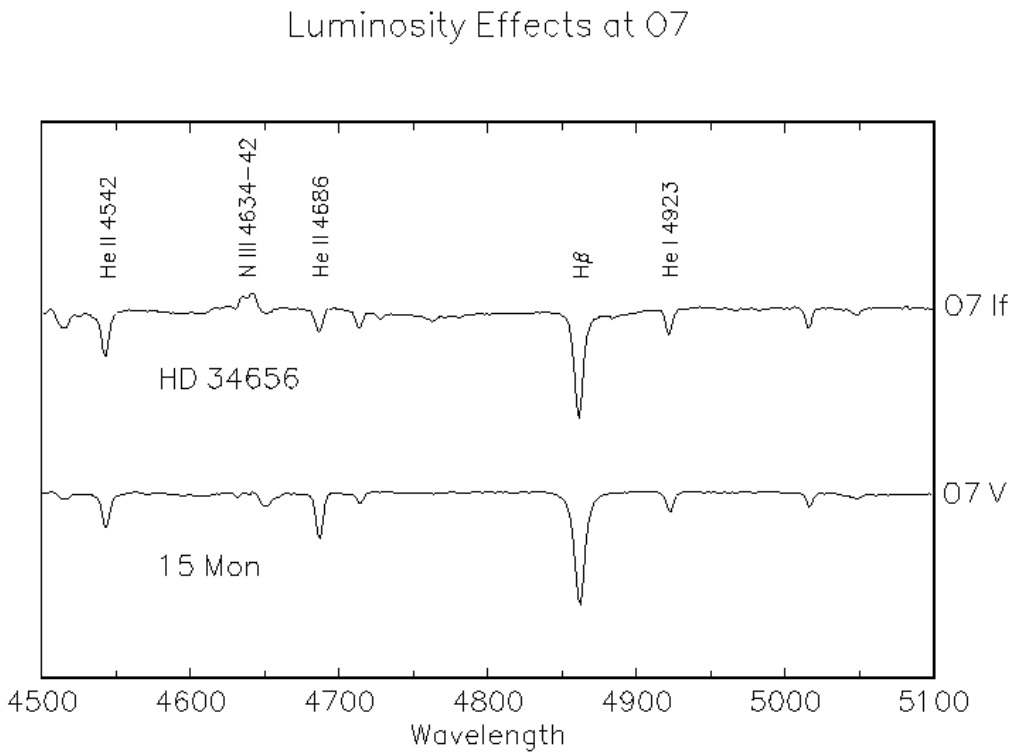

Figure 4.2: The luminosity sequence at O7. Figure taken from: `http://ned.ipac.caltech.edu/level5/Gray/frames.html`. [22]

As goes for notable luminosity effects, at O9 the hydrogen lines become more sensitive to differences in luminosity than at earlier types, the spectra are shown in the figure 4.3 below. [22]

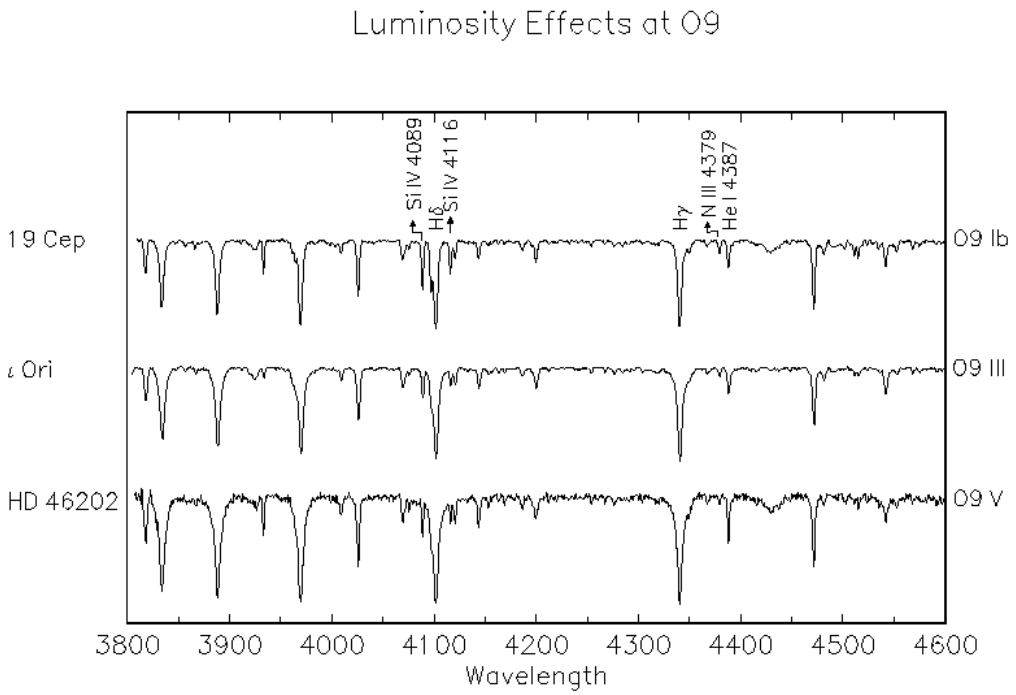

Figure 4.3: The luminosity sequence at O9. Figure taken from: `http://ned.ipac.caltech.edu/level5/Gray/frames.html`. [22]

After careful inspection, it can be noticed that, the ratio of Si IV 4089, which increases in strength as does luminosity, to Hδ, which becomes weaker with increasing luminosity, the ratio of Si IV 4116 to the neighbouring He I 4121 line, and the ratio of N III 4379 to He I 4387 pose as possible criteria for luminosity classification at spectral class O9. [22, 25, 26]

The helium lines of O type stars can be significantly influenced by metallicity effects: the smaller the value of metallicity, the stronger the ionized He absorbtion lines will be. The absorbtion lines of He I are affected more strongly than lines of He II. The He lines individually change according to effective temperature and luminosity class and, when used in certain ratios, may even shift the classification results to one subtype later. [1, 25, 26, 27]

4.2 B type stars

B type stars are a group of blue-white hot stars with temperatures of 10 000 – 28 000 K, typically situated in OB associations. B type stars are typically slightly smaller (1.8 – 6.6 R_S) and less massive (2.9 – 18 M_S) than O type stars, their "lifetimes" spent as main sequence stars may, however, be many times longer.

The main difference between the spectra of O and B stars is in the presence / absence of lines of singly ionized helium. B type stellar spectra contain lines of helium exclusively in its neutral state. Also, in the spectra we can observe not only stronger lines of ionized hydrogen, but also lines of neutral hydrogen. In a similar way as ratios of ionized / neutral helium were used for classification of O type stars, ratios of H I / He I can be used for quantitative classification of B type stars. Some weaker lines in the wavelength range 3 600 – 4 800 Å can be used for the classification, but the number of observable elements drops towards the later B type stars and so all of the visible lines should be used in order to classify B5-A0 stars. The Yerkes system uses ratios of He I, Si II, III and IV and Mg II. [24, 25, 26, 28] This method of classification may, however, sometimes lead to flawed results, as the elements may behave in an abnormal way, for instance in helium stars and CNO objects. One of the approaches to this problem was only using He and Si lines, as suggested Nolan R. Walborn [29], stars with Si anomalies were not known yet at the time, but stars with He anomalies were known to exist and so the general approach became to use the rest of the ratios to confirm the classification result. [24] Figure 4.4 shows spectra of the early main sequence B type stars.

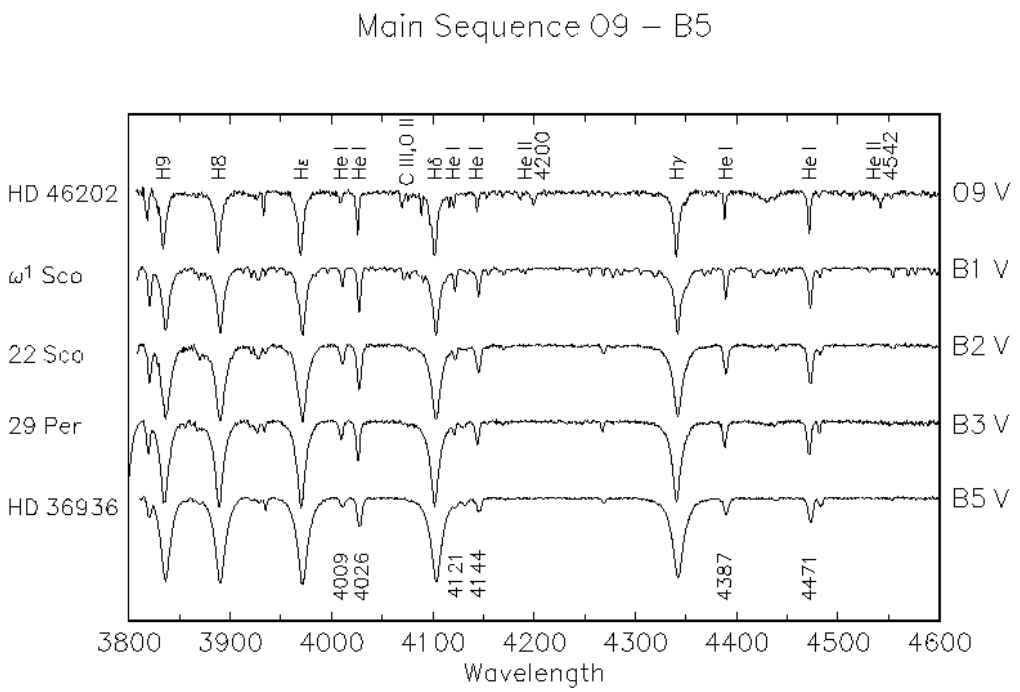

Figure 4.4: The main sequence from O9 to B5. Figure taken from: `http://ned.ipac.caltech.edu/level5/Gray/frames.html`. [22]

The intensity of the lines of He I reaches a maximum at approximately B2 and for cooler B type stars it weakens. A possible criterion of classification of spectral type lies in the ratio of He I 4471 / Mg II 4481 [22] and also N II 3995 / He I 4009 [28], although these spectral lines could be difficult to resolve on low resolution spectra.

Toward later types, the strength of helium lines decreases, until they disappear in spectra of this resolution at a spectral type of about A0. Even here, the validity of the ratio He I 4471 / Mg II 4481 holds. The threshold at the spectral class A0 is marked by the appearance of Ca II K-line, as can be seen in the figure 4.5. [22, 24, 25, 26]

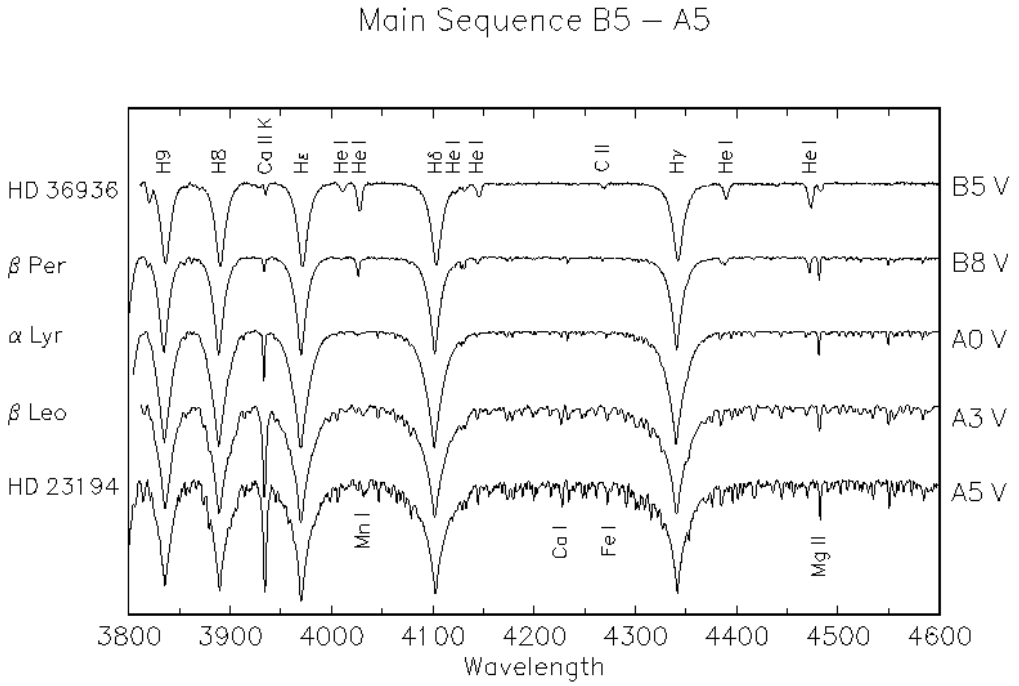

Figure 4.5: The main sequence from B5 to A5. Figure taken from: `http://ned.ipac.caltech.edu/level5/Gray/frames.html`. [22]

The luminosity classification is based on criteria that vary with the spectral type. As for the early B type stars (fig. 4.6), the width and strength of the hydrogen lines is a feasible luminosity criterion - the hydrogen and the He I spectral lines tend to weaken with increasing luminosity. But for the temperatures of B1, using ratio of the H or He spectral lines with the O II 4070-6 blend, the O II 4348 or the O II 4416 spectral lines may lead to greater precision of luminosity classification. Very important is also the Si III 4553 absorption spectral line, that can be used to discern between the dwarf and giant luminosity classes of this type and its immediate spectral progression neighbors.

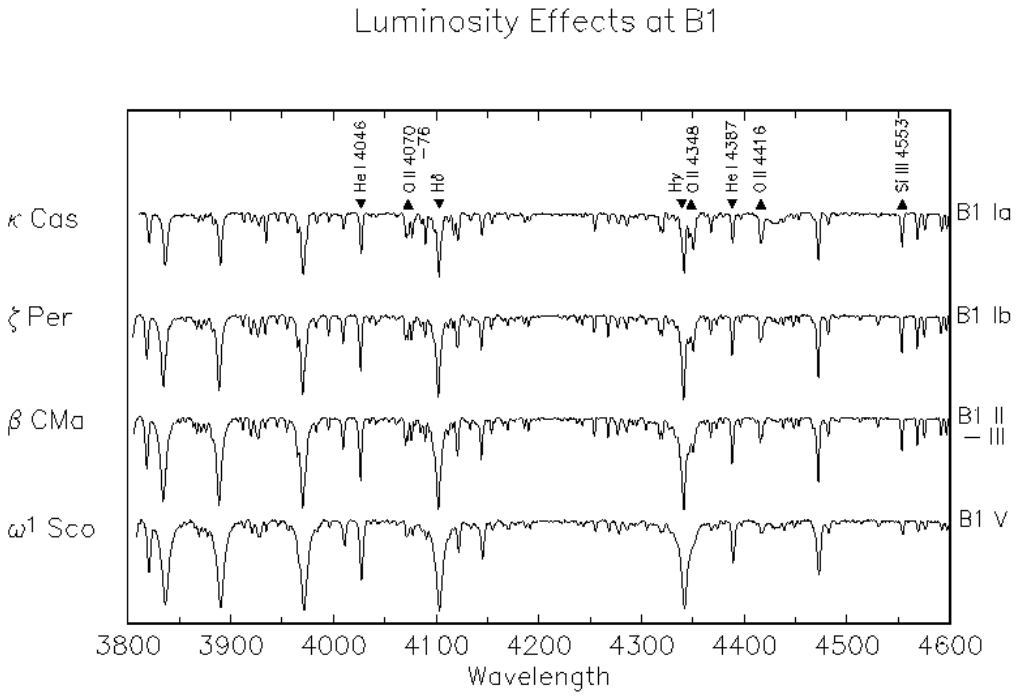

Figure 4.6: The luminosity sequence at B1. Figure taken from: `http://ned.ipac.caltech.edu/level5/Gray/frames.html`. [22]

As it has been stated, the strength of the Balmer lines is weakening with increasing luminosity, which is especially important for the luminosity classification of late B type stars, where the He I spectral lines no longer show any luminosity sensitivity. The luminosity sensitivity of the hydrogen lines is however greater here, than it was at early B type stars. [22, 24, 30] The strengths of C II spectral lines are also luminosity dependent, yet their usage is unsure due to possible abnormal chemical abundances. Features of spectra of different luminosity classes of B5 type stars are shown in the figure 4.7.

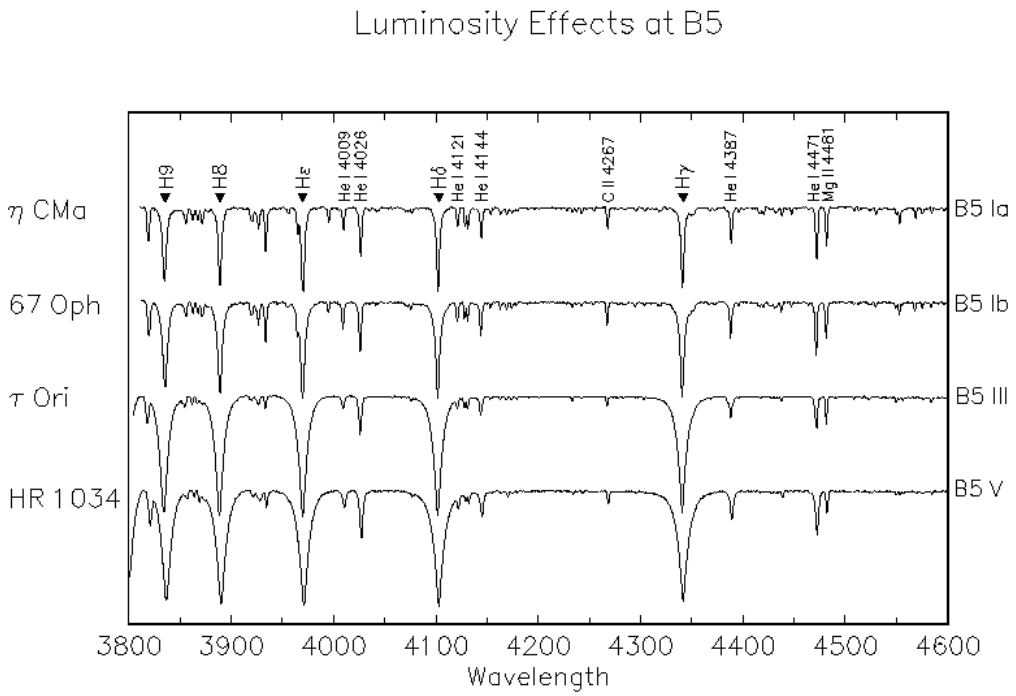

Figure 4.7: The luminosity sequence at B5. Figure taken from: `http://ned.ipac.caltech.edu/level5/Gray/frames.html`. [22]

Moreover, some of the stars of spectral type B show spectra containing spectral lines called type Be, which are characteristic by emission spectral lines accompanied by absorption spectral lines in the central cores of the profile of the emission line. These spectra may originate from B type supergiants and Herbig Be stars, pre-main sequence stars that are still in the phases of stellar contraction to their main sequence radius. Spectra of some Be stars may also show spectral features that are generally interpreted as a detached shell of gas surrounding the star, most likely in the form of a disc or ring. In the case, that this ring-like shell is aligned in our direction, we can observe very narrow absorption lines in the spectrum. Be stars are often visually and spectroscopically variable. In the case that a disc feature is observed, the star is being counted among the Gamma Cassiopeiae variables group and if the origin of variability is thought to be pulsation, the Be star is considered to be a part of the Lambda Eridani variables group. [22, 25, 26]

Another distinct group of B type stars are the chemically peculiar B type He-weak and He-strong stars, showing either exceptionally weak or strong spectral lines of neutral helium.

The figure 4.8 shows that the hydrogen lines of 3 Sco clearly belong to a star similar to the B3 V and B5 V standards, while the strength of the helium lines would suggest a spectral type of at least B8. Some B type spectroscopic variables can become helium-strong at one stage and helium-weak at different stage of their cycle. [1, 22]

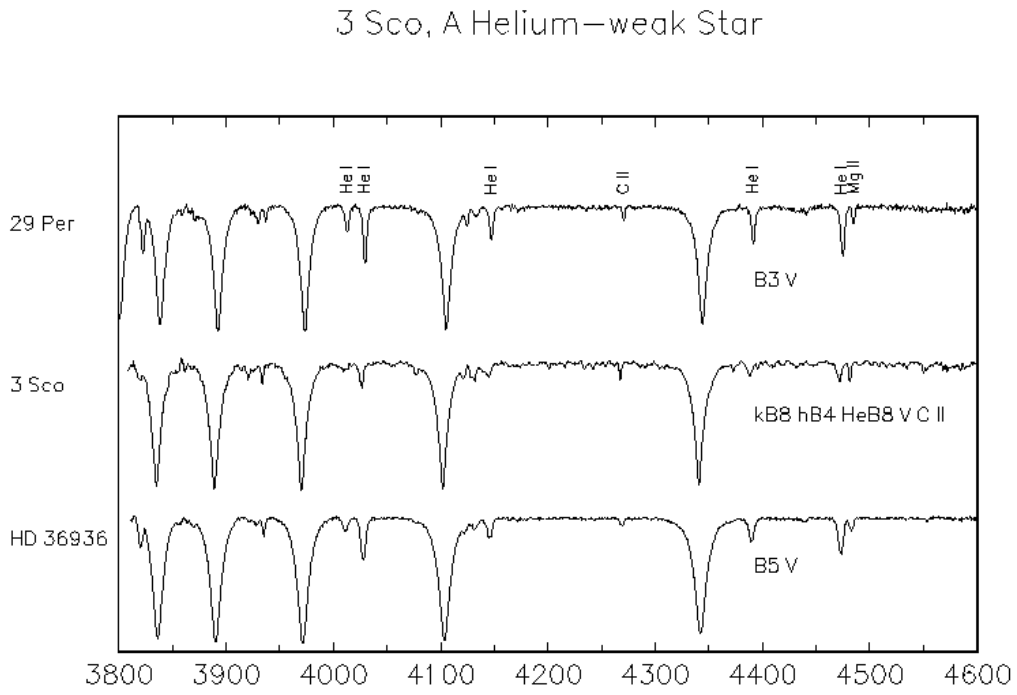

Figure 4.8: The B type Helium-weak star 3 Sco compared to B3 V and B5 V standards. Figure taken from: `http://ned.ipac.caltech.edu/level5/Gray/frames.html`. [22]

4.3 A type stars

A type stars are next in the temperature order, with temperatures ranging from 7 300 K to 10 000 K. A type stars are white, typically fast rotating stars, that are rather common, when compared to the rarity of stars of types O and B in the solar neighbourhood. A type stars, although the maximum of the spectral distribution of their radiation lies in the visible part of the spectrum, often also radiate strongly in the infrared part of the spectrum. This phenomena is attributed to a presence of dust in the system. [14]

A type stellar spectra exhibit strong absorption of the Balmer series, which is their prime characteristics as are strong lines of ionized metals. Hence, for classification of A type stars we can generally use ratios of relative intensities of lines of Hydrogen, Fe I, Fe II,

Mg II, Ti II, Ca I and Sr II. In the spectra of early A type stars, neutral helium lines are present, although much weaker, when compared to B type stars. The neutral helium lines become no longer observable in the later A type stars. [4, 24] As it was mentioned in the B type section, the threshold at the spectral class A0 is marked by the appearance of Ca II K-line. Its strength increases further throughout the cooler A type stars, as can be seen in the figure 4.9. [22, 25, 26]

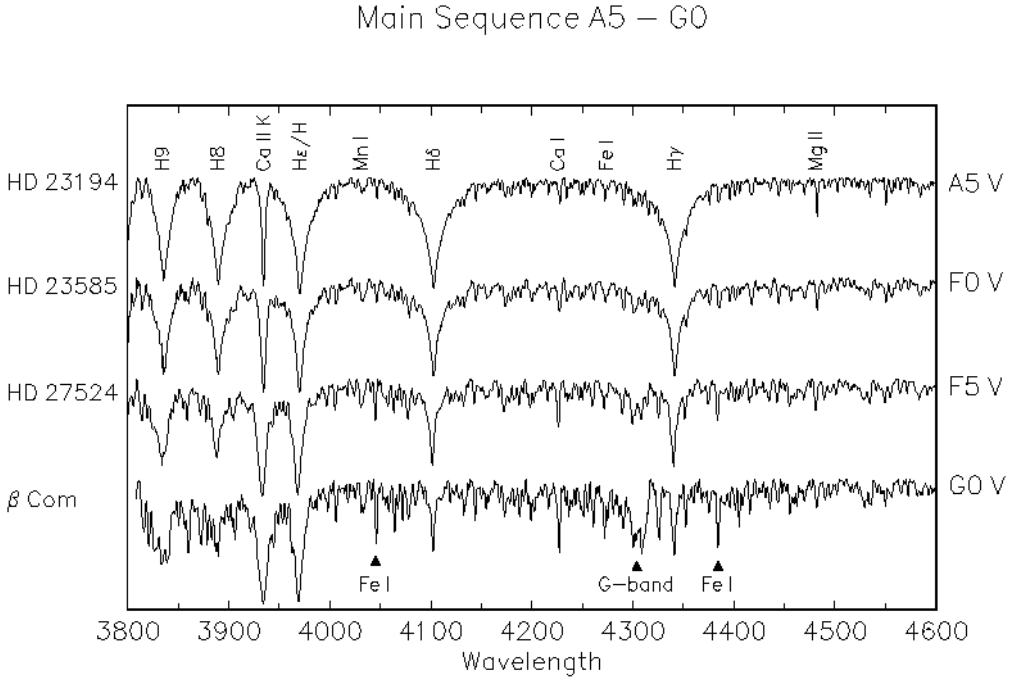

Figure 4.9: The main sequence from A5 to G0. Figure taken from: `http://ned.ipac.caltech.edu/level5/Gray/frames.html`. [22]

A note should be made at the Ca II K-line, as peculiar A type stars exist, in which these spectral lines are hardly observable. Similarly as the Ca II lines, the general metallic-line spectrum appears and strengthens at the A type stars. A spectral type classification criterion can be found in the ratios of lines such as Mn I 4030-4, Ca I 4226, and Fe I 4271. [22, 24, 25, 26]

As for luminosity criteria, in the temperature vicinity of the A0 subtype (fig. 4.10) the main spectral feature of interest is the weakening of hydrogen lines with increasing luminosity. The A0 supergiants can be identified by pronounced spectral lines of ionized iron, namely the Fe II 4233 spectral line and the Fe II + Ti II blend at 4172-8 Å, as well as the Si II blend at 4128-32 Å. [1, 22, 25, 26]

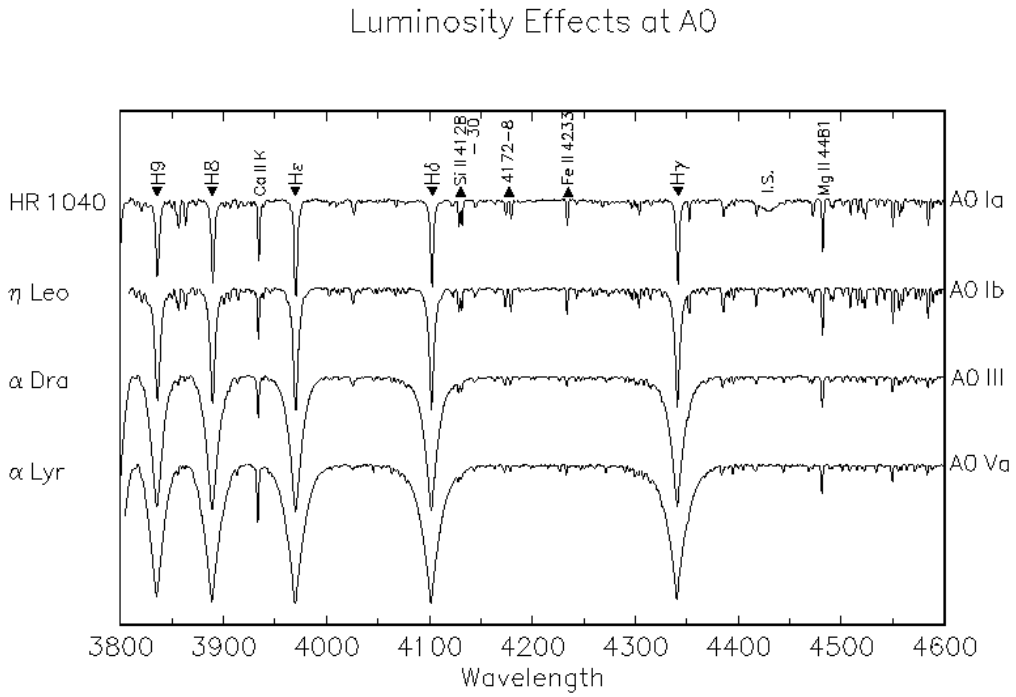

Figure 4.10: The luminosity sequence at A0. Figure taken from: `http://ned.ipac.caltech.edu/level5/Gray/frames.html`. [22]

What some would consider a special case of an A type star, Herbig Ae stars are a group of young pre-main sequence stars, that still have not fully contracted to their main sequence radius. These stars are thus still surrounded by the remnants of their circumstellar discs, unless they have already developed massive stellar winds. Their spectra can change very rapidly, even on the scale of single days.

The spectra of Herbig Ae stars (fig. 4.11) generally display emissions in the Hα spectral line, and also quite often emissions in Hβ and even Hγ lines and spectral lines in their spectra can have P Cygni and inverse P Cygni profiles. It is possible to classify these stars by comparing emission or abnormal absorption in the lines of the Fe II blend and the strength of the Balmer series, while also keeping track of the character of the Hβ emission line. [22]

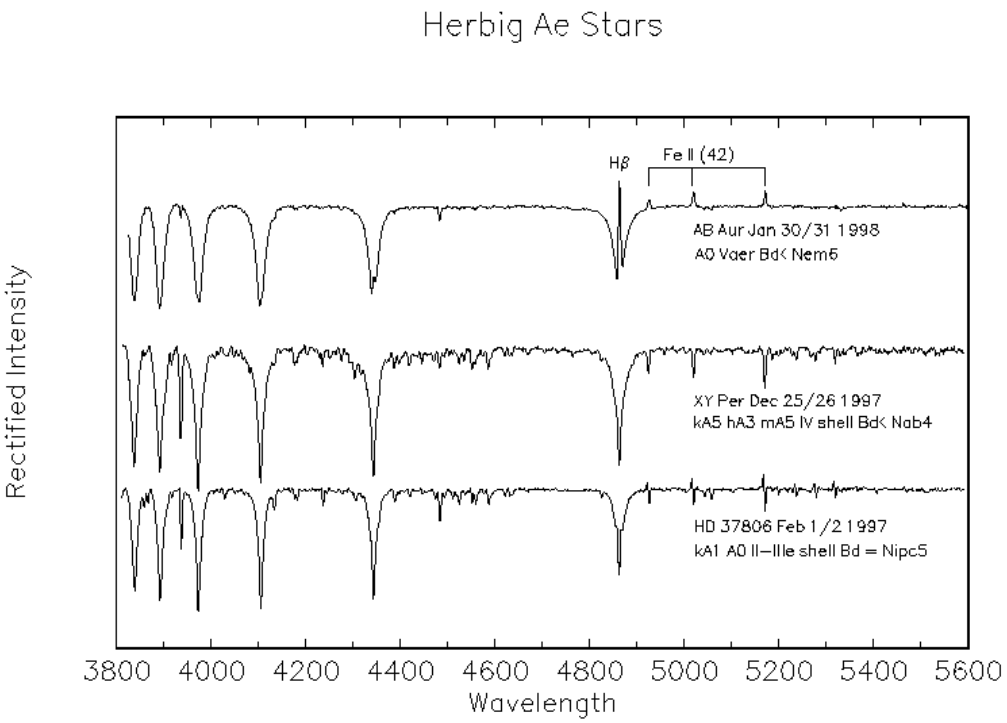

Figure 4.11: The Herbig Ae stars. Figure taken from: `http://ned.ipac.caltech.edu/level5/Gray/frames.html`. [22]

A type stellar spectra may be peculiar in a multitude of ways. Spectra of A type peculiar stars, Ap stars, three of which are shown in the figure 4.12, show abnormal strength of the Si II 4128-32 blend, for which they are called silicon stars, but they may also possess enhancements of abundances of other elements. Silicon stars often generate very powerful magnetic fields. [22]

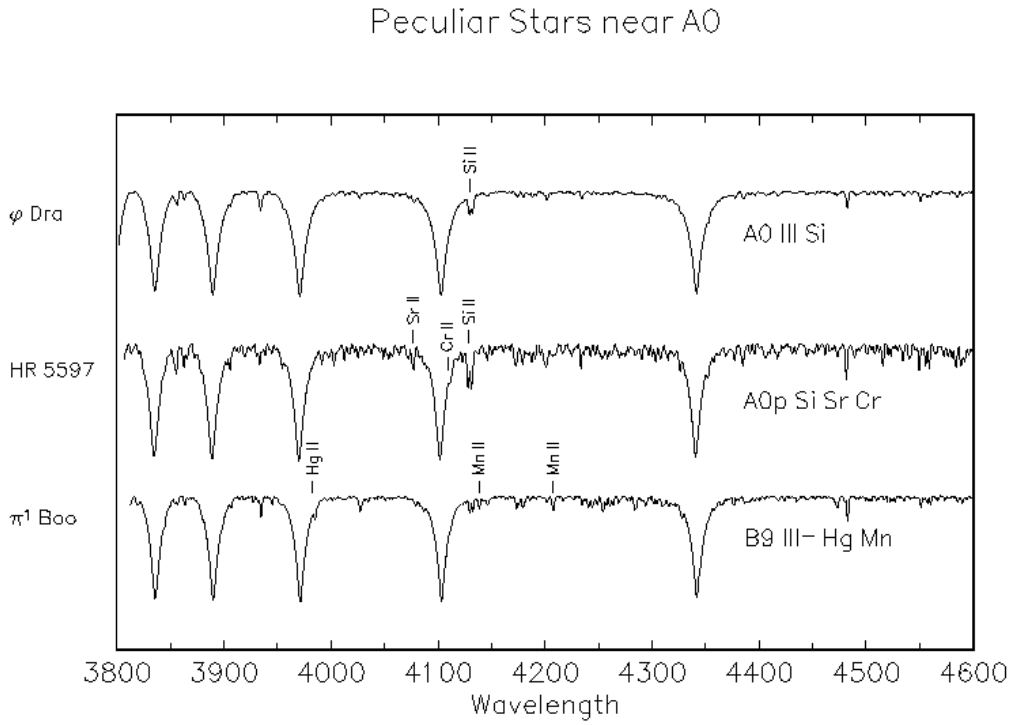

Figure 4.12: The chemically peculiar Ap stars. Figure taken from: `http://ned.ipac.caltech.edu/level5/Gray/frames.html`. [22]

In some of the Ap type spectra the Si II 4128-32 blend may be accompanied by the Sr II 4077 and Cr II 4111 spectral lines. The last Ap spectrum shown in the figure 4.12 belongs to a mercury-manganese star, characteristic by strong lines of Hg II 3984, Mn II 4136 and Mn II 4206. The HgMn Ap stars appear to be quite different to their Si Ap stellar cousins, as they seemingly do not create huge magnetospheres. [22, 25, 26]

A type stellar spectra can also display abnormal spectral lines of metals. These stars are sometimes called "Metallic line A type stars", hence they are designated as Am stars. In the figure 4.13, an Am stellar spectrum is compared to that of a A2 IV standard star. [22]

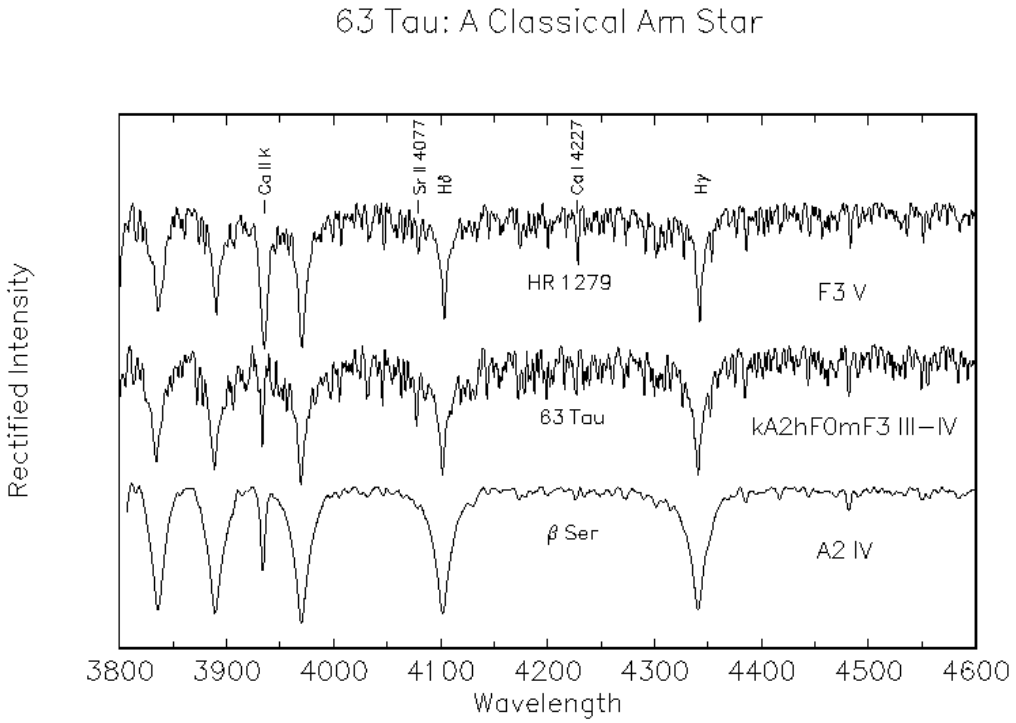

Figure 4.13: A "metallic-line" Am star compared to a A2 IV standard star. Figure taken from: `http://ned.ipac.caltech.edu/level5/Gray/frames.html`. [22]

The Am stars are most often determined by comparing the metallic lines with the Ca II K-line. [22]

4.4 F type stars

F type stars, while at main sequence often termed as yellow-white dwarfs, range in radii from $1.0R_S$ to $1.4R_S$ and effective temperatures from 6 000 K to 7 300 K. Famous examples include Procyon A, the helium fusing supergiant Canopus (second brightest star on our sky) and perhaps the most famous star of all, the F7 bright giant Polaris.

Approaching the cooler type stars along the main sequence, we can notice hydrogen lines weakening, as we reach the threshold between types A and F, and the Ca II K-line and metallic lines strengthening instead. In the spectra of early F type stars, the strength of the quite sharp Ca II K-line is comparable, or slightly lesser to the strength of the Hγ spectral line, but by F5 this relation is reversed and Ca II K-line, being almost saturated,

becomes much stronger than Hγ. The strength of metallic lines (Fe I, Cr I, Mg II) is growing steadily, but the lines still remain relatively weak by reaching the later end of the F type. The molecular G-band, composed of large number of closely spaced CH spectral lines, first appears in the spectra of the F2 type stars, given the resolution is sufficient. [22, 24, 25, 26]

As said before, upon reaching F0, the hydrogen spectral lines are already weakening significantly, which causes them to lose most of their sensitivity to luminosity. Instead, in the proximity of the F0 threshold (fig. 4.14), the luminosity class is determined from the strength of spectral lines of ionized metals, namely Fe II and Ti II. Particularly important luminosity dependent features include the Fe II, Ti II blend at 4172-8 Å, and similar blends at 4395-4400, 4417 and 4444 Å. These would be then compared to the strength to other less luminosity dependent features, such as Ca I 4226, Fe I 4271 and Mg II 4481. [22, 25, 26]

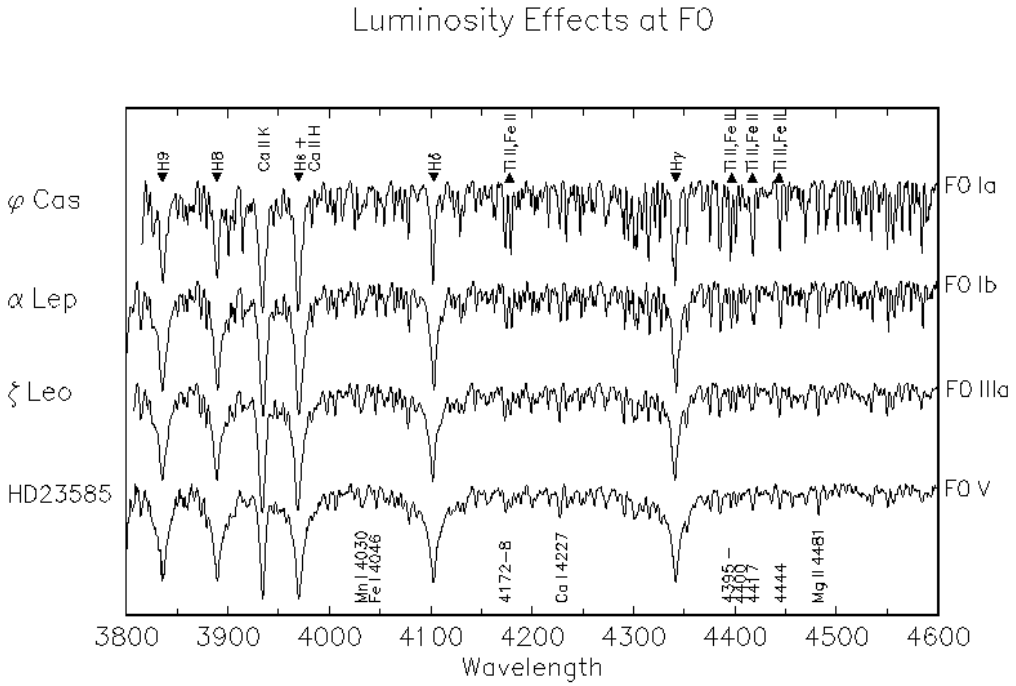

Figure 4.14: The luminosity sequence at F0. Figure taken from: `http://ned.ipac.caltech.edu/level5/Gray/frames.html`. [22]

Another interesting threshold lies at the F5 temperatures (fig. 4.15), where the H lines have lost sensitivity to luminosity almost completely. From this point onward, only spectral lines and blends originating from transitions of ionized elements are reliable for the luminosity classification of the F-type stars.

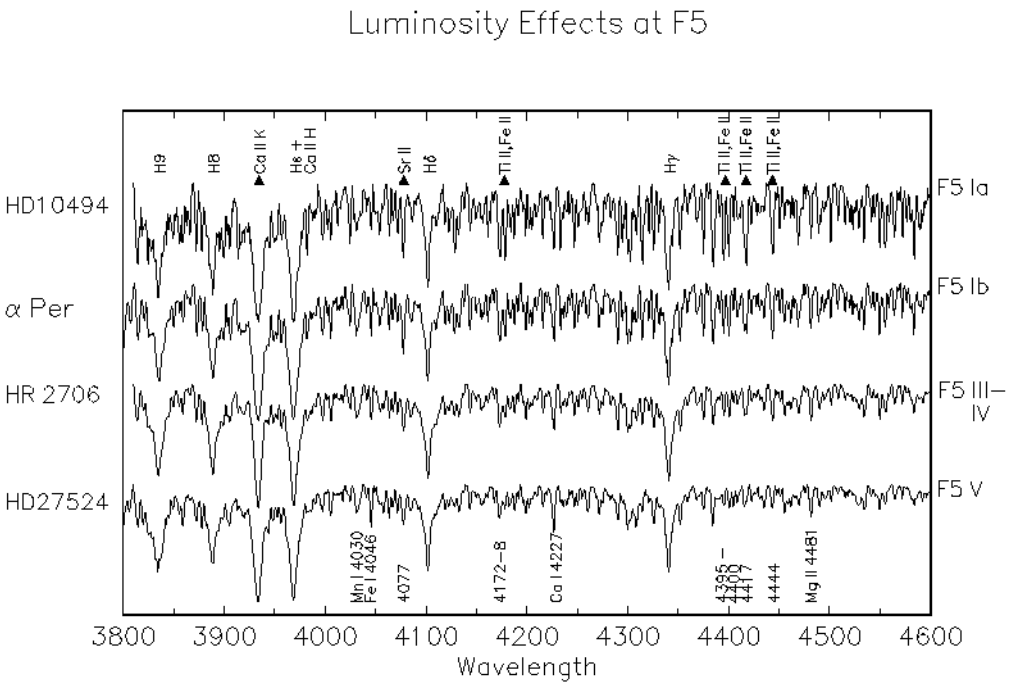

Figure 4.15: The luminosity sequence at F5. Figure taken from: `http://ned.ipac.caltech.edu/level5/Gray/frames.html`. [22]

The luminosity classification criteria based on metallic blends at F0 still hold for the F5 temperatures, except that, given the spectra is of sufficient resolution, Sr II 4077 can be possibly used as a luminosity sensitive feature also. This sensitivity can also be noticed in the broadening of Ca II K-line, that appears slightly broader in the spectra of more luminous stars. [22, 25, 26]

4.5 G type stars

After reaching G0, moving further toward the later types along the main sequence, the hydrogen spectral lines gradually weaken, while the strength of the general metallic-line spectrum continues to increase, as does the strength of the the Ca I 4226 and G-band. These two spectral features continue this trend until reaching the temperature threshold belonging to K-type stars (about K2), and then the G-band starts weakening, while the strength of Ca I 4226 increases greatly by reaching the K5 temperature threshold. [22, 25, 26]

The possibility that the observed star might be metal-weak or metal-rich bares us from using the ratios of Fe I 4046 / Hδ and Fe I 4325 / Hγ, otherwise it could aid us in spectral classification greatly. Instead, in spectra of at least intermediate resolution, we can use the ratio of Cr I 4254 spectral line with the two neighboring Fe I lines at 4250 and 4260. The ratio of the strength of the Cr I spectral line compared to the strengths of the neighboring Fe I lines grows in the spectra of later G and K type stars. [22, 25, 26]

Considering the luminosity criteria at G0 (fig. 4.16), the most important are the strengths of Sr II 4077 and these of metallic blends of Ti II and Fe II, the same used the F-type luminosity criteria. Some of the spectral lines might already not be resolvable in spectra of lower resolution, but particularly the ratio of the two blends Ti II + Fe II 4172-8 and Ti II + Fe II 4444 with Mg II 4481 might yield results usable for luminosity classification. [22, 25, 26]

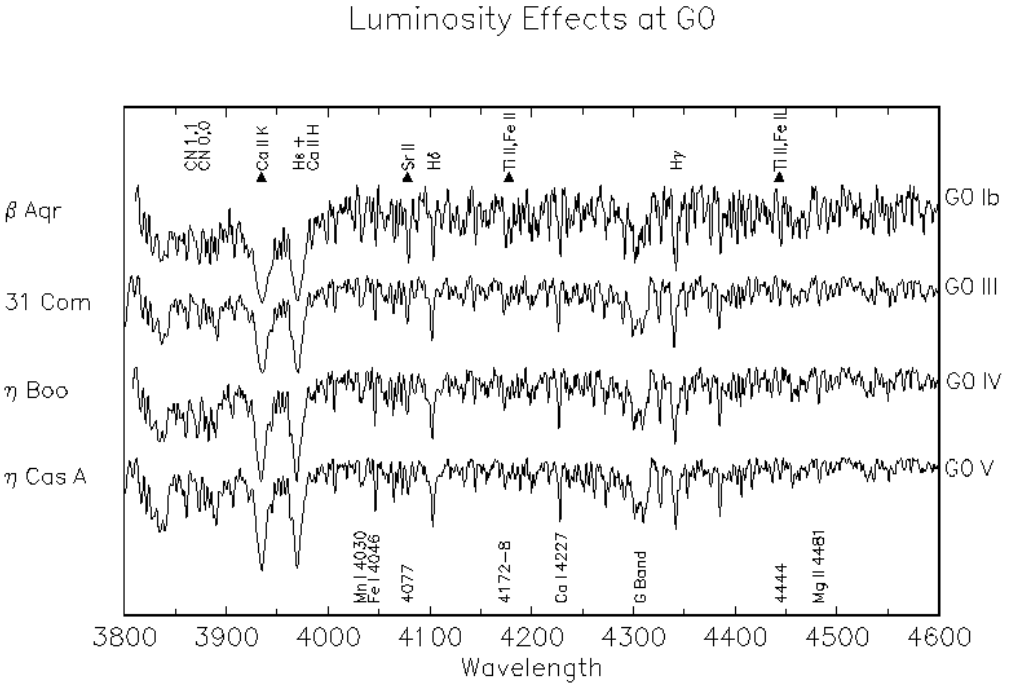

Figure 4.16: The luminosity sequence at G0. Figure taken from: `http://ned.ipac.caltech.edu/level5/Gray/frames.html`. [22]

Another possible criterion at G0 are the cyanogen CN molecular blends at 3883 and 3871, that appear in spectra as a depression of the continuum in area surrounding said wavelengths. These spectral features display an intriguing behavior in stars near to G0. These bands increase in strength as luminosity increases from class V to IV, but then weaken again in the region of luminosity class III, but strengthening again in the spectra of supergiant stars.

For the late G-type stars (fig. 4.17), the ratio of Sr II 4077 to iron lines (Fe I 4046, 4063, 4071) holds as a valid luminosity classification criterion. The CN bands at 4216 Å, present in the spectra of supergiant and giant, also display a significant sensitivity to luminosity, if resolved. Another fine criterion for discerning the luminosity classes can be achieved through the ratio of spectral lines Y II 4376 to Fe I 4383. [22, 25, 26]

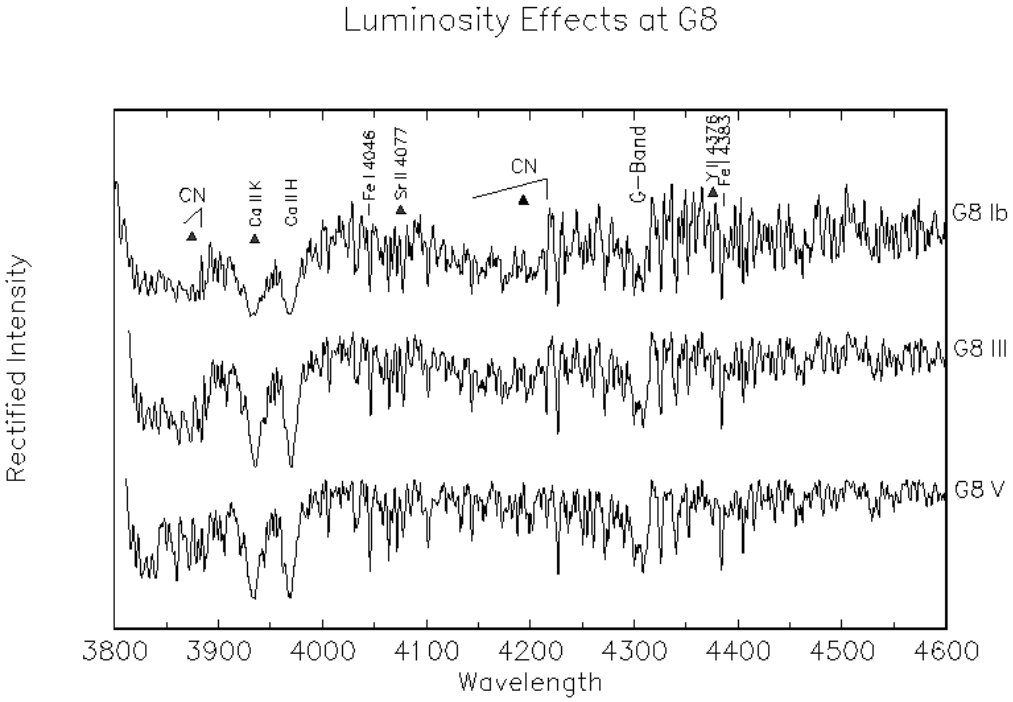

Figure 4.17: The luminosity sequence at G8. Figure taken from: `http://ned.ipac.caltech.edu/level5/Gray/frames.html`. [22]

4.6 K type stars

The K-type stars are a large group of stars, varying in perceived color from orange to orange-red, to which belong some of the most prominent stars on our night sky, for instance the K-type giants Aldebaran, Dubhe, or Kochab. To the K type dwarfs on the other hand belong several of our nearest stars, for example Alpha Centauri B and Epsilon Indi.

In the spectra of K type stars (fig. 4.18) we observe spectral lines of ionized and neutral iron Fe II and Fe I, strong lines of ionized and neutral calcium Ca II and Ca I and also many molecular bands, CN and CO usually being the most prominent in the spectra of K-type giants. Namely, CN 4216 is a molecular band frequently used for luminosity class classification. Considering spectral type classification, in the spectra of K-type dwarfs, a usable criterion lies in the ratio of Ca I 4226 to Fe I 4383, as the ratio grows toward later types. The tooth-like MgH molecular absorption feature appears at 4780 Å,

halfway through the K-type – this molecular band later on becomes a blend with the TiO molecular band. The TiO molecular bands first appear at around at K7, but the TiO 5448 band can just barely be detected here, although its strength increases dramatically in the later types. Across the temperature interval of the K type, the G-band gradually fades from the stellar spectra. Another criterion usable for spectral classification is the forementioned Cr I 4254 spectral line in ratio with the two neighboring Fe I 4250 and Fe I 4260 spectral lines. [22, 25, 26]

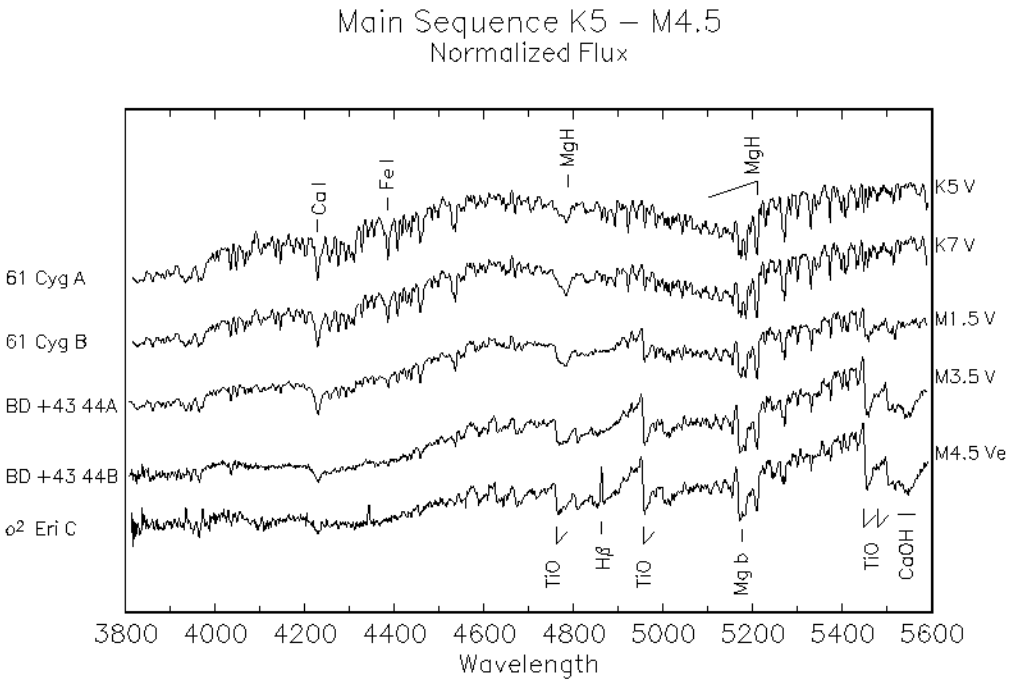

Figure 4.18: The main sequence from K5 to M4.5. Figure taken from: `http://ned.ipac.caltech.edu/level5/Gray/frames.html`. [22]

The threshold between K and M types can be somewhat blurry for giants and supergiants, for the main sequence the main sign of reaching the M type are the sufficiently strong TiO bands.

4.7 M type stars

M-type stars are the latest of spectral types and coolest of stars, usually have quite complex spectra and may vary in luminosity greatly. The brightest of M-type stars can have luminosities reaching ten orders higher than that of the least luminous ones and given their low temperature, immensely different radii. The main sequence M-type stars – red dwarfs typically have both mass and radius about an order lesser than that of a M_S and R_S and

with temperatures ranging from 2 600 K to 3 900 K are too dim to be seen with eyesight only, yet they may be making up to 85 % of all stars. On the other hand, the bright M-type stars, for instance the M2 Iab red supergiant Betelguese, have radii comparable to the distance between the Sun and Jupiter. M-type stars are usually a lot more violent than earlier types, their atmospheres can have various features, including strong flares and spots that may decrease the stars luminosity by up to 40 %. Red dwarfs are famous for their long lifetimes on the main sequence, hypothetically reaching up to ten trillion years, although they do not stay constant during this period, as they have a complex evolution even before leaving the main sequence. What is also noteworthy, is the fact that all observed red dwarfs contain spectral lines of metals – implying all of them are metal rich stars of population I. This is reflected in the accepted theory that low mass stars like red dwarfs could not form in the metal poor population II. M-type giants and supergiants, even though 1010 times brighter than red dwarfs, can have very low surface temperatures and are often variable stars, for instance the Mira stars. Mira stars are an important group of K-type and M-type (most often M1-M6) pulsating variable stars located on asymptotic giant branch, that represent stars in the very last stages of their stellar evolution. Their periods are hundreds of days (characteristic period approx. 300 days) and the rate of pulsation is greater for hotter and smaller stars, while cooler and larger stars have a greater period of pulsation. [22, 25, 26]

Spectra of M-type stars are rather complex, as they contain many spectral lines of not only atomic origin, but also a number of molecular spectral lines, bands and blends. For some, the number of spectral lines may reach thousands. Generally, the spectra of M-type dwarfs show metallic spectral lines, absorption lines of TiO and VO and also a blend of H_2O molecular spectral lines. The infrared region also shows absorption that is due to the blend of CO molecular spectral lines. [22, 25, 26]

As of reaching the temperature threshold of M0, TiO molecular bands are visible in the spectrum, and strengthen toward later types, gradually overpowering the atomic spectral lines of metals (Fe, Ti), that are strongest in the spectra of early M-type stars (fig. 4.19). At M4.5 the TiO bands are usually one of the dominant spectral features. As these TiO bands intensify, the MgH + TiO feature at 4780 that first appeared in the spectra of K-type dwarfs, becomes increasingly flat-bottomed. The shape of this MgH + TiO blend is one of the criteria for luminosity classification – for dwarf stars the tooth-like MgH dominates the flat-looking TiO in the blend. At around M2, another criterion for luminosity classification should be sought in the variations of the Ca I 4226 spectral line – for giants, it continues to grow in strengths even past the threshold of M5 (fig. 4.20). [22, 25, 26]

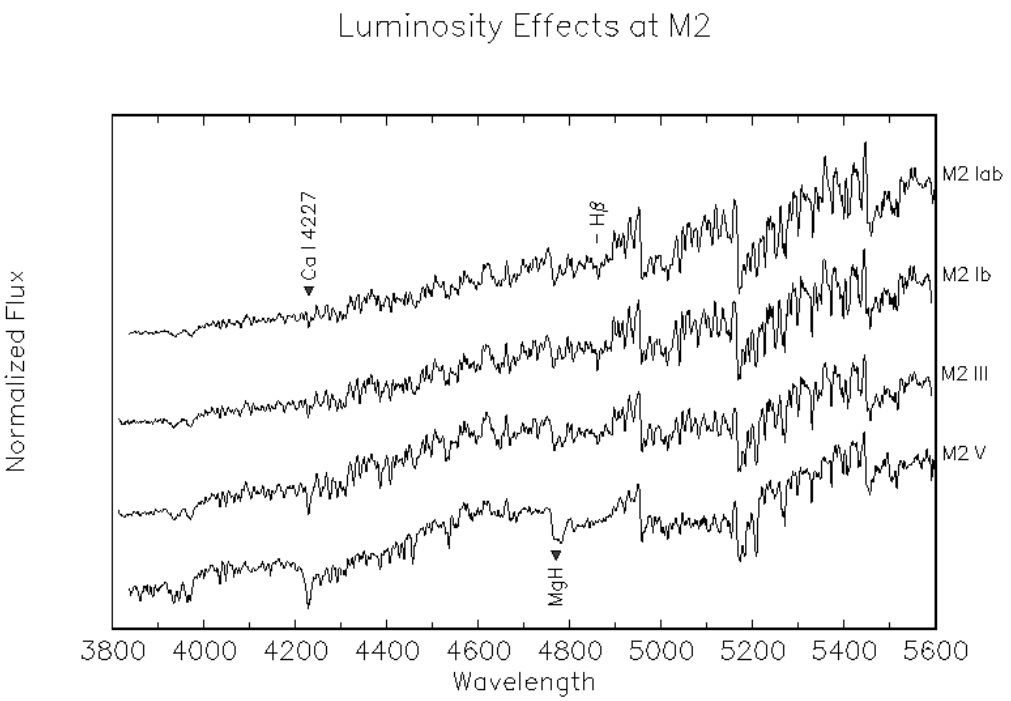

Figure 4.19: The luminosity sequence at M2. Figure taken from: `http://ned.ipac.caltech.edu/level5/Gray/frames.html`. [22]

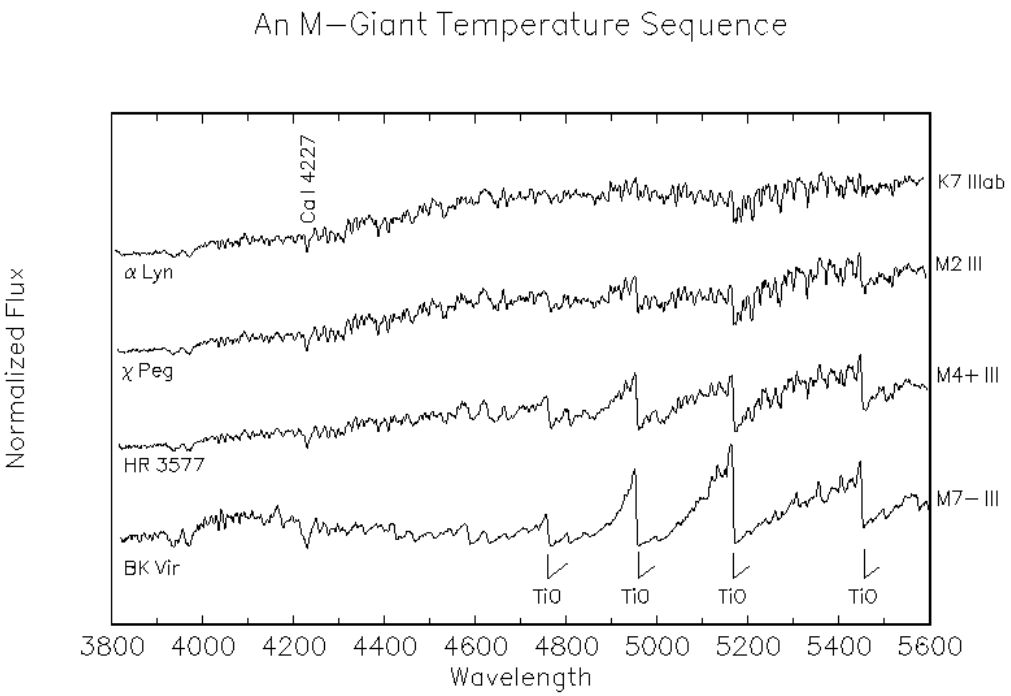

Figure 4.20: The temperature sequence of M type giants. Figure taken from: `http://ned.ipac.caltech.edu/level5/Gray/frames.html`. [22]

The TiO bands also play a major role in temperature classification of M-type giants. Again going from the earlier to the later types, the strength of TiO bands increases, the strongest of TiO bands becoming saturated after passing the M3 threshold. Spectral features of some of the stars, particularly variable Mira stars, may be faded due to abundance or population effects, which of course implies lower eq. width values of measured spectral lines, but this shouldn't impede the classification itself, if we use the eq. widths in correct criterion ratios (meaning, as long both lines in question are equally faded).

Surprising to some might be the presence of Hβ emission spectral line in many of the M-type spectra. These originate in active chromospheres that many M-type dwarf stars possess. These stars – flare stars, exhibit strong flares many times more powerful than solar flares. One of the manifestations of these energetic events is the emission in the hydrogen lines.

The Mira variable stars are a special case even concerning their spectra. The cycle of pulsations of these giant M and K type stars affects their spectra greatly and significant changes can even appear in their spectra during each cycle. Their spectra are characterized by the presence of emission lines (fig. 4.21), most often in the spectral lines of hydrogen, which originate from shock waves in their pulsating atmospheres. These emission lines do strengthen for the greater luminosity classes, but this effect isn't a very reliable luminosity classification predictor. Some Mira stars may also show emissions in the lines

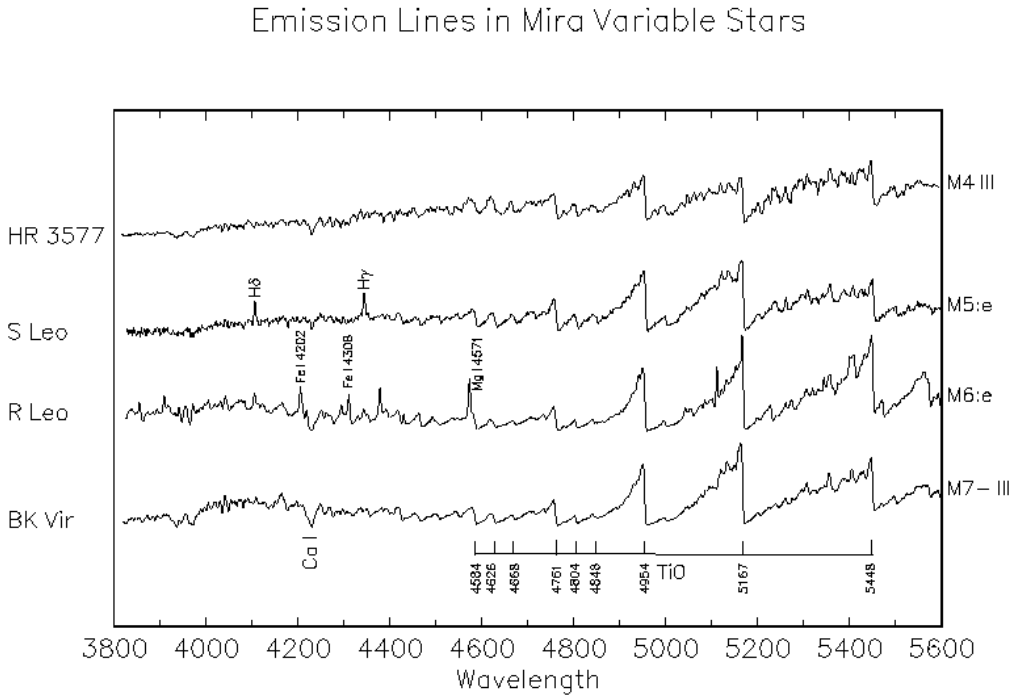

Figure 4.21: The temperature sequence of Mira variable stars. Figure taken from: `http://ned.ipac.caltech.edu/level5/Gray/frames.html`. [22]

of Fe I 4202, Fe I 4308 and Mg I 4571, which seem to appear in the absence of hydrogen emissions. [22]

Certain phases of the Mira star pulsation cycle may show the quite unusual molecular bands of AlO. As it was already mentioned, spectral features, most notably the molecular TiO bands, of Mira stars may appear faded and the general profile of spectral lines is broader and less pronounced. This is generally attributed to presence of high-level atmospheric clouds that veil and affect the spectrum in such way.

Chapter 5

SpecOp 2 application

5.1 On the aim of the application

The SpecOp 2 application has been developed, for the purposes of this thesis, but also with the aim to bring greater accessibility to stellar classification for both professional astrophysicists and astronomers and amateurs and also make it significantly less time consuming, while offering the convenience and user friendly graphical interface (fig. 5.1) the Microsoft Windows NT users are used to. It is a continuation of my previous work – I started the project as a side-product of my bachelor thesis on classification of hot stars, yet it grew somewhat to be the centerpiece of my work. It went through great changes and many features were added over the time. While the task of making the classification process fully automatized is rather complicated, going through the procedure in a semi-automatic, sequenced approach, with funded supervision of each step proved to be the more realistic solution, while also maintaining as much of the capabilities with my limited resources. Thus the semi-automatic approach was chosen and work began on turning the software into an expert oriented spectroscopic suite. Expansions of the code include improved user interface, stellar parameter estimation, batch processing and HR plotting capabilities, but also integrating in a build of the expert application MKClass, written by R. O. Gray *et al.* [31] MKClass is the application I deem to be the most successful attempt at fully automatizing spectral classification. It however still requires an expert user, and unfortunately does not have a build dedicated to the Win systems and so I hope to have provided the small service of modifying the source code to fit the operating system and creating GUI to control in through SpecOp for users that prefer the casualty of Windows. Users can of course also use the built executables with Windows shell, without using SpecOp. Another of my aims was making a software capable of generating equivalent width enhanced HR diagrams directly from a given spectral library, granting enhanced awareness of studied collection of spectra.

5.2 On the current release SpecOp 2.0b

The development cycle of the SpecOp software has progressed to the version of 2.0b, reaching the phase of closed beta test, boasting a range of capabilities that will be described here, including ability to measure equivalent widths of a refined collection of a hundred spectral lines spanning the region 3 800 – 8 400 Å.

The SpecOp 2 software carries these stellar spectra libraries:

- A Stellar Spectral Flux Library: 1150-25000 Å, A. J. Pickles, 1998 [32] – 131 spectra of O5-M5 type stars of luminosity classes I-V, 1 150 – 25 000 Å, resolution = 5 Å
- A library of stellar spectra, George H. Jacoby, Deidre A. Hunter and Carol A. Christian, 1984 [33] – 161 spectra of O5-M5 type stars of luminosity classes I, III and V, 3 510 – 7 427 Å, resolution = 4.5 Å
- An Atlas of Southern MK Standards From 5800 to 10200 Å, Anthony C. Danks and Michel Dennefeld [34] – 126 spectra of O5-M7 stars of luminosity classes I, III and V, 5 800 – 10 200 Å, resolution = 4.3 Å

Furthermore included is a selection of the POLLUX synthetic spectra [35], that's distributed as a separate addon due to their considerable size. Users can additionally load desired custom data in `.txt`, `.dat`, `.ascii`, or `.tsv` format files, minimalizing the needed reformatting of the imported libraries, that can be stored in `flux.dat` files, tab separated values, or simply in (wavelength, spectral flux) columns.

SpecOp's current capabilities include loading, viewing, evaluating and plotting stellar spectra, all in the single frame standardized user environment (fig. 5.1). SpecOp 2 is capable of estimating continuum of loaded spectra using smoothing, handled by the iterative peak striping method and its variations and normalize the data according to the estimated continuum. Users are free to choose a set of smoothing parameters, accommodating various aspects of different spectra. One of the core features is the determination of equivalent widths. The studied spectrum is scanned for variations and matched against a refined set of criterion spectral lines and features of interest. The detected spectral lines are then measured with the use of block integration. Depending on user's choice, After evaluating the ratios of found values, output tables of equivalent widths measured for each applicable spectral line as well as the ratios themselves are stored in a `.txt` file in ascii format.

5.3 SpecOp 2.0b features and capabilities

The UI of the SpecOp 2 software has been greatly expanded to accommodate for a number of new features. The controls of all toolsets have been categorized into separated tabs, that are easy to control and allow flexibility and ease of access, while also avoiding overwhelming the user with too many preferences. The illustration bellow (fig. 5.1) shows the general overview of the application.

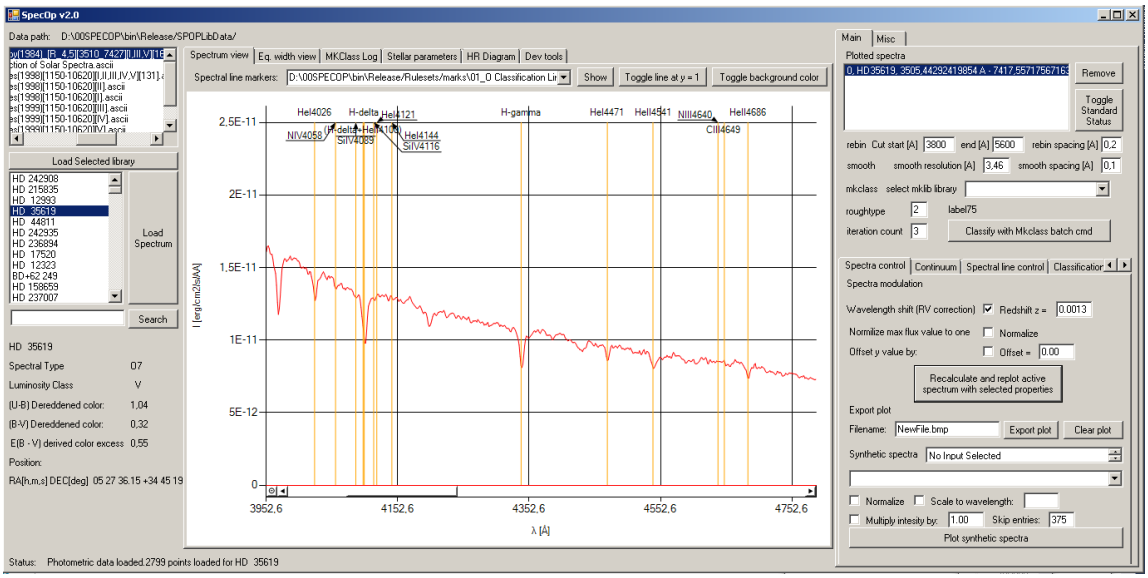

Figure 5.1: User interface of the SpecOp 2 software.

The first of the user control menus is the menu maintaining loading of libraries of stellar spectra and their contents, accompanied by some of the details pertaining to the star, contained in the library header file. Upon loading a spectrum, it is immediately plotted in the Spectrum view (fig. 5.2) window and assigned a layer in the plotted spectra list on the right. The Spectrum plot view window is interactive, as the user can zoom in and out to desired position on the plot with the left mouse button and reset the view with the right mouse button and also display the plot with altered visuals for higher contrast. To display sets of spectral lines, the user can use the controls above the spectrum plot in the Spectrum view, or in the separated control tab for spectral lines.

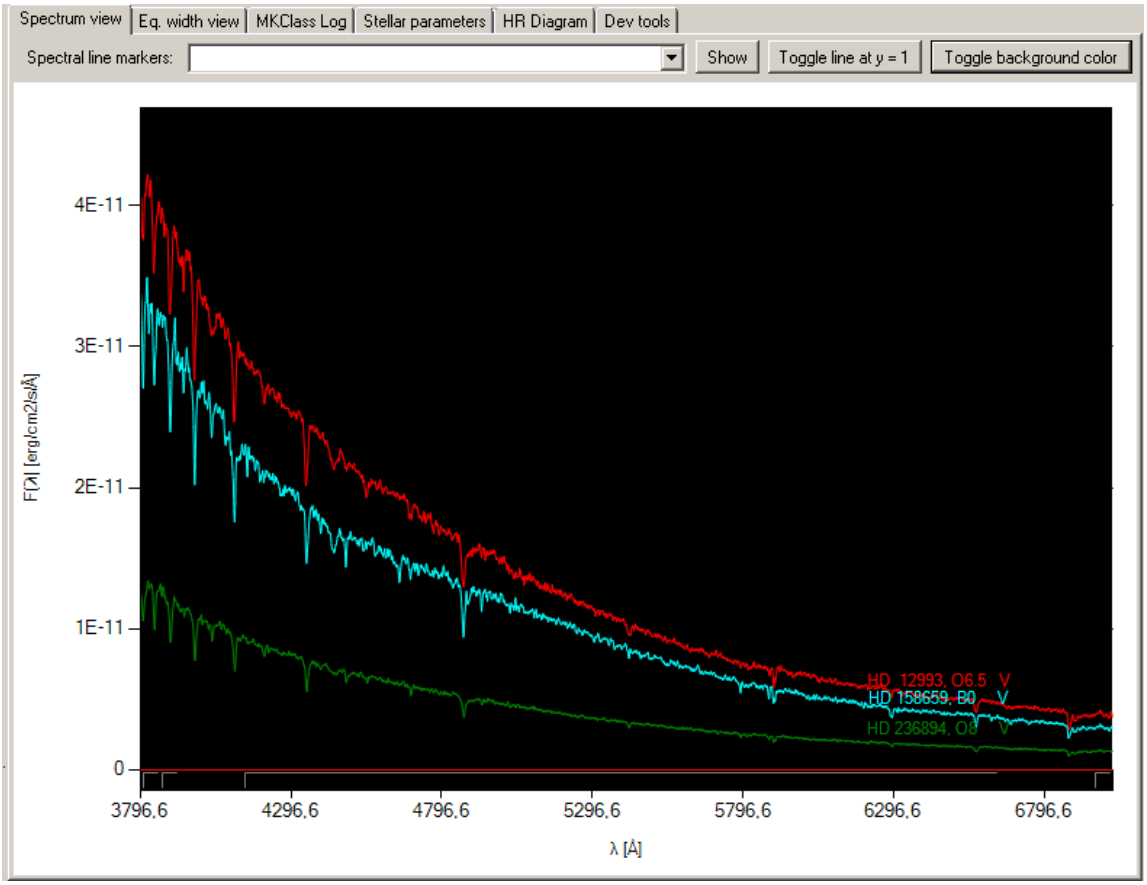

Figure 5.2: Spectrum view UI of the SpecOp 2 software.

Loaded spectra can be modulated in the Spectra control tab, which allows for a couple of basic operations like scaling options and recalculating the spectrum for a set value of radial velocity. Following the Spectra control tab is the Continuum tab, that handles the parameters of continuum smoothing and continuum normalization, the Spectral line control tab and finally, the Classification control tab. After normalizing a spectrum to its continuum, here the user can select which set of classification criteria ratios is going to be calculated. There is also an option to only calculate equivalent widths of loaded lines, which can be useful when processing a large collection of spectra. The equivalent width values can be output to a file, but they also display in the Equivalent width view window.

The window Stellar parameters (fig. 5.3) contains a sizeable table, making up a grid of spectral types and luminosity classes and their parameters. It is designed to aid in calculating stellar parameters so that the star can be plotted onto HR diagram. This tab also hosts the controls for batch processing all stars of the selected library.

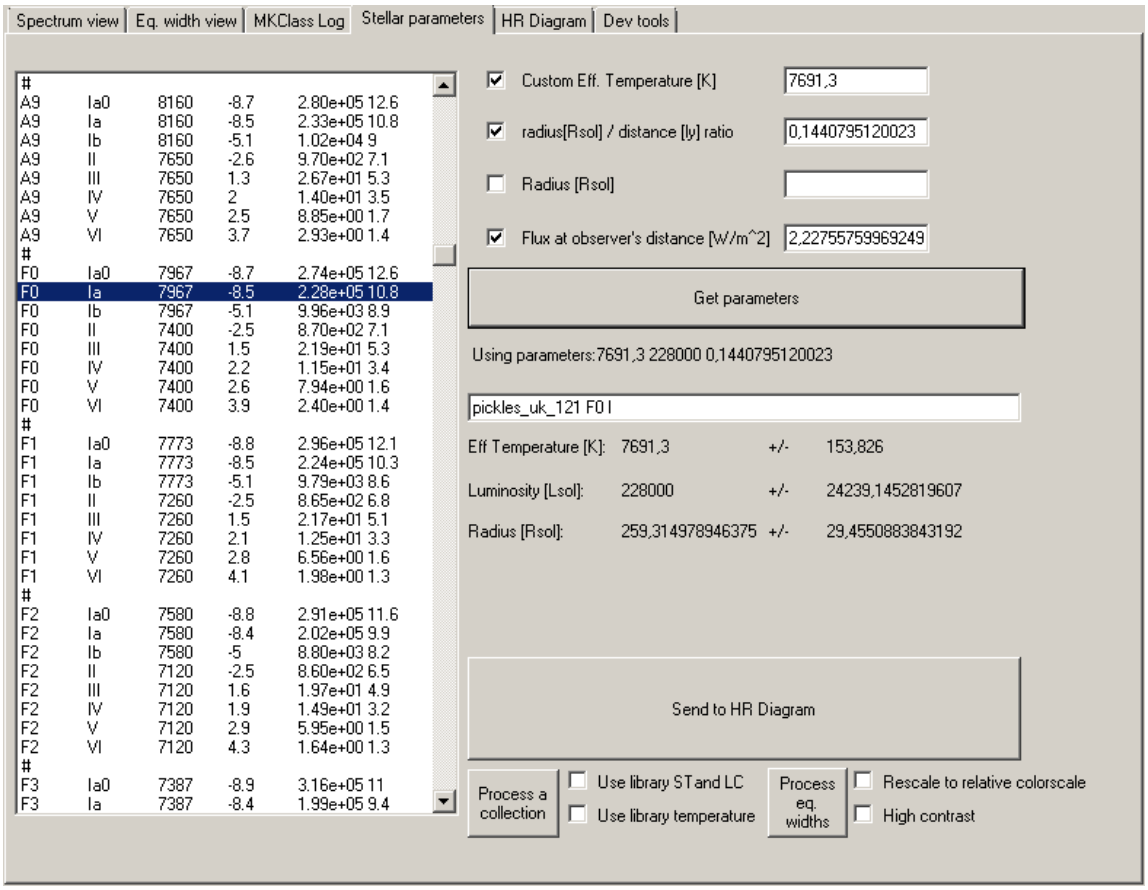

Figure 5.3: The window Stellar parameters of the SpecOp 2 software.

After clicking the "Send to HR Diagram" button, a point is created in the Herztsprung-Russel diagram in the following window, along with error bars denoting statistical uncertainty of the luminosity values. Either going through the full collection of stars in library, or, more comfortably, batching through the library will then project contained stars onto the diagram, as shown in the fig. 5.4. This particular HR diagram shows main sequence standards of the Pickles library.

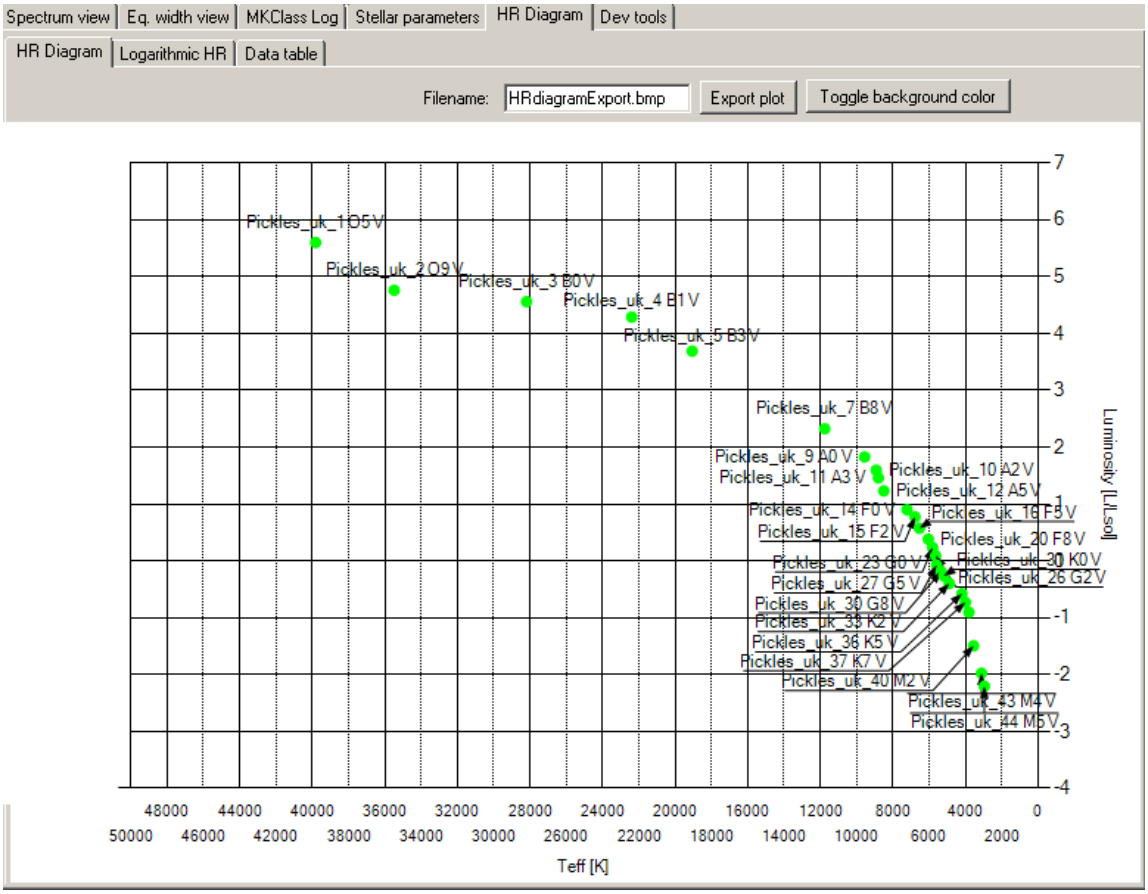

Figure 5.4: The HR diagram constructed from Pickles main sequence stars of the SpecOp 2 software.

In that case, the HR diagram was quite basic, but SpecOp 2 can also plot its more advanced forms, for example when also displaying measured equivalent widths (fig. 5.5), although this capability is still being developed.

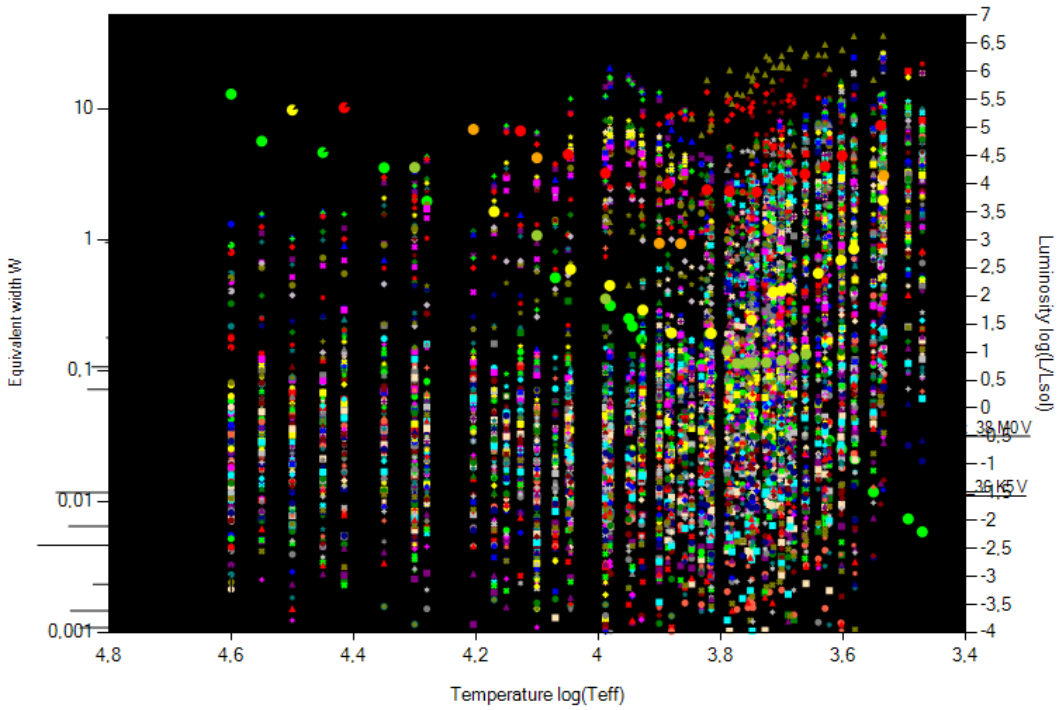

Figure 5.5: Figure 5.2: The HR diagram constructed from the whole Pickles library with displayed measured equivalent widths.

Equivalent widths in this diagram use a high contrast coloring, in order to help the user visually separate the progression of lines, but options to use true coloring, derived from the wavelength values, or to rescale the measured interval of wavelengths to the visible region are also included.

The window MKClass is dedicated to the outputs of the MKClass scripts, that are controllable from the main window on the right. Communication between SpecOp and the MKClass software is maintained by custom built scripts and temporary spectrum files that are stored in the folder `/mkclass`. The usage of MKClass requires inputting correct parameters for the handling of the spectra, which is assisted by the SpecOp automated routines. A result from a classification routine, or rather the last page of the output, done by MKClass as viewed in the SpecOp interface is seen in the fig. 5.6. This particular routine succeeded in classifying an M2 V star.

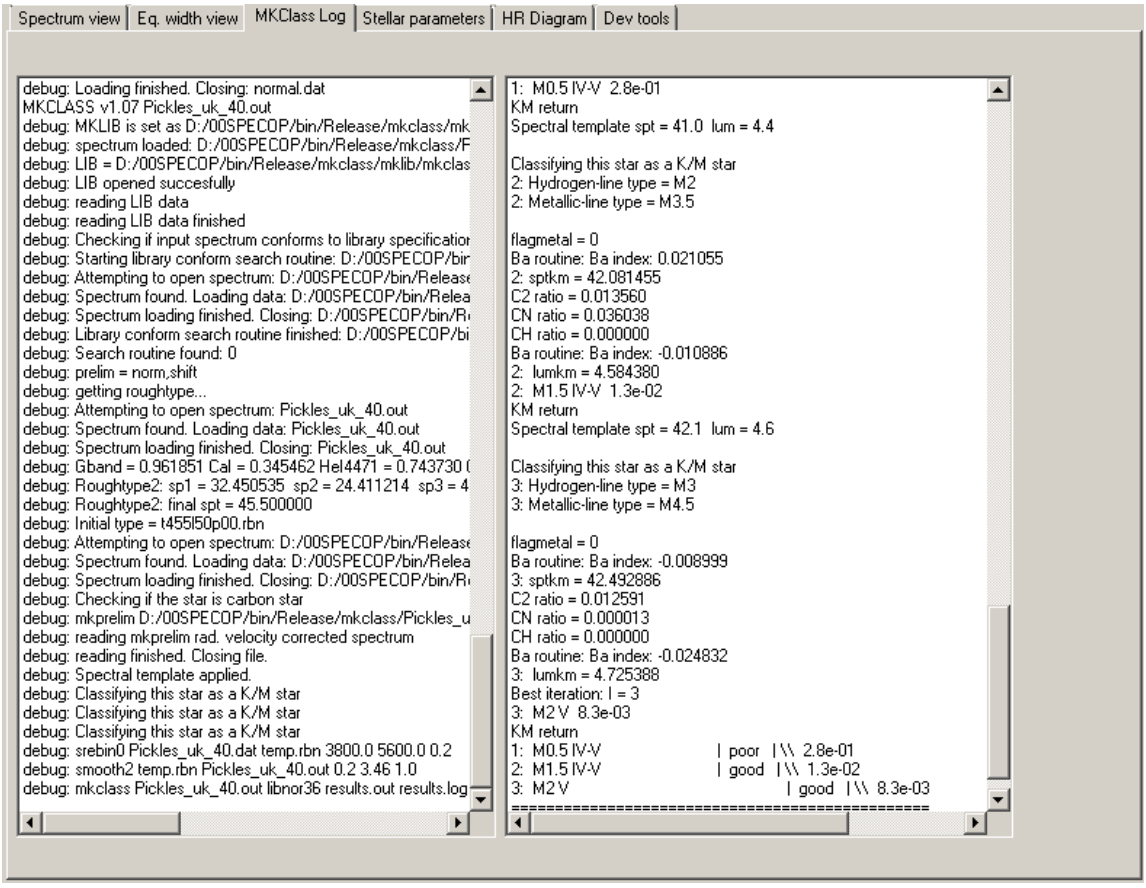

Figure 5.6: The MKClass output example.

5.4 Continuum smoothing

Continuum estimation is most likely the step bringing the main part of uncertainty when measuring equivalent widths. It is the process of attempting to approximate the continuum of a star as it would look if all the spectral lines were absent, most often involving certain kind of iterative smoothing. The smoothing function of the SpecOp software uses the so called peak stripping method and its various modifications. To estimate the continuum of a spectrum, the smoothing function iterates over the values of wavelength and compares the values of flux at given wavelength with the mean flux value of the area, with the area interval being set by a parameter. For instance, the most simple version of the peak stripping method only uses the mean value of the two neighboring values $m_i = (y_{i-1} + y_{i+1}) / 2$ and then takes the greater of m_i and y_i. In this way, the spectrum is iterated through many times, for this specific use of this method, 300 to 1 000 cycles are made to gain an estimate of the continuum, depending on spacing of the values of the studied spectrum. [36] The illustration 5.7 shows the continuum estimates after (a) 300, (b) 500, (c) 800 iterations.

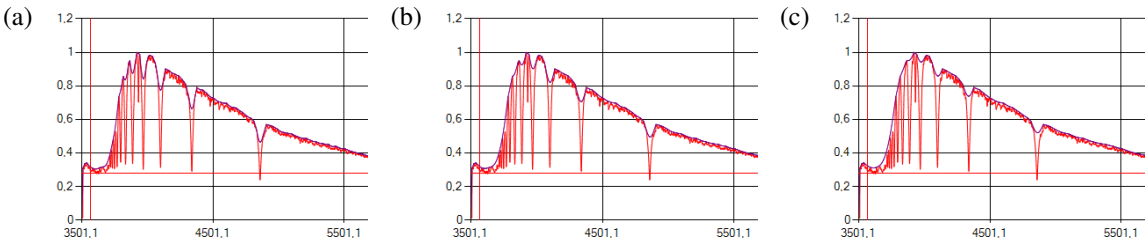

Figure 5.7: The use of the standard peak striping method after (a) 300, (b) 500 and (c) 800 iterations.

The standard version of the peak stripping method works well on spectra containing mostly absorption spectral lines, but its estimate may fade out any present emission spectral lines. Modifications of this method exist, that can be used to gain better estimates of continua of spectra containing both absorption and emission spectral lines, but the quality of the fit varies depending on the resolution of the spectra and parameters used. If the star is suspected of containing emission spectral lines in its spectra, that are essential to its classification, it would be reasonable to consider using such modification of the peak stripping method in addition to the standard one. One such use is illustrated in the fig. 5.8. In this case the smoothing area is 2, and the smoothing function modifications include sensitivity and offsetting. The sensitivity parameter acts as a threshold, limiting the replacement of y_i with m_i, unless the "pull" of the local average is too strong, and offset, which adds to values of y_i, if the sensitivity check passes. Estimations of continua using either of these smoothing methods won't always yield globally reliable continua, their correct usage

usually implies choice of a specific region at which the final smoothened spectrum represents the continuum accurately. [1]

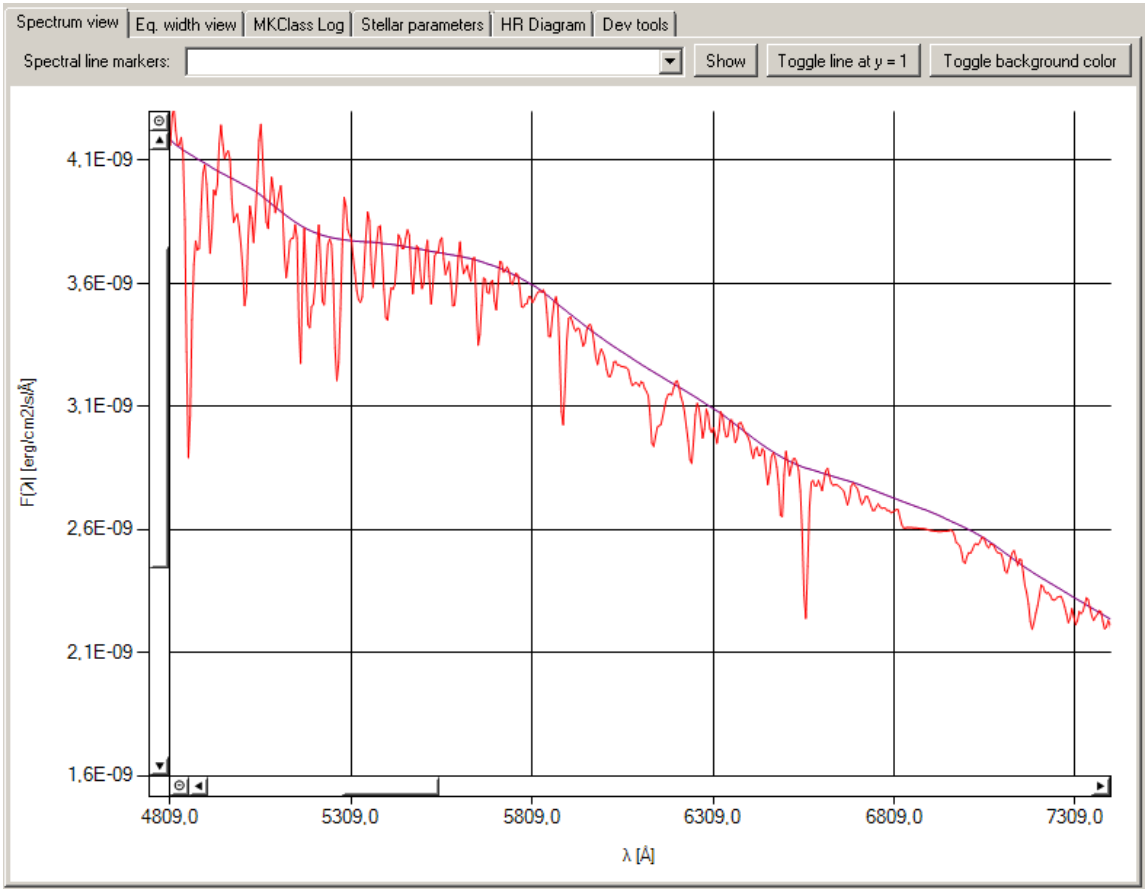

Figure 5.8: The use of the advanced peak striping method with parameters: smoothing area = 2, sensitivity = 8e-5, offset = 2.2e-4, 150 cycles.

5.5 Future of the application

The SpecOp 2 software has evolved from a minimalistic tool to a robust spectroscopic suite and the underlying classification system growing with it. It was this system that is more or less setting the course of the development, which is a trend that will possibly continue in the future. Possible expansions might focus on expanding to C type, S type, Wolf-Rayet stars and degenerate stars but also to different spectral regions.

Results

Used spectra

Spectra used in this thesis are from the ESO 2007 [37] republishing of A Stellar Spectral Flux Library: 1 150 – 25000 Å, Pickles A. J., 1998 [32] of resolution 5 Å.

Refined system of spectral lines

The new list of spectral classification criterion lines was refined once again. In order to make classification as precise as possible, the wavelengths of associated spectral lines were researched and corrected to a precision of .1 Å using tables of atomic spectra [38, 39].

Spectral lines used for each spectral type are listed with their associated wavelengths in the table I.

Table I: Table of spectral lines measured for each type. [38, 39, 40, 41]

O		B		A		F		G		K		M	
spectral line	λ [Å]	spectral line	λ [Å]	spectral line	λ [Å]	spectral line	λ [Å]	spectral line	λ [Å]	spectral line	λ [Å]	spectral line	λ [Å]
Hγ	4340.46	Hα	6562.76	Hα	6562.76	Hα	6562.76	Hα	6562.76	Hα	6562.76	Ca I 4226	4226.73
Hδ + He II 4100	4100.00	Hβ	4861.31	Hβ	4861.31	Hβ	4861.31	Hβ	4861.31	Hβ	4861.31	Ca II triplet 8498+8542+8662	8567.42
He I 4026	4026.19	Hγ	4340.46	Hγ	4340.46	Hγ	4340.46	Hγ	4340.46	Hγ	4340.46	Cr I 4254	4254.33
He I 4121	4120.82	Hδ	4101.74	Hδ	4101.74	Hδ	4101.74	Hδ	4101.74	Hδ	4101.74	Cr I 4274	4274.81
He I 4144	4143.76	He I 4009	4009.27	Ca I 4226	4226.73	Ca I 4226	4226.73	Ca I 4226	4226.73	Ca I 4226	4226.73	Cr I 4290	4289.73
He I 4471	4471.68	He I 4026	4026.19	Fe I 4045	4045.81	Ca II H-line	3968.47	Ca II H-line	3968.47	Cr I 4254	4254.33	Fe I 4045	4045.81
He II 4541	4541.00	He I 4121	4120.82	Fe I 4271	4271.76	Ca II K-line	3933.66	Ca II K-line	3933.66	Cr I 4274	4274.81	Fe I 4063	4063.59
He II 4686	4686.60	He I 4144	4143.76	Fe I 4485	4485.68	Fe I 4045	4045.81	Cr I 4254	4254.33	Fe I 4005	4005.24	Fe I 4250	4250.79
C III 4649	4649.57	He I 4387	4387.93	Fe II 4173	4173.47	Fe I 4063	4063.59	Cr I 4274	4274.81	Fe I 4045	4045.81	Fe I 4383	4383.55
N IV 4058	4058.0	He I 4471	4471.68	Fe II 4351	4351.76	Fe I 4071	4071.74	Fe I 4045	4045.81	Fe I 4063	4063.59	K I 7699	7698.97
N III 4640	4640.00	Mg II + Mg II 4481	4481.23	Fe I + Fe II 4383-5	4384.47	Fe I 4271	4271.76	Fe I 4063	4063.59	Fe I 4071	4071.74	Na I 8183	8183.26
Si IV 4089	4088.85	N II 3995	3995.00	Fe II + Ti II 4417	4417.27	Fe II + Ti II 4172-8	4175.00	Fe I 4071	4071.74	Fe I 4143	4143.87	Na I 8195	8194.81
Si IV 4116	4116.10	O II 4348	4348.00	Mg II + Mg II 4481	4481.23	Fe II + Ti II 4395-4400	4397.50	Fe I 4143	4143.87	Fe I 4250	4250.79	Sr II 4077	4077.71
		O II 4416	4416.97	Mn I + Mn I 4030-4	4032.63	Fe II + Ti II 4417	4417.27	Fe I 4250	4250.79	Fe I 4260	4260.48	Sr II + Fe I 4216	4215.85
		O II + O II 4070-6	4071.75	O I triplet 7771-5	7773.83	Fe II + Ti II 4444	4443.80	Fe I 4260	4260.48	Fe I 4271	4271.76	Y II + Fe I 4376	4375.43
		Si IV 4089	4088.85	Sr II 4215	4215.52	Mg II + Mg II 4481	4481.23	Fe I 4271	4271.76	Fe I 4325	4325.76	MgH band	5130.00
		Si IV 4116	4116.10	Ti I 4300	4300.55	Mn I + Mn I 4030-4	4032.63	Fe I 4325	4325.76	Fe I 4383	4383.55	MgH + TiO band	4770.00
		Si III 4552	4552.62			O I triplet 7771-5	7773.83	Fe I 4383	4383.55	Fe I 4405	4404.75	CaH band 6346	6346.00
		Si II + Si II4128-32	4129.48			Si II + Si II 4128-32	4129.48	Fe II + Ti II 4172-8	4175.00	Mg I triplet 5167-83	5174.54	CaH band 6382	6382.00
						Sr II 4077	4077.71	Fe II + Ti II 4444	4443.80	Sr II 4077	4077.71	CaH band 6750	6750.00
						G-band	4307.74	Mg II + Mg II 4481	4481.23	Ti I 3999	3998.64	TiO band 4422	4422.00
								Mg I triplet 5167-83	5174.54	Ti II 4400	4399.77	TiO band 4584	4584.00
								Sr II 4077	4077.71	CN 0,0 band	3883.40	TiO band 4626	4626.00
								Sr II + Fe I 4216	4215.85	CN 1,1 band	3871.00	TiO band 4761	4761.00
								Y II + Fe I 4376	4375.43	CN 4216	4216.00	TiO band 4954	4954.00
								CN 0,0 band	3883.40	MgH band	5130.00	TiO band 5448	5448.00

Table I: (Continued) Table of spectral lines measured for each type [38, 39, 40, 41].

O		B		A		F		G		K		M	
spectral line	λ [Å]	spectral line	λ [Å]	spectral line	λ [Å]	spectral line	λ [Å]	spectral line	λ [Å]	spectral line	λ [Å]	spectral line	λ [Å]
								CN 1,1 band	3871.00	TiO band 4422	4422.00	TiO band 5759	5759.00
								CN 4216	4216.00	TiO band 4584	4584.00	TiO band 5810	5810.00
										TiO band 4626	4626.00	TiO band 6322	6322.00
										TiO band 4761	4761.00	TiO band 6569	6569.00
										TiO band 4954	4954.00	TiO band 6651	6651.00
										TiO band 7045	7045.00	TiO band 7045	7045.00
										TiO band 7053	7053.00	TiO band 7053	7053.00
										TiO band 7088	7088.00	TiO band 7088	7088.00
										TiO band 7126	7126.00	TiO band 7126	7126.00
										TiO band 7589	7589.00	TiO band 7589	7589.00
										TiO band 8432	8432.00	TiO band 7666	7666.00
												TiO band 8206	8206.00
												TiO band 8432	8432.00
												VO band 5737	5737.00
												VO band 7334	7334.00
												VO band 7373	7373.00
												VO band 7851	7851.00
												VO band 7865	7865.00
												VO band 7865	7896.00

Compiled classification criteria

Of the researched spectral and luminosity classification criteria in the 3 800 – 8 400 Å region, the accepted and used ones are listed in the tables II, III, IV and V.

Table II: Compiled criteria used for spectral and luminosity classification of O and B subtypes. [22, 23, 24, 25, 26, 28, 29, 30, 42, 43, 44, 45]

	O		B	
	Spectral	Luminosity	Spectral	Luminosity
Main criteria	He I / He II He I / H N IV / N III	C III / He II Si IV / He I	SI IV / Si III Si III / Si II Mg II, Si II / He I H / He I	He I / O II Mg II / He I N II / He I, H Si IV, Si III / He I profiles of Balmer lines
0		C III 4649 blend / He I 4686	Si IV 4089 / Si III 4552 Si III4552 / Si II4128-32	Hγ / O II 4348 He I 4026 / O II 4070-6 He I 4387 / O II 4416 Mg II + Mg II 4481 / He I 4471 N II 3995 / Hγ, Hδ, He I 4009 Si IV 4089 / He I 4026 Si IV 4116 / He I 4121 Si III 4552 / He I 4387
1		C III 4649 blend / He I 4686	Si IV 4089 / Si III 4552 Si III4552 / Si II4128-32	Hγ / O II 4348 He I 4026 / O II 4070-6 He I 4387 / O II 4416 Mg II + Mg II 4481 / He I 4471 N II 3995 / Hγ, Hδ, He I 4009 Si IV 4089 / He I 4026 Si IV 4116 / He I 4121 Si III 4552 / He I 4387
2	He I 4471 / He II 4541 He I 4471 /Hγ N IV 4058 / N III 4640	C III 4649 blend / He I 4686 He I 4471 / He II 4541	Si IV 4089 / Si III 4552 Si III4552 / Si II4128-32 Si II 4128-32 / He I 4121 Si II 4128-32 / He I 4144	Hγ / O II 4348 He I 4026 / O II 4070-6 He I 4387 / O II 4416 Mg II + Mg II 4481 / He I 4471 N II 3995 / Hγ, Hδ, He I 4009 Si IV 4089 / He I 4026 Si IV 4116 / He I 4121 Si III 4552 / He I 4387
3	He I 4471 / He II 4541 He I 4471 /Hγ N IV 4058 / N III 4640	C III 4649 blend / He I 4686 He I 4471 / He II 4541	Si IV 4089 / Si III 4552 Si III4552 / Si II4128-32 Si II 4128-32 / He I 4121 Si II 4128-32 / He I 4144	Hδ / Hγ, Hγ / Hβ, Hβ / Hα Mg II + Mg II 4481 / He I 4471 N II 3995 / Hγ, Hδ, He I 4009 Si IV 4089 / He I 4026 Si IV 4116 / He I 4121 Si III 4552 / He I 4387
4	He I 4471 / He II 4541 He I 4471 /Hγ N IV 4058 / N III 4640	C III 4649 blend / He I 4686 He I 4471 / He II 4541	Hδ / He I 4471 Mg II + Mg II 4481 / He I 4471 Si II 4128-32 / He I 4121 Si II 4128-32 / He I 4144	Hδ / Hγ, Hγ / Hβ, Hβ / Hα Mg II + Mg II 4481 / He I 4471 N II 3995 / Hγ, Hδ, He I 4009 Si IV 4089 / He I 4026 Si IV 4116 / He I 4121 Si III 4552 / He I 4387
5	He I 4471 / He II 4541 He I 4471 /Hγ Hδ + He II 4100 / He II 4541	C III 4649 blend / He I 4686	Hδ / He I 4471 Mg II + Mg II 4481 / He I 4471 Si II 4128-32 / He I 4121 Si II 4128-32 / He I 4144	Hδ / Hγ, Hγ / Hβ, Hβ / Hα Mg II + Mg II 4481 / He I 4471 N II 3995 / Hγ, Hδ, He I 4009 Si IV 4089 / He I 4026 Si IV 4116 / He I 4121 Si III 4552 / He I 4387
6	He I 4471 / He II 4541 He I 4471 /Hγ Hδ + He II 4100 / He II 4541	C III 4649 blend / He I 4686 Si IV 4089 / He I 4026 Si IV 4089 / He I 4144 Si IV 4116 / He I 4121 Si IV 4116 / He I 4144	Hδ / He I 4471 Mg II + Mg II 4481 / He I 4471 Si II 4128-32 / He I 4121 Si II 4128-32 / He I 4144	Hδ / Hγ, Hγ / Hβ, Hβ / Hα Mg II + Mg II 4481 / He I 4471 N II 3995 / Hγ, Hδ, He I 4009 Si IV 4089 / He I 4026 Si IV 4116 / He I 4121 Si III 4552 / He I 4387
7	He I 4471 / He II 4541 He I 4471 /Hγ Hδ + He II 4100 / He II 4541	C III 4649 blend / He I 4686 Si IV 4089 / He I 4026 Si IV 4089 / He I 4144 Si IV 4116 / He I 4121 Si IV 4116 / He I 4144	Hδ / He I 4471 Mg II + Mg II 4481 / He I 4471 Si II 4128-32 / He I 4121 Si II 4128-32 / He I 4144	Hδ / Hγ, Hγ / Hβ, Hβ / Hα Mg II + Mg II 4481 / He I 4471 N II 3995 / Hγ, Hδ, He I 4009 Si IV 4089 / He I 4026 Si IV 4116 / He I 4121 Si III 4552 / He I 4387
8	He I 4471 / He II 4541 He I 4471 /Hγ	C III 4649 blend / He I 4686 Si IV 4089 / He I 4026 Si IV 4089 / He I 4144 Si IV 4116 / He I 4121 Si IV 4116 / He I 4144	Hδ / He I 4471 Mg II + Mg II 4481 / He I 4471 Si II 4128-32 / He I 4121 Si II 4128-32 / He I 4144	Hδ / Hγ, Hγ / Hβ, Hβ / Hα Mg II + Mg II 4481 / He I 4471 N II 3995 / Hγ, Hδ, He I 4009 Si IV 4089 / He I 4026 Si IV 4116 / He I 4121 Si III 4552 / He I 4387
9	He I 4471 / He II 4541 He I 4471 /Hγ	C III 4649 blend / He I 4686 Si IV 4089 / Hδ Si IV 4089 / He I 4026 Si IV 4089 / He I 4144 Si IV 4116 / He I 4121 Si IV 4116 / He I 4144	Hδ / He I 4471 Mg II + Mg II 4481 / He I 4471 Si II 4128-32 / He I 4121 Si II 4128-32 / He I 4144	Hδ / Hγ, Hγ / Hβ, Hβ / Hα Mg II + Mg II 4481 / He I 4471 N II 3995 / Hγ, Hδ, He I 4009 Si IV 4089 / He I 4026 Si IV 4116 / He I 4121 Si III 4552 / He I 4387

Table III: Compiled criteria used for spectral and luminosity classification of A and F subtypes. [22, 23, 24, 25, 26, 28, 29, 30, 42, 43, 44, 45]

	A		F	
	Spectral	Luminosity	Spectral	Luminosity
Main criteria	Ca I / Mg II Fe I / Fe II Fe II + Ti II / Mg II Mn I, Ti I / H	profiles of Balmer lines Fe II / Mg II Fe II + Ti II / Mg II Sr II / Ca I O I triplet	Ca II K-line, Ca II H-line Mn I / Mn II G-band	Fe II + Ti II / Ca I, Fe I, Mg II Sr II / Fe I O I triplet
0	Ca I 4226 / Hβ, Hγ Ca I 4226 / Mg II + Mg II 4481 Fe I 4271 / Hβ, Hγ Fe I 4045 / Fe II 4173 Mg II + Mg II 4481 / Fe I 4485 Mn I 4030-4 / Hβ, Hγ Ti I 4300 / Hβ, Hγ	Hδ / Hγ, Hγ / Hβ, Hβ / Hα Fe II 4351 / Mg II + Mg II 4481 Fe I + Fe II 4383-5 / Mg II + Mg II 4481 Fe II + Ti II 4417 / Mg II + Mg II 4481 Sr II 4215 / Ca I 4226 O I triplet 7771-5 / Hα, Hβ, Hγ	Ca I 4226 / Hγ Fe I 4045 / Hδ Mn I 4030-4 / Si II 4128-32 Ca II K line / Hα, Hβ, Hγ Ca II H line / Hα, Hβ, Hγ	Fe II + Ti II 4172-8, 4395-4400, 4417, 4444 / Ca I 4226, Fe I 4271, Mg II + Mg II 4481 Sr II 4077 / Hδ, Fe I 4045 O I triplet 7771-5 / Hα, Hβ, Hγ
1	Ca I 4226 / Hβ, Hγ Ca I 4226 / Mg II + Mg II 4481 Fe I 4271 / Hβ, Hγ Fe I 4045 / Fe II 4173 Mg II + Mg II 4481 / Fe I 4485 Mn I 4030-4 / Hβ, Hγ Ti I 4300 / Hβ, Hγ	Fe II 4351 / Mg II + Mg II 4481 Fe I + Fe II 4383-5 / Mg II + Mg II 4481 Fe II + Ti II 4417 / Mg II + Mg II 4481 Sr II 4215 / Ca I 4226 O I triplet 7771-5 / Hα, Hβ, Hγ	Ca I 4226 / Hγ Fe I 4045 / Hδ Mn I 4030-4 / Si II 4128-32 Ca II K line / Hα, Hβ, Hγ Ca II H line / Hα, Hβ, Hγ	Fe II + Ti II 4172-8, 4395-4400, 4417, 4444 / Ca I 4226, Fe I 4271, Mg II + Mg II 4481 Sr II 4077 / Hδ, Fe I 4045 O I triplet 7771-5 / Hα, Hβ, Hγ
2	Ca I 4226 / Hβ, Hγ Ca I 4226 / Mg II + Mg II 4481 Fe I 4271 / Hβ, Hγ Fe I 4045 / Fe II 4173 Mg II + Mg II 4481 / Fe I 4485 Mn I 4030-4 / Hβ, Hγ Ti I 4300 / Hβ, Hγ	Fe II 4351 / Mg II + Mg II 4481 Fe I + Fe II 4383-5 / Mg II + Mg II 4481 Fe II + Ti II 4417 / Mg II + Mg II 4481 Sr II 4215 / Ca I 4226 O I triplet 7771-5 / Hα, Hβ, Hγ	Ca I 4226 / Hγ Fe I 4045 / Hδ Mn I 4030-4 / Si II 4128-32 Ca II K line / Hα, Hβ, Hγ Ca II H line / Hα, Hβ, Hγ G-band / Hα, Hβ, Hγ	Fe II + Ti II 4172-8, 4395-4400, 4417, 4444 / Ca I 4226, Fe I 4271, Mg II + Mg II 4481 Sr II 4077 / Hδ, Fe I 4045 O I triplet 7771-5 / Hα, Hβ, Hγ
3	Ca I 4226 / Hβ, Hγ Ca I 4226 / Mg II + Mg II 4481 Fe I 4271 / Hβ, Hγ Fe I 4045 / Fe II 4173 Mg II + Mg II 4481 / Fe I 4485 Mn I 4030-4 / Hβ, Hγ Ti I 4300 / Hβ, Hγ	Fe II 4351 / Mg II + Mg II 4481 Fe I + Fe II 4383-5 / Mg II + Mg II 4481 Fe II + Ti II 4417 / Mg II + Mg II 4481 Sr II 4215 / Ca I 4226 O I triplet 7771-5 / Hα, Hβ, Hγ	Ca I 4226 / Hγ Fe I 4045 / Hδ Mn I 4030-4 / Si II 4128-32 Ca II K line / Hα, Hβ, Hγ Ca II H line / Hα, Hβ, Hγ G-band / Hα, Hβ, Hγ	Fe II + Ti II 4172-8, 4395-4400, 4417, 4444 / Ca I 4226, Fe I 4271, Mg II + Mg II 4481 Sr II 4077 / Hδ, Fe I 4045 O I triplet 7771-5 / Hα, Hβ, Hγ
4	Ca I 4226 / Hβ, Hγ Ca I 4226 / Mg II + Mg II 4481 Fe I 4271 / Hβ, Hγ Fe I 4045 / Fe II 4173 Mg II + Mg II 4481 / Fe I 4485 Mn I 4030-4 / Hβ, Hγ Ti I 4300 / Hβ, Hγ	Fe II 4351 / Mg II + Mg II 4481 Fe I + Fe II 4383-5 / Mg II + Mg II 4481 Fe II + Ti II 4417 / Mg II + Mg II 4481 Sr II 4215 / Ca I 4226 O I triplet 7771-5 / Hα, Hβ, Hγ	Ca I 4226 / Hγ Fe I 4045 / Hδ Mn I 4030-4 / Si II 4128-32 Ca II K line / Hα, Hβ, Hγ Ca II H line / Hα, Hβ, Hγ G-band / Hα, Hβ, Hγ	Fe II + Ti II 4172-8, 4395-4400, 4417, 4444 / Ca I 4226, Fe I 4271, Mg II + Mg II 4481 Sr II 4077 / Hδ, Fe I 4045 O I triplet 7771-5 / Hα, Hβ, Hγ
5	Ca I 4226 / Hβ, Hγ Ca I 4226 / Mg II + Mg II 4481 Fe I 4271 / Hβ, Hγ Fe I 4045 / Fe II 4173 Mg II + Mg II 4481 / Fe I 4485 Mn I 4030-4 / Hβ, Hγ Ti I 4300 / Hβ, Hγ	Fe II 4351 / Mg II + Mg II 4481 Fe I + Fe II 4383-5 / Mg II + Mg II 4481 Fe II + Ti II 4417 / Mg II + Mg II 4481 Sr II 4215 / Ca I 4226 O I triplet 7771-5 / Hα, Hβ, Hγ	Ca I 4226 / Hγ Fe I 4045 / Hδ Mn I 4030-4 / Si II 4128-32 Ca II K line / Hα, Hβ, Hγ Ca II H line / Hα, Hβ, Hγ G-band / Hα, Hβ, Hγ	Fe II + Ti II 4172-8, 4395-4400, 4417, 4444 / Ca I 4226, Fe I 4271, Mg II + Mg II 4481 Sr II 4077 / Hδ, Ca I 4226, Fe I 4045, 4063, 4071 O I triplet 7771-5 / Hα, Hβ, Hγ Ca II K line / Hα, Hβ, Hγ
6	Ca I 4226 / Hβ, Hγ Ca I 4226 / Mg II + Mg II 4481 Fe I 4271 / Hβ, Hγ Fe I 4045 / Fe II 4173 Mg II + Mg II 4481 / Fe I 4485 Mn I 4030-4 / Hβ, Hγ Ti I 4300 / Hβ, Hγ	Fe II 4351 / Mg II + Mg II 4481 Fe I + Fe II 4383-5 / Mg II + Mg II 4481 Fe II + Ti II 4417 / Mg II + Mg II 4481 Sr II 4215 / Ca I 4226 O I triplet 7771-5 / Hα, Hβ, Hγ	Ca I 4226 / Hγ Fe I 4045 / Hδ Mn I 4030-4 / Si II 4128-32 Ca II K line / Hα, Hβ, Hγ Ca II H line / Hα, Hβ, Hγ G-band / Hα, Hβ, Hγ	Fe II + Ti II 4172-8, 4395-4400, 4417, 4444 / Ca I 4226, Fe I 4271, Mg II + Mg II 4481 Sr II 4077 / Hδ, Ca I 4226, Fe I 4045, 4063, 4071 O I triplet 7771-5 / Hα, Hβ, Hγ Ca II K line / Hα, Hβ, Hγ
7	Ca I 4226 / Hβ, Hγ Ca I 4226 / Mg II + Mg II 4481 Fe I 4271 / Hβ, Hγ Fe I 4045 / Fe II 4173 Mg II + Mg II 4481 / Fe I 4485 Mn I 4030-4 / Hβ, Hγ Ti I 4300 / Hβ, Hγ	Fe II 4351 / Mg II + Mg II 4481 Fe I + Fe II 4383-5 / Mg II + Mg II 4481 Fe II + Ti II 4417 / Mg II + Mg II 4481 Sr II 4215 / Ca I 4226 O I triplet 7771-5 / Hα, Hβ, Hγ	Ca I 4226 / Hγ Fe I 4045 / Hδ Mn I 4030-4 / Si II 4128-32 Ca II K line / Hα, Hβ, Hγ Ca II H line / Hα, Hβ, Hγ G-band / Hα, Hβ, Hγ	Fe II + Ti II 4172-8, 4395-4400, 4417, 4444 / Ca I 4226, Fe I 4271, Mg II + Mg II 4481 Sr II 4077 / Hδ, Ca I 4226, Fe I 4045, 4063, 4071 Ca II K line / Hα, Hβ, Hγ
8	Ca I 4226 / Hβ, Hγ Ca I 4226 / Mg II + Mg II 4481 Fe I 4271 / Hβ, Hγ Fe I 4045 / Fe II 4173 Mg II + Mg II 4481 / Fe I 4485 Mn I 4030-4 / Hβ, Hγ Ti I 4300 / Hβ, Hγ	Fe II 4351 / Mg II + Mg II 4481 Fe I + Fe II 4383-5 / Mg II + Mg II 4481 Fe II + Ti II 4417 / Mg II + Mg II 4481 Sr II 4215 / Ca I 4226 O I triplet 7771-5 / Hα, Hβ, Hγ	Ca I 4226 / Hγ Fe I 4045 / Hδ Mn I 4030-4 / Si II 4128-32 Ca II K line / Hα, Hβ, Hγ Ca II H line / Hα, Hβ, Hγ G-band / Hα, Hβ, Hγ	Fe II + Ti II 4172-8, 4395-4400, 4417, 4444 / Ca I 4226, Fe I 4271, Mg II + Mg II 4481 Sr II 4077 / Hδ, Ca I 4226, Fe I 4045, 4063, 4071 Ca II K line / Hα, Hβ, Hγ
9	Ca I 4226 / Hβ, Hγ Ca I 4226 / Mg II + Mg II 4481 Fe I 4271 / Hβ, Hγ Fe I 4045 / Fe II 4173 Mg II + Mg II 4481 / Fe I 4485 Mn I 4030-4 / Hβ, Hγ Ti I 4300 / Hβ, Hγ	Fe II 4351 / Mg II + Mg II 4481 Fe I + Fe II 4383-5 / Mg II + Mg II 4481 Fe II + Ti II 4417 / Mg II + Mg II 4481 Sr II 4215 / Ca I 4226 O I triplet 7771-5 / Hα, Hβ, Hγ	Ca I 4226 / Hγ Fe I 4045 / Hδ Mn I 4030-4 / Si II 4128-32 Ca II K line / Hα, Hβ, Hγ Ca II H line / Hα, Hβ, Hγ G-band / Hα, Hβ, Hγ	Fe II + Ti II 4172-8, 4395-4400, 4417, 4444 / Ca I 4226, Fe I 4271, Mg II + Mg II 4481 Sr II 4077 / Hδ, Ca I 4226, Fe I 4045, 4063, 4071 Ca II K line / Hα, Hβ, Hγ

Table IV: Compiled criteria used for spectral and luminosity classification of G and K subtypes. [22, 23, 24, 25, 26, 28, 29, 30, 42, 43, 44, 45]

	G		K	
	Spectral	Luminosity	Spectral	Luminosity
Main criteria	Ca I, Fe I / H Cr I / Fe I	Fe II + Ti II / Mg II Sr II / Ca I, Fe I CN bands	Ca I, Cr I, Ti I / Fe I Ti O bands MgH band	Sr II, Ti II / Fe I CN band Mg I triplet
0	Ca I 4226 / Hδ Fe I 4045 / Hδ Fe I 4143 / Hδ Fe I 4383 / Hγ Cr I 4254 / Fe I 4250, 4260 Cr I 4274 / Fe I 4271	Fe II + Ti II 4172-8, 4444 / Mg II + Mg II 4481 Sr II 4077 / Hδ, Ca I 4226, Fe I 4045, 4063, 4071 Sr II + Fe I 4216 / Ca I 4226 Y II + Fe I 4376 / Fe I 4383 CN 0,0 3883 / Hα, Hβ, Hγ CN 1,1 3871 / Hα, Hβ, Hγ	Ca I 4226 / Fe I 4250 Fe I 4045, 4143 / Hδ Fe I 4325 / Hγ Cr I 4254 / Fe I 4250, 4260 Cr I 4274 / Fe I 4271 Ti I 3999 / Fe I 4005	Hδ / Fe I 4071 Sr II 4077 / Fe I 4063 Ti II 4400 / Fe I 4405 CN 0,0 3883 / Hα, Hβ, Hγ CN 1,1 3871 / Hα, Hβ, Hγ CN 4216 / Hα, Hβ, Hγ Mg I triplet 5167-83 / Hα, Hβ, Hγ
1	Ca I 4226 / Hδ Fe I 4045 / Hδ Fe I 4143 / Hδ Fe I 4383 / Hγ Cr I 4254 / Fe I 4250, 4260 Cr I 4274 / Fe I 4271	Fe II + Ti II 4172-8, 4444 / Mg II + Mg II 4481 Sr II 4077 / Hδ, Ca I 4226, Fe I 4045, 4063, 4071 Sr II + Fe I 4216 / Ca I 4226 Y II + Fe I 4376 / Fe I 4383 CN 0,0 3883 / Hα, Hβ, Hγ CN 1,1 3871 / Hα, Hβ, Hγ	Ca I 4226 / Fe I 4250 Fe I 4045, 4143 / Hδ Fe I 4325 / Hγ Cr I 4254 / Fe I 4250, 4260 Cr I 4274 / Fe I 4271 Ti I 3999 / Fe I 4005	Hδ / Fe I 4071 Sr II 4077 / Fe I 4063 Ti II 4400 / Fe I 4405 CN 0,0 3883 / Hα, Hβ, Hγ CN 1,1 3871 / Hα, Hβ, Hγ CN 4216 / Hα, Hβ, Hγ Mg I triplet 5167-83 / Hα, Hβ, Hγ
2	Ca I 4226 / Hδ Fe I 4045 / Hδ Fe I 4143 / Hδ Fe I 4383 / Hγ Cr I 4254 / Fe I 4250, 4260 Cr I 4274 / Fe I 4271	Fe II + Ti II 4172-8, 4444 / Mg II + Mg II 4481 Sr II 4077 / Hδ, Ca I 4226, Fe I 4045, 4063, 4071 Sr II + Fe I 4216 / Ca I 4226 Y II + Fe I 4376 / Fe I 4383 CN 0,0 3883 / Hα, Hβ, Hγ CN 1,1 3871 / Hα, Hβ, Hγ	Ca I 4226 / Fe I 4250 Fe I 4045, 4143 / Hδ Fe I 4325 / Hγ Cr I 4254 / Fe I 4250, 4260 Cr I 4274 / Fe I 4271 Ti I 3999 / Fe I 4005	Hδ / Fe I 4071 Sr II 4077 / Fe I 4063 Ti II 4400 / Fe I 4405 CN 0,0 3883 / Hα, Hβ, Hγ CN 1,1 3871 / Hα, Hβ, Hγ CN 4216 / Hα, Hβ, Hγ Mg I triplet 5167-83 / Hα, Hβ, Hγ
3	Ca I 4226 / Hδ Fe I 4045 / Hδ Fe I 4143 / Hδ Fe I 4383 / Hγ Cr I 4254 / Fe I 4250, 4260 Cr I 4274 / Fe I 4271	Fe II + Ti II 4172-8, 4444 / Mg II + Mg II 4481 Sr II 4077 / Hδ, Ca I 4226, Fe I 4045, 4063, 4071 Sr II + Fe I 4216 / Ca I 4226 Y II + Fe I 4376 / Fe I 4383 CN 0,0 3883 / Hα, Hβ, Hγ CN 1,1 3871 / Hα, Hβ, Hγ	Ca I 4226 / Fe I 4250 Fe I 4045, 4143 / Hδ Fe I 4325 / Hγ Cr I 4254 / Fe I 4250, 4260 Cr I 4274 / Fe I 4271 Ti I 3999 / Fe I 4005	Hδ / Fe I 4071 Sr II 4077 / Fe I 4063 Ti II 4400 / Fe I 4405 CN 0,0 3883 / Hα, Hβ, Hγ CN 1,1 3871 / Hα, Hβ, Hγ CN 4216 / Hα, Hβ, Hγ Mg I triplet 5167-83 / Hα, Hβ, Hγ
4	Ca I 4226 / Hδ Fe I 4045 / Hδ Fe I 4143 / Hδ Fe I 4383 / Hγ Cr I 4254 / Fe I 4250, 4260 Cr I 4274 / Fe I 4271	Fe II + Ti II 4172-8, 4444 / Mg II + Mg II 4481 Sr II 4077 / Hδ, Ca I 4226, Fe I 4045, 4063, 4071 Sr II + Fe I 4216 / Ca I 4226 Y II + Fe I 4376 / Fe I 4383 CN 0,0 3883 / Hα, Hβ, Hγ CN 1,1 3871 / Hα, Hβ, Hγ	Ca I 4226 / Fe I 4250 Fe I 4045, 4143 / Hδ Fe I 4325 / Hγ Cr I 4254 / Fe I 4250, 4260 Cr I 4274 / Fe I 4271 Ti I 3999 / Fe I 4005	Hδ / Fe I 4071 Sr II 4077 / Fe I 4063 Ti II 4400 / Fe I 4405 CN 0,0 3883 / Hα, Hβ, Hγ CN 1,1 3871 / Hα, Hβ, Hγ CN 4216 / Hα, Hβ, Hγ Mg I triplet 5167-83 / Hα, Hβ, Hγ
5	Ca I 4226 / Hδ Fe I 4045 / Hδ Fe I 4325 / Hγ Cr I 4254 / Fe I 4250, 4260 Cr I 4274 / Fe I 4271	Fe II + Ti II 4172-8, 4444 / Mg II + Mg II 4481 Sr II 4077 / Hδ, Ca I 4226, Fe I 4045, 4063, 4071 Sr II + Fe I 4216 / Ca I 4226 Y II + Fe I 4376 / Fe I 4383 CN 0,0 3883 / Hα, Hβ, Hγ CN 1,1 3871 / Hα, Hβ, Hγ	Ca I 4226 / Fe I 4250, 4383 Fe I 4045, 4143 / Hδ Fe I 4325 / Hγ Cr I 4254 / Fe I 4250, 4260 Cr I 4274 / Fe I 4271 Ti I 3999 / Fe I 4005 MgH band 5130 / Hα, Hβ, Hγ	Hδ / Fe I 4071 Sr II 4077 / Fe I 4063 Ti II 4400 / Fe I 4405 CN 0,0 3883 / Hα, Hβ, Hγ CN 1,1 3871 / Hα, Hβ, Hγ CN 4216 / Hα, Hβ, Hγ Mg I triplet 5167-83 / Hα, Hβ, Hγ
6	Ca I 4226 / Hδ Fe I 4045 / Hδ Fe I 4325 / Hγ Cr I 4254 / Fe I 4250, 4260 Cr I 4274 / Fe I 4271	Fe II + Ti II 4172-8, 4444 / Mg II + Mg II 4481 Sr II 4077 / Hδ, Ca I 4226, Fe I 4045, 4063, 4071 Sr II + Fe I 4216 / Ca I 4226 Y II + Fe I 4376 / Fe I 4383 CN 0,0 3883 / Hα, Hβ, Hγ CN 1,1 3871 / Hα, Hβ, Hγ	Ca I 4226 / Fe I 4250, 4383 Fe I 4143 / Hδ Cr I 4254 / Fe I 4250, 4260 Cr I 4274 / Fe I 4271 Ti I 3999 / Fe I 4005 MgH band 5130 / Hα, Hβ, Hγ	Hδ / Fe I 4071 Sr II 4077 / Fe I 4063 Ti II 4400 / Fe I 4405 CN 0,0 3883 / Hα, Hβ, Hγ CN 1,1 3871 / Hα, Hβ, Hγ CN 4216 / Hα, Hβ, Hγ
7	Ca I 4226 / Hδ Fe I 4045 / Hδ Fe I 4325 / Hγ Cr I 4254 / Fe I 4250, 4260 Cr I 4274 / Fe I 4271	Fe II + Ti II 4172-8, 4444 / Mg II + Mg II 4481 Sr II 4077 / Hδ, Ca I 4226, Fe I 4045, 4063, 4071 Sr II + Fe I 4216 / Ca I 4226 Y II + Fe I 4376 / Fe I 4383 CN 0,0 3883 / Hα, Hβ, Hγ CN 1,1 3871 / Hα, Hβ, Hγ	Ca I 4226 / Fe I 4250, 4383 Fe I 4143 / Hδ Cr I 4254 / Fe I 4250, 4260 Cr I 4274 / Fe I 4271 Ti I 3999 / Fe I 4005 TiO bands 4422-8432 / Hα, Hβ, Hγ MgH band 5130 / Hα, Hβ, Hγ	Hδ / Fe I 4071 Sr II 4077 / Fe I 4063 Ti II 4400 / Fe I 4405 CN 0,0 3883 / Hα, Hβ, Hγ CN 1,1 3871 / Hα, Hβ, Hγ CN 4216 / Hα, Hβ, Hγ
8	Ca I 4226 / Hδ Fe I 4045 / Hδ Fe I 4325 / Hγ Cr I 4254 / Fe I 4250, 4260 Cr I 4274 / Fe I 4271	Sr II 4077 / Hδ, Fe I 4045, 4063, 4071 Sr II + Fe I 4216 / Ca I 4226 Y II + Fe I 4376 / Fe I 4383 CN 4216 / Hα, Hβ, Hγ Mg I triplet 5167-83 / Hα, Hβ, Hγ Ca II K line / Hα, Hβ, Hγ Ca II H line / Hα, Hβ, Hγ	Ca I 4226 / Fe I 4250, 4383 Fe I 4143 / Hδ Cr I 4254 / Fe I 4250, 4260 Cr I 4274 / Fe I 4271 Ti I 3999 / Fe I 4005 TiO bands 4422-8432 / Hα, Hβ, Hγ MgH band 5130 / Hα, Hβ, Hγ	Hδ / Fe I 4071 Sr II 4077 / Fe I 4063 Ti II 4400 / Fe I 4405 CN 0,0 3883 / Hα, Hβ, Hγ CN 1,1 3871 / Hα, Hβ, Hγ CN 4216 / Hα, Hβ, Hγ
9	Ca I 4226 / Hδ Fe I 4045 / Hδ Fe I 4325 / Hγ Cr I 4254 / Fe I 4250, 4260 Cr I 4274 / Fe I 4271	Sr II 4077 / Hδ, Fe I 4045, 4063, 4071 Sr II + Fe I 4216 / Ca I 4226 Y II + Fe I 4376 / Fe I 4383 CN 4216 / Hα, Hβ, Hγ Mg I triplet 5167-83 / Hα, Hβ, Hγ Ca II K line / Hα, Hβ, Hγ Ca II H line / Hα, Hβ, Hγ	Ca I 4226 / Fe I 4250, 4383 Fe I 4143 / Hδ Cr I 4254 / Fe I 4250, 4260 Cr I 4274 / Fe I 4271 Ti I 3999 / Fe I 4005 TiO bands 4422-8432 / Hα, Hβ, Hγ MgH band 5130 / Hα, Hβ, Hγ	Hδ / Fe I 4071 Sr II 4077 / Fe I 4063 Ti II 4400 / Fe I 4405 CN 0,0 3883 / Hα, Hβ, Hγ CN 1,1 3871 / Hα, Hβ, Hγ CN 4216 / Hα, Hβ, Hγ

Table V: Compiled criteria used for spectral and luminosity classification of M subtype. [22, 23, 24, 25, 26, 28, 29, 30, 42, 43, 44, 45]

	M	
	Spectral	Luminosity
Main criteria	Ca I / Fe I Ti O bands VO bands CaH bands	Ca I, Ca II, Cr I / H Sr II / Fe I K I, Na I / H MgH + TiO blend
0	Ca I 4226 / Fe I 4383 CaH band 6346, 6382, 6750 / Hα, Hβ, Hγ TiO bands 4422-8432 / Hα, Hβ, Hγ	Ca I 4226 / Hα, Hβ, Hγ Ca II triplet 8498 + 8542 + 8662 / Hα, Hβ, Hγ Cr I 4254, 4274, 4290 / Hα, Hβ, Hγ Sr II 4077 / Fe I 4045, 4063 Sr II + Fe I 4216 / Fe I 4250 Y II + Fe I 4376 / Fe I 4383 K I 7699 / Hα, Hβ, Hγ Na I 8183, 8195 / Hα, Hβ, Hγ
1	Ca I 4226 / Fe I 4383 CaH band 6346, 6382, 6750 / Hα, Hβ, Hγ TiO bands 4422-8432 / Hα, Hβ, Hγ	Ca I 4226 / Hα, Hβ, Hγ Ca II triplet 8498 + 8542 + 8662 / Hα, Hβ, Hγ Cr I 4254, 4274, 4290 / Hα, Hβ, Hγ Sr II 4077 / Fe I 4045, 4063 Sr II + Fe I 4216 / Fe I 4250 Y II + Fe I 4376 / Fe I 4383 K I 7699 / Hα, Hβ, Hγ Na I 8183, 8195 / Hα, Hβ, Hγ
2	Ca I 4226 / Fe I 4383 CaH band 6346, 6382, 6750 / Hα, Hβ, Hγ TiO bands 4422-8432 / Hα, Hβ, Hγ	Ca I 4226 / Hα, Hβ, Hγ Ca II triplet 8498 + 8542 + 8662 / Hα, Hβ, Hγ Cr I 4254, 4274, 4290 / Hα, Hβ, Hγ Sr II 4077 / Fe I 4045, 4063 Sr II + Fe I 4216 / Fe I 4250 Y II + Fe I 4376 / Fe I 4383 K I 7699 / Hα, Hβ, Hγ Na I 8183, 8195 / Hα, Hβ, Hγ MgH + TiO blend 4770 / Hα, Hβ, Hγ
3	Ca I 4226 / Fe I 4383 CaH band 6346, 6382, 6750 / Hα, Hβ, Hγ TiO bands 4422-8432 / Hα, Hβ, Hγ	Ca I 4226 / Hα, Hβ, Hγ Ca II triplet 8498 + 8542 + 8662 / Hα, Hβ, Hγ Cr I 4254, 4274, 4290 / Hα, Hβ, Hγ Sr II 4077 / Fe I 4045, 4063 Sr II + Fe I 4216 / Fe I 4250 Y II + Fe I 4376 / Fe I 4383 K I 7699 / Hα, Hβ, Hγ Na I 8183, 8195 / Hα, Hβ, Hγ MgH + TiO blend 4770 / Hα, Hβ, Hγ
4	Ca I 4226 / Fe I 4383 CaH band 6346, 6382, 6750 / Hα, Hβ, Hγ TiO bands 4422-8432 / Hα, Hβ, Hγ	Ca I 4226 / Hα, Hβ, Hγ Ca II triplet 8498 + 8542 + 8662 / Hα, Hβ, Hγ Cr I 4254, 4274, 4290 / Hα, Hβ, Hγ Sr II 4077 / Fe I 4045, 4063 Sr II + Fe I 4216 / Fe I 4250 Y II + Fe I 4376 / Fe I 4383 K I 7699 / Hα, Hβ, Hγ Na I 8183, 8195 / Hα, Hβ, Hγ MgH + TiO blend 4770 / Hα, Hβ, Hγ
5	Ca I 4226 / Fe I 4383 CaH band 6346, 6382, 6750 / Hα, Hβ, Hγ TiO bands 4422-8432 / Hα, Hβ, Hγ	Ca I 4226 / Hα, Hβ, Hγ Ca II triplet 8498 + 8542 + 8662 / Hα, Hβ, Hγ Cr I 4254, 4274, 4290 / Hα, Hβ, Hγ Sr II 4077 / Fe I 4045, 4063 Sr II + Fe I 4216 / Fe I 4250 Y II + Fe I 4376 / Fe I 4383 K I 7699 / Hα, Hβ, Hγ Na I 8183, 8195 / Hα, Hβ, Hγ MgH + TiO blend 4770 / Hα, Hβ, Hγ
6	CaH band 6346, 6382, 6750 / Hα, Hβ, Hγ TiO bands 4422-8432 / Hα, Hβ, Hγ	Ca I 4226 / Hα, Hβ, Hγ Ca II triplet 8498 + 8542 + 8662 / Hα, Hβ, Hγ Cr I 4254, 4274, 4290 / Hα, Hβ, Hγ Sr II 4077 / Fe I 4045, 4063 Sr II + Fe I 4216 / Fe I 4250 Y II + Fe I 4376 / Fe I 4383 K I 7699 / Hα, Hβ, Hγ Na I 8183, 8195 / Hα, Hβ, Hγ MgH + TiO blend 4770 / Hα, Hβ, Hγ
7	CaH band 6346, 6382, 6750 / Hα, Hβ, Hγ TiO bands 4422-8432 / Hα, Hβ, Hγ VO bands 5737-7896 / Hα, Hβ, Hγ	Ca I 4226 / Hα, Hβ, Hγ Ca II triplet 8498 + 8542 + 8662 / Hα, Hβ, Hγ Cr I 4254, 4274, 4290 / Hα, Hβ, Hγ Sr II 4077 / Fe I 4045, 4063 Sr II + Fe I 4216 / Fe I 4250 Y II + Fe I 4376 / Fe I 4383 K I 7699 / Hα, Hβ, Hγ Na I 8183, 8195 / Hα, Hβ, Hγ MgH + TiO blend 4770 / Hα, Hβ, Hγ

8	CaH band 6346, 6382, 6750 / Hα, Hβ, Hγ TiO bands 4422-8432 / Hα, Hβ, Hγ VO bands 5737-7896 / Hα, Hβ, Hγ	Ca I 4226 / Hα, Hβ, Hγ Ca II triplet 8498 + 8542 + 8662 / Hα, Hβ, Hγ Cr I 4254, 4274, 4290 / Hα, Hβ, Hγ Sr II 4077 / Fe I 4045, 4063 Sr II + Fe I 4216 / Fe I 4250 Y II + Fe I 4376 / Fe I 4383 K I 7699 / Hα, Hβ, Hγ Na I 8183, 8195 / Hα, Hβ, Hγ MgH + TiO blend 4770 / Hα, Hβ, Hγ
9	CaH band 6346, 6382, 6750 / Hα, Hβ, Hγ TiO bands 4422-8432 / Hα, Hβ, Hγ VO bands 5737-7896 / Hα, Hβ, Hγ	Ca I 4226 / Hα, Hβ, Hγ Ca II triplet 8498 + 8542 + 8662 / Hα, Hβ, Hγ Cr I 4254, 4274, 4290 / Hα, Hβ, Hγ Sr II 4077 / Fe I 4045, 4063 Sr II + Fe I 4216 / Fe I 4250 Y II + Fe I 4376 / Fe I 4383 K I 7699 / Hα, Hβ, Hγ Na I 8183, 8195 / Hα, Hβ, Hγ MgH + TiO blend 4770 / Hα, Hβ, Hγ

HR Diagrams

In order to test the ability of SpecOp, a set of HR diagrams was generated using the software. It spans the grid of the stars of types O-M, classes I-V included in the Pickles library. The stars plotted are colored by luminosity class, the main sequence stars – green, subgiants – lime, giants – yellow, supergiants – orange and hypergiants – red. Measurement of equivalent widths was done for all lines of the system. The values of equivalent widths are scaled onto the HR diagram (fig. I) with the formula $y = 3.5 * log_{10}W + 1.5$.

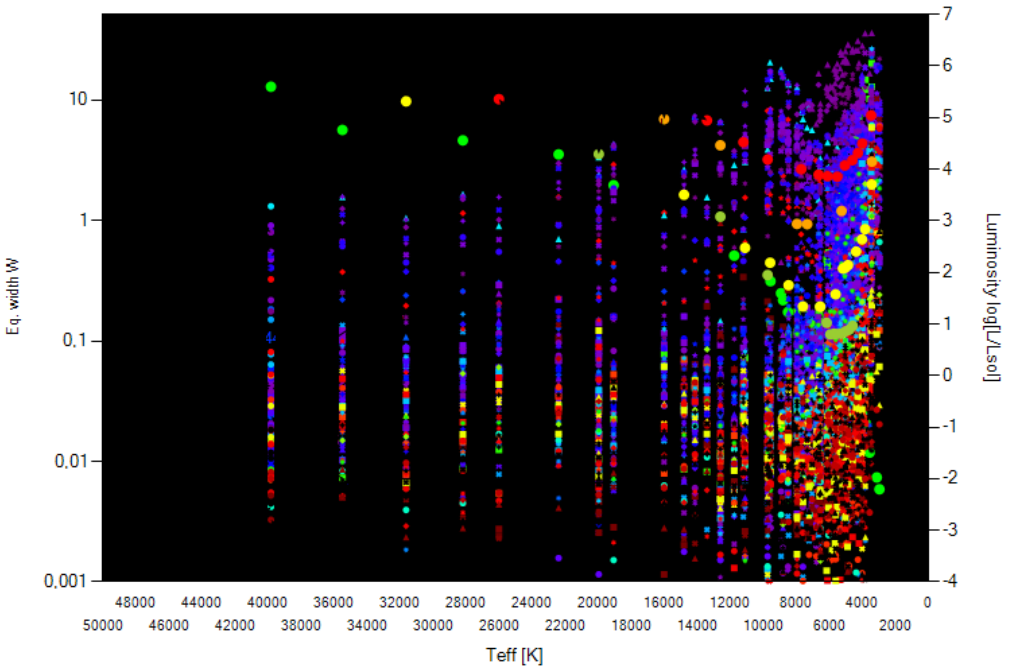

Figure I: HR diagram constructed from the Pickles library, displaying values of measured equivalent widths.

The coloring of the spectral lines corresponds to the color of their radiation, derived from the wavelength of the spectral line. The assigned colors are shown in the fig. II.

Figure II: Color coding derived from wavelengths of included criteria spectral lines.

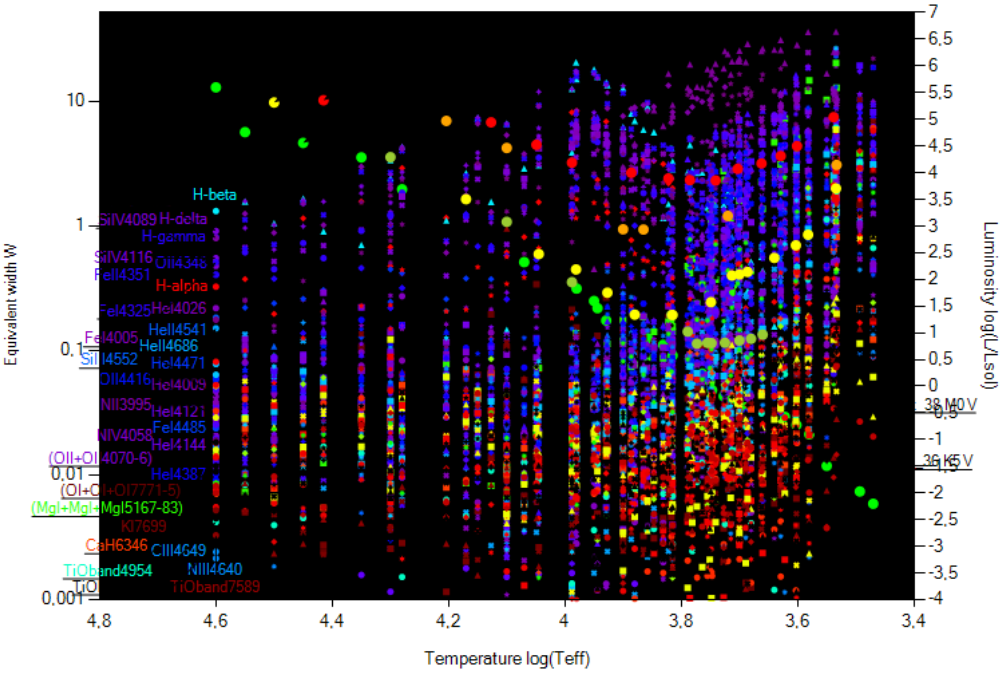

Figure III: HR diagram constructed from the Pickles library, realistic coloring of spectral lines.

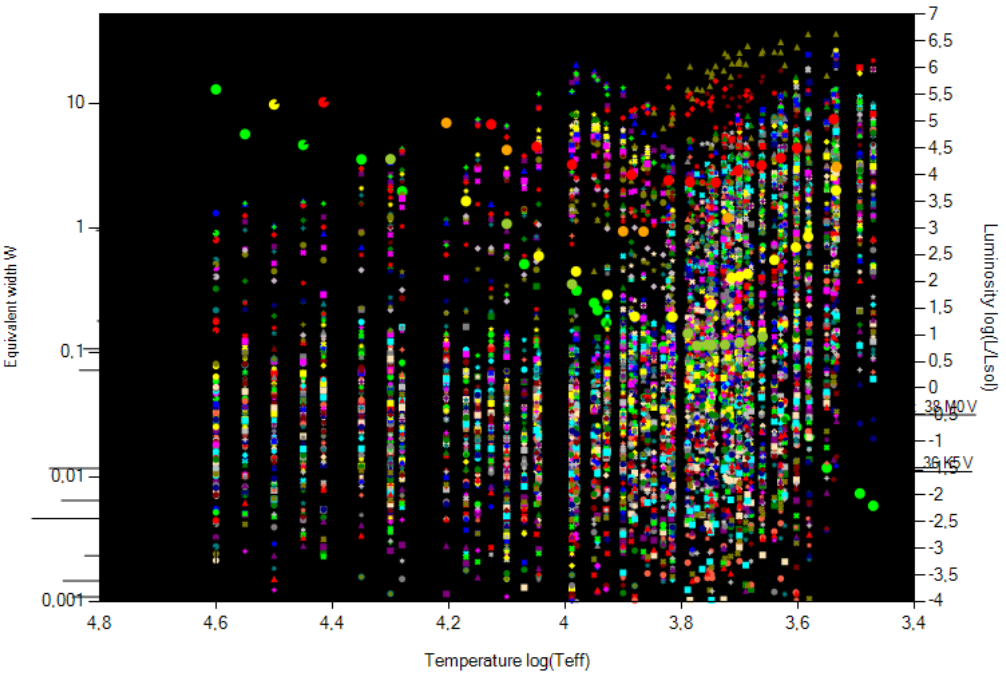

Figure IV: HR diagram constructed from the Pickles library, contrast coloring of spectral lines.

Following HR diagrams (fig. V, VI and VII) are results of luminosity classes V, III and I being plotted separately, equivalent width being colored realistically on the left (a) and with contrast coloring on the right (b):

(a) (b)

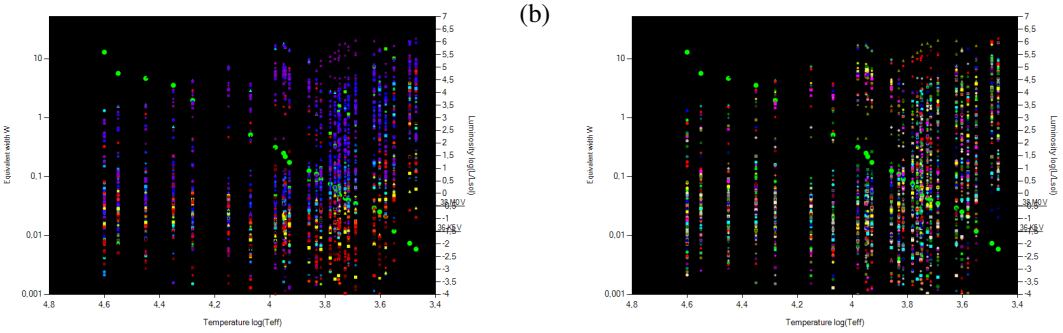

Figure V: HR diagrams of luminosity class V; (a) realistic and (b) contrast coloring of equivalent widths.

(a) (b)

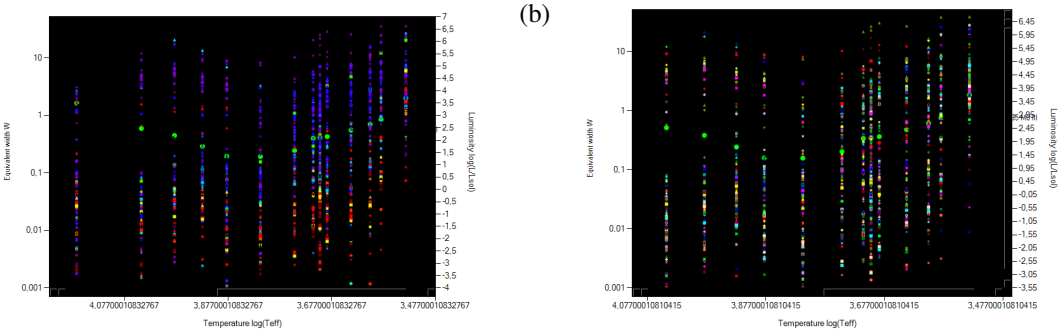

Figure VI: HR diagrams of luminosity class III; (a) realistic and (b) contrast coloring of equivalent widths.

(a) (b)

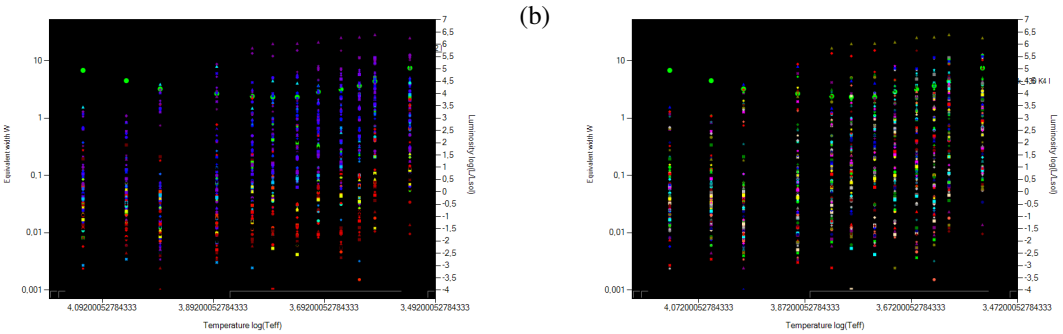

Figure VII: HR diagrams of luminosity class I; (a) realistic and (b) contrast coloring of equivalent widths.

Discussion

Refined system of the MK classification criteria

A major part of this thesis has been devoted to collecting, researching and refining criteria applicable in classification according to the MK system in the visible to the near infrared region of radiation. The sources of implemented criteria were [22, 23, 24, 25, 26, 28, 29, 30, 42, 43, 44, 45]. The collected criteria were integrated into the software developed over the time period of two years, but the classification system can of course be used by itself as well, and as such, represents a major part of this thesis and also a significant portion of the work done, to the extent it could be seen as the main result. Refined system of classification criteria is supported by a refined collection of spectral lines, molecular bands and blends, wavelengths of which were refined using [38, 39, 40, 41].

The SpecOp 2 software

The developed software SpecOp 2 can serve as a suite for handling of spectral data including continuum estimations, measurement of equivalent widths, basic stellar parameters estimations, dynamic plotting of HR diagrams from spectral libraries and can even serve as an interface to a fully automatic MK classification provided by the implemented software MKClass. [31]

HR diagrams of the Pickles library

The processing of the data contained in the Pickles library into an automatically generated HR diagram and enhancing it with measured equivalent widths was meant to be a test of the capabilities of the software as well as the refined classification system. All criterion spectral lines of the system were measured for all spectra of the Pickles library. However, it is important to note, that the equivalent widths of spectral lines shown in this diagram are not necessarily accurate for spectral types not associated with each given spectral line: at different effective temperature, radiation coming from different spectral lines having

similar wavelengths might be detected instead, especially if the resolution of the spectra isn't very high and the smoothing is done automatically, by a preset set of parameters. It is important to interpret the equivalent widths in the context of applicable criteria that are different for each spectral type, that make the measured values valid. While it might seem unusual to attempt to measure equivalent widths of all of the classification criteria spectral lines for all of the stars of the collection, rather than using specific sets of spectral lines for stars suspect of belonging to specific spectral types (the way the classification process is typically done), by choosing this approach and disregarding the invalid spectral lines we still retain the possibility of visually identifying anomalous spectra in large collections of data. Developing a set of MK classification criteria spectral lines, based on using only the weak lines on high resolution spectra, that would be applicable to the complete temperature progression without the issue of encountering strong neighboring spectral lines is one of the future aims for this software.

The values of the criterion spectral lines of each type show values comparable to those found in literature [46, 47]. Measurements of a several of the equivalent widths of non-criteria (for the given spectral type) spectral lines were measured erroneously, an outcome which was expected. The HR diagrams show a couple of interesting features. While the upper values of the equivalent width scale are mostly occupied by blue spectral lines, this is most likely related to most of the spectral lines used by the system being situated in that region, which poses as a bias effect, although it could also be hinting a flaw in the form of skewed normalization and other systematic errors. The red lines visibly strengthen significantly in the lower end of the temperature scale. Spectral lines of hydrogen are unsurprisingly generally dominant in many of the spectra, the lines of the Balmer series being positioned in the upper area of all of the diagrams. Ca II lines are represented strongly across the temperature progression of the cooler spectral types as expected, but some were also erroneously measured as greater than unity at high effective temperatures, most often being unresolved due to proximity of strong spectral lines, most often those due to hydrogen. An interesting feature are the two sharp separation points, first at 10 000 K and second at 6 000 K, the first being due to ionized metals and the second marking the appearance of lines of neutral metals, particularly spectral lines of Fe I. The yellow TiO bands can be seen clumping at low values across the progression, but any measurements bellow effective temperature of 4 000 K are likely only measuring different minor spectral lines and/or the noise of the spectra. After reaching low enough temperatures, the yellow markers clearly lift off to valid measured values, being a valid criterion spectral line in the M type spectra. The onset of yellow TiO bands is preceded on the temperature scale by the appearance of the light blue spectral lines of the same molecule. Quite interesting is the behavior of the green MgH molecular band that reaches values nearing unity in the later spectral types.

Generally, most of the physical aspects of the HR diagrams can be considered valid estimates, at the very least at the criteria spectral lines own to each spectral type . It must be noted though, that using the software to process a collection of spectra of significantly varying spectral types using a static system of spectral lines may lead to erroneous values of measured equivalent widths of non-criterion spectral lines. While this causes the need to disregard some of the measurements, it is also a way to determine the criteria that stay valid even in these settings.

Conclusions

In this thesis I have researched, compiled and refined a set of stellar MK classification criteria applicable to stars of spectral types O-M and luminosity classes I-V in the visible to the near infrared region of 3 800 – 8 400 Å as well as a set of refined spectral lines supporting it. The refined MK classification system was implemented in the software SpecOp 2, development of which was the second, although not secondary, aim of this work. To test the capabilities of the software, a set of automatically generated HR diagrams was produced with it, enhanced by appending values of equivalent widths of criterion spectral lines for each star in the Pickles library. Additional functionality of fully automatic classification according to MK system was achieved by implementing a custom build of the software MKClass by R. O. Gray *et al.*

References

[1] FAKTOR, J. *Jaká kritéria jsou vhodná ke klasifikaci hvězd horní části hlavní posloupnosti?* Brno, 2016. Bakalářská práce. Masarykova univerzita, Přírodovědecká fakulta.

[2] KIRCHHOFF, G. and R. BUNSEN. Chemical Analysis by Observation of Spectra. *Annalen der Physik und der Chemie*. 1860, vol. 110, p. 161-189.

[3] *MIT Spectroscopy Lab* [online]. Massachusetts Institute of Technology. [cit. 2018-11-10]. Retrieved from: `http://web.mit.edu/spectroscopy/history/spec-history.html`.

[4] MIKULÁŠEK, Z. and J. KRTIČKA. *Základy fyziky hvězd*. Brno: Masaryk university, 2005.

[5] HALLIDAY, D., R. RESNICK and J. WALKER. *Fyzika: vysokoškolská učebnice obecné fyziky*. Brno: VUTIUM, 2007. ISBN 80-214-1868-0.

[6] MIKULÁŠEK, Z. and M. ZEJDA. *Proměnné hvězdy*. Brno: Masaryk university, 2002.

[7] HOLLAS, J. M. *Modern spectroscopy*. 4th ed. Hoboken: J. Wiley, 2004. ISBN 04-708-4416-7.

[8] COLLINS, G. W. *The Fundamentals of Stellar Astrophysics*. New York: W. H. Freeman, 1989. ISBN 07-167-1993-2.

[9] KRTIČKA, J. *Horké hvězdy II*. Brno: Masaryk university, 2015.

[10] PALMER, C. and E. LOEWEN. *Diffraction Grating Handbook*. 6th ed. New York: Newport Corporation, 2005.

[11] MORGAN, W. W. and P. C. KEENAN. Spectral Classification. *Annual Review of Astronomy and Astrophysics* [online]. 1973, vol. 11, p. 29-50 [cit. 2018-11-11]. DOI: 10.1146/annurev.aa.11.090173.000333.

[12] UNDERHILL, A. B. *The Early Type Stars*. Dordrecht: D. Reidel Publishing Company, 1966. ISBN 978-940-1035-583.

[13] MORGAN, W. W., P. C. KEENAN and E. KELLMAN. *An atlas of stellar spectra, with an outline of spectral classification*. Chicago: The University of Chicago press, 1943.

[14] *Spectral Classification of Stars* [online]. Bruce MacEvoy. (2013). [cit. 2018-11-11]. Retrieved from: `http://www.handprint.com/ASTRO/specclass.html`.

[15] CONTI, P. S. and W. R. ALSCHULER. Spectroscopic Studies of O-Type Stars. I. Classification and Absolute Magnitudes. *The Astrophysical Journal* [online]. 1971, vol. 170, p. 325-344 [cit. 2018-11-20]. DOI: 10.1086/151218.

[16] BISIACCHI, G. F., C. FIRMANI, R. ORTEGA and R. PENICHE. Spectral classification of early type stars. Calibration using a TV-vidicon multichannel system. *Revista Mexicana de Astronomía y Astrofísica* [online]. 1976, vol. 2, p. 13-21 [cit. 2018-11-20].

[17] MIKULÁŠEK, Z. *Fyzika horkých hvězd I*. Brno: Masaryk university, 2011.

[18] SMALLEY, B. T_{eff} and log g Determinations. *Memorie della Società Astronomica Italiana* [online]. 2005, vol. 8, p. 130-141 [cit. 2018-11-20].

[19] METCHEV, S. *Stellar Phenomenology and Stellar Properties* [PDF document]. (2011). [cit. 2018-11-20]. Retrieved from: `http://www.astro.sunysb.edu/metchev/PHY521/lecture2.pdf`

[20] CIARDULLO, R. *Characteristics of Main Sequence Stars* [PDF document]. (2007). [cit. 2018-11-28]. Retrieved from: `http://www2.astro.psu.edu/users/rbc/a534/lec18.pdf`.

[21] DURIC, N. *Advanced astrophysics*. Cambridge: Cambridge University Press, 2004. ISBN 978-051-1800-177.

[22] GRAY, R. O. *A Digital Spectral Classification Atlas v1.02* [online]. (2000). [cit. 2018-11-28]. Retrieved from: `http://ned.ipac.caltech.edu/level5/Gray/frames.html`

[23] GOSWAMI, A. and B. E. REDDY (eds.). *Principles and perspectives in cosmochemistry: lecture notes of the Kodai School on 'synthesis of elements in stars' held at Kodaikanal Observatory, India, April 29 – May 13, 2008*. New York: Springer Verlag, 2010. ISBN 978-364-2103-520.

[24] JASCHEK, C. and M. JASCHEK. *The classification of stars*. New York: Cambridge University Press, 1987. ISBN 05-212-6773-0.

[25] GIRIDHAR, S. Advances in spectral classification. *Bulletin of the Astronomical Society of India* [online]. 2010, vol. 38, p. 1-33 [cit. 2018-12-12].

[26] GIRIDHAR, S. Spectral Classification, Old and Contemporary. *Principles and Perspectives in Cosmochemistry* [online]. 2010, p. 1-17 [cit. 2018-12-12]. DOI: 10.1007/978-3-642-10352-0_3.

[27] MARKOVA, N., L. BIANCHI, B. EFREMOVA and J. PULS. Metallicity effects in the spectral classification of O-type stars. Theoretical consideration. *Bulgarian Astronomical Journal* [online]. 2009, vol. 12, p. 21-28 [cit. 2018-12-14].

[28] DUFAY, J. *Introduction to Astrophysics: The Stars*. New York: Dover Publications, 2012. ISBN 978-048-6607-719.

[29] WALBORN, N. R., I. D. HOWARTH, D. J. LENNON, P. MASSEY, M. S. OEY, A. F. J. MOFFAT, G. SKALKOWSKI, N. I. MORRELL, L. DRISSEN and J. W. PARKER. A New Spectral Classification System for the Earliest O Stars: Definition of Type O2. *The Astronomical Journal* [online]. 2002, vol. 123, p. 2754-2771 [cit. 2018-12-14]. DOI: 10.1086/339831.

[30] GRAY, R. O. and C. J. CORBALLY. *Stellar spectral classification*. Princeton: Princeton University Press, 2009. ISBN 06-911-2511-2.

[31] GRAY, R. O. and C. J. CORBALLY. AN EXPERT COMPUTER PROGRAM FOR CLASSIFYING STARS ON THE MK SPECTRAL CLASSIFICATION SYSTEM. *The Astronomical Journal* [online]. 2014, vol. 147, p. 1-7 [cit. 2018-10-30]. DOI: 10.1088/0004-6256/147/4/80.

[32] PICKLES, A. J. A Stellar Spectral Flux Library: 1150–25000 Å. *Publications of the Astronomical Society of the Pacific* [online]. 1998, vol. 110, p. 863-878 [cit. 2018-10-30]. DOI: 10.1086/316197.

[33] JACOBY, G. H., D. A. HUNTER and C. A. CHRISTIAN. A library of stellar spectra. *The Astrophysical Journal Supplement Series* [online]. 1984, vol. 56, p. 257-281 [cit. 2018-10-30]. DOI: 10.1086/190983.

[34] DANKS, A. C. and M. DENNEFELD. An atlas of southern MK standards from 5800 to 10200 Å. *Publications of the Astronomical Society of the Pacific* [online]. 1994, vol. 106, p. 382-396 [cit. 2018-12-18]. DOI: 10.1086/133390.

[35] PALACIOS, A., M. GEBRAN, E. JOSSELIN, F. MARTINS, B. PLEZ, M. BELMAS and A. LÈBRE. POLLUX: a database of synthetic stellar spectra. *Astronomy and Astrophysics* [online]. 2010, vol. 516, p. 1-9 [cit. 2018-12-18]. DOI: 10.1051/0004-6361/200913932.

[36] GRIEKEN, R. van and A. A. MARKOWICZ (eds.). *Handbook of X-Ray Spectrometry*. 2nd ed. New York: Marcel Dekker, 2002. ISBN 08-247-0600-5.

[37] ESO - Library of Stellar Spectra. *European Southern Observatory* [online]. 2007. [cit. 2018-12-18]. Retrieved from: `https://www.eso.org/sci/facilities/paranal/decommissioned/isaac/tools/lib.html`.

[38] STRIGANOV, A. R. and N. S. SVENTITSKII. *Tables of Spectral Lines of Neutral and Ionized Atoms*. New York: Springer-Verlag, 2013. ISBN 978-1-4757-6612-7.

[39] ZAIDEL, A. N., V. K. PROKOFEV, S. M. RAISKII, V. A. SLAVNYI and E. Y. SHREIDER. *Tables of Spectral Lines*. New York: Plenum Publishing Corporation, 1970. ISBN 978-1-4757-1603-0.

[40] U.S. DEPARTMENT OF COMMERCE / National Bureau of Standards Monograph 145. *Tables of Spectral-Line Intensities – Arranged by Elements*. 2nd ed. Washington: U.S. Government Printing Office, 1975.

[41] SANSONETTI, J. E. and W. C. MARTIN. Handbook of Basic Atomic Spectroscopic Data. *Journal of Physical and Chemical Reference Data* [online]. 2005, vol. 34, p. 1559-2259 [cit. 2018-12-18]. DOI: 10.1063/1.1800011.

[42] MORGAN, W. W., H. A. ABT and J. W. TAPSCOTT. *Revised MK Spectral Atlas for stars earlier than the Sun*. Williams Bay: Yerkes Observatory, and Tucson: Kitt Peak National Observatory, 1978.

[43] YAMASHITA, Y. and K. NARIAI. *An Atlas of representative stellar spectra*. Tokyo: University of Tokyo Press, 1977.

[44] LANDI, J., M. JASCHEK and C. JASCHEK. *An atlas of grating stellar spectra at intermediate dispersion*. Córdoba: Universidad Nacional de Córdoba, 1977.

[45] NORDLANDER, T. *Analyses of cool stars using molecular lines* [online]. 2012 [cit. 2018-12-18]. Retrieved from: `https://uu.diva-portal.org/smash/get/diva2:528152/FULLTEXT01.pdf. Uppsala Universitet`.

[46] CANANZI, K., R. AUGARDE and J. LEQUEUX. An atlas of Balmer lines (Hδ and Hγ). *Astronomy and Astrophysics Supplement* [online]. 1993, vol. 101, p. 599-619 [cit. 2018-12-20].

[47] STETSON, P. B. and E. PANCINO. DAOSPEC: An Automatic Code for Measuring Equivalent Widths in High-Resolution Stellar Spectra. *Publications of the Astronomical Society of the Pacific* [online]. 2008, vol. 120, p. 1332-1354 [cit. 2018-12-20]. DOI: 10.1086/596126.